

RICE UNIVERSITY

**Numerical Treatment of Stochastic Dynamic Systems with
Fractional Laplacian Terms**

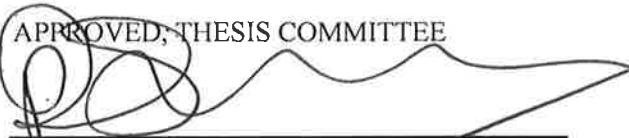
by

Yiyu Jiao

A THESIS SUBMITTED IN PARTIAL FULFILLMENT OF THE
REQUIREMENTS FOR THE DEGREE

Doctor of Philosophy

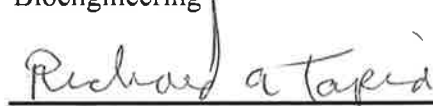
APPROVED, THESIS COMMITTEE



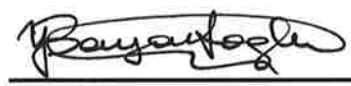
Pol D. Spanos, Chair
Lewis B. Ryon Professor in Mechanical &
Civil Engineering



Fathi H. Ghorbel
Professor of Mechanical Engineering &
Bioengineering



Richard A. Tapia
University Professor
Maxfield-Oshman Professor in Engineering



Yildiz Bayazitoglu
Harry S. Cameron Chair in Mechanical
Engineering

HOUSTON, TEXAS
August 2018

Abstract

Numerical Treatment of Stochastic Dynamic Systems with Fractional Laplacian Terms

by

Yiyu Jiao

The fractional Laplacian is an integro-differential operator that is currently widely used in nonlocal models, such as the anomalous diffusion, which arises when a particle moves randomly in the space involving a random process that allows long jumps. Determining the response of such dynamic systems is a daunting task, as general analytical solutions are not available. This thesis proposes approximate and numerical methods for determining the response of dynamic systems containing fractional Laplacian terms. Based on the Riesz-Marchaud and Caputo-type representations of the fractional Laplacian, two Boundary Element Methods (BEM) are introduced to treat fractional dynamic systems. Further, a modal expansion is proposed as a novel expression of the fractional Laplacian. Furthermore, based on the proposed eigenfunctions, statistical linearization procedures are developed to approximate the response statistics.

A BEM-based numerical algorithm is first introduced to estimate the solution of the fractional Poisson equation based on the Riesz-Marchaud definition of the fractional Laplacian. Further, the algorithm is applied to a fractional diffusion equation. The properties of the Caputo-type fractional Laplacian are next investigated. Then, a different BEM-based algorithm is developed for time domain simulation of the response of dynamic systems with Caputo-type fractional Laplacian terms. The analog equation is constructed with the unknown load, which is used in calculation of the fractional Laplacian of the response. A discretization and numerical integration scheme are then employed for estimating the response.

It is shown that a frequency domain analysis of a nonlinear fractional diffusion equation

with stochastic excitation can be conducted by a statistical linearization procedure. The approach is implemented by introducing non-orthogonal eigenfunctions of the fractional Laplacian of the response, which are transformed from the linear modes of the classical diffusion equation solution. Such a representation allows deriving an MDOF nonlinear ordinary differential equation, which is linearized in the mean square sense. Further, a simplified statistical linearization approximation method is proposed. The variance and the power spectral density of the response are then calculated by an iterative procedure.

Numerical results pertaining to linear and nonlinear systems exposed to periodic and stochastic excitation are provided to demonstrate the effectiveness of the proposed methods.

Acknowledgements

I would like to express my deepest gratitude to my advisor Professor Pol D. Spanos for his mentorship through my incredible years at Rice University. His patient guidance and unending encouragement pushed me to continue improving myself and exploring unrestrictedly new ideas. I am very grateful for this great experience he has offered.

I would also like to thank Professor Fathi H. Ghorbel, Professor Yildiz Bayazitoglu and Professor Richard A. Tapia for serving on my thesis committee and providing me with insightful feedback. Professor Ghorbel's lectures on nonlinear dynamics built a strong foundation for my research.

I also want to thank all my professors, instructors and friends at Rice University for making my life extremely enjoyable.

I would like to express my strong appreciation to Professor Wei Xu in Northwestern Polytechnical University for his help and support. Further, I wish to thank my friend Dr. Giovanni Malara in Mediterranea University of Reggio Calabria for his advice and cooperation in research work. Furthermore, I want to thank the China Scholarship Council for providing me financial aid to study in Rice University.

Finally, I would like to thank my parents Antong Jiao and Qingping Qu for their unconditional love and encouragement.

Table of Contents

Abstract	ii
Acknowledgements	iv
Table of Contents	v
List of Figures	vii
List of Tables	x
1. Introduction	1
1.1. Thesis Perspective.....	1
1.2. Thesis Outline.....	10
2. Mathematical Background	13
2.1. Preliminary Remark.....	13
2.2. Fractional Diffusion.....	14
2.3. The Fractional Laplacian.....	16
2.4. The Boundary Element Method.....	23
2.5. Statistical Linearization.....	25
3. The Boundary Element Method (Riesz-Marchaud) for Dynamic Systems with the Fractional Laplacian	28
3.1. Preliminary Remark.....	28
3.2. The Boundary Element Method Based Algorithm (BEMrm) for Static Problem...	28
3.3. BEMrm for Fractional Diffusion Equation.....	34
3.4. Synopsis.....	38
4. The Caputo-type Fractional Laplacian and the Boundary Element Method (Caputo)	39

4.1. Preliminary Remark.....	39
4.2. Property of the Caputo-type Fractional Laplacian.....	39
4.3. The Boundary Element Method Based Approach (BEMc) for Fractional Diffusion Equation.....	43
4.4. Evaluation of the Singular Integrals in the BEM discretization.....	47
4.5. Examples.....	48
4.6. Synopsis.....	51
5. Modal Expansion and Statistical Linearization Methods for Fractional Diffusion Equation.....	52
5.1. Preliminary Remark.....	52
5.2. The Non-Orthogonal Modal Expansion.....	52
5.3. Simplified Statistical Linearization Approximation.....	56
5.4. Complete Statistical Linearization Method.....	61
5.5. Examples.....	64
5.6. Synopsis.....	80
6. Concluding Remarks.....	82
References.....	86

List of Figures

Fig 1.1	Absolute values of $GL_j^{(\alpha)}$	6
Fig 2.1	The experiment of the rotating annulus to illustrate the anomalous diffusion.....	15
Fig 2.2	Evaluation of the fractional Laplacian based on Riesz-Marchaud and Caputo-type definition.....	21
Fig 2.3	Evaluation of the fractional Laplacian based on Riesz-Marchaud and Caputo-type definition on the whole axis.....	22
Fig 2.4	Relative difference of the evaluated fractional Laplacian at the point $x = 0$	22
Fig 2.5	Discretization of the beam into N equal elements.....	25
Fig 3.1	Discretization of the domain.....	29
Fig 3.2	The exact solution and BEMrm solution of Eq. (3.24) with order $\alpha = 1.9$ and $\alpha = 1.7$	33
Fig 3.3	Square Domain and internal points of Example 3.2.....	34
Fig 3.4	The rectangular domain with Dirichlet boundary condition.....	36
Fig 3.5	Standard deviation and the power spectral density of the response with white noise input and $\alpha = 1.9$	37
Fig 3.6	Standard deviation and the power spectral density of the response with white noise input and coefficient $k = 0.1$	38
Fig 4.1	The coordinates on the considered domain.....	40
Fig 4.2	The element and local coordinate.....	48
Fig 4.3	Response calculated by BEMc and BEMrm with order $\alpha = 1.9$ and $\alpha = 1.7$ on a 10×5 rectangular plate.....	49
Fig 4.4	Response calculated by BEMc and BEMrm with $\alpha = 1.7$ on a 100×50 rectangular plate and a 1000×500 rectangular plate.....	50
Fig 4.5	Relative difference of the variance of the response calculated by BEMc and BEMrm with $\alpha = 1.7$	50
Fig 5.1	Power spectral density of the response when $\alpha = 1.9$ and $\alpha = 1.7$	65
Fig 5.2	Power spectral density of the response calculated by SL-1 and SL-2.....	66
Fig 5.3	Standard deviation and the power spectral density of the response with white	

noise input and fractional order 1.9.....	66
Fig 5.4 Standard deviation and the power spectral density of the response with white noise input and coefficient $k = 0.1$	67
Fig 5.5 Power spectrum of u calculated by BEMc simulation and SL-2 with white noise when $\alpha = 1.9$	67
Fig 5.6 Power spectrum of u calculated by BEMc simulation and SL-2 with white noise when $\alpha = 1.5$	68
Fig 5.7 Variance by BEMc simulation and SL-2 with white noise when $\alpha = 1.9$ and relative error.....	68
Fig 5.8 Variance by BEMc simulation and SL-2 with white noise when $\alpha = 1.5$ and relative error.....	69
Fig 5.9 Standard deviation and the power spectral density of the response with the fractional order 1.9.....	70
Fig 5.10 Standard deviation and the power spectral density of the response with the coefficient $k = 0.1$	70
Fig 5.11 Power spectrum of u calculated by BEMc simulation and SL-2 when $\alpha = 1.9$...	71
Fig 5.12 Power spectrum of u calculated by BEMc simulation and SL-2 when $\alpha = 1.5$...	71
Fig 5.13 Variance by BEMc simulation and SL-2 when $\alpha = 1.9$ and relative error.....	72
Fig 5.14 Variance by BEMc simulation and SL-2 when $\alpha = 1.5$ and relative error.....	72
Fig 5.15 Rectangular domain with mixed boundary condition.....	73
Fig 5.16 Standard deviation and the power spectral density of the response with mixed boundary conditions and fractional order 1.9.....	77
Fig 5.17 Standard deviation and the power spectral density of the response with mixed boundary conditions and $k = 0.1$	78
Fig 5.18 Power spectrum of u calculated by BEMc simulation and SL-2 with mixed boundary conditions when $\alpha = 1.9$	78
Fig 5.19 Power spectrum of u calculated by BEMc simulation and SL-2 with mixed boundary conditions when $\alpha = 1.5$	79
Fig 5.20 Variance by BEMc simulation and SL-2 with mixed boundary conditions when $\alpha = 1.9$ and relative error.....	79

Fig 5.21 Variance by BEMc simulation and SL-2 with mixed boundary conditions when $\alpha = 1.5$ and relative error.....	80
---	----

List of Tables

Table 3.1 Internal values computed by SBM and BEMrm when $\alpha = 1.9$	34
Table 3.2 Internal values computed by SBM and BEMrm when $\alpha = 1.5$	34

Chapter 1

Introduction

1.1 Thesis Perspective

Fractional calculus pertains to the theory of integrals and derivatives of arbitrary order. Although this theory is named fractional, the order could actually be any number: fractional, irrational, or complex. The idea of non-integer order derivatives was first discussed by Leibniz when the classical calculus theory was just established. For centuries, the theory of fractional calculus was treated merely as a pure mathematical topic, until recent decades when many authors have pointed out that the integrals and derivatives of non-integer order are suitable for the description of non-local properties of various real materials.

Since the first comment by Leibniz, many mathematicians, including Euler, Laplace, Fourier, Liouville and Riemann made contributions to the theory about non-integer derivatives and integrals from different approaches. This fact led to different definitions of fractional derivatives and integrals (Kilbas, Srivastava and Trujillo, 2006. Miller and Ross, 1993). From the perspective of dynamics, in this thesis, the fractional derivatives are defined via the Fourier transform in the frequency domain. Nevertheless, the mostly used definitions, such as Riemann-Liouville derivative and Grunwald-Letnikov derivative, can be regarded as being defined in the time domain.

Specifically, the Fourier transform of a function $f(t), t \in \mathbb{R}$ is defined as

$$\hat{f}(\omega) = \mathbb{F}\{f(t), \omega\} = \int_{\mathbb{R}} f(t) e^{-i\omega t} dt. \quad (1.1)$$

And the inverse Fourier transform is

$$f(t) = \frac{1}{2\pi} \int_{\mathbb{R}} \hat{f}(\omega) e^{i\omega t} d\omega. \quad (1.2)$$

It is well known that the Fourier transform of the n -th derivative of $f(t)$ is

$$\mathbb{F}\left\{\frac{d^n}{dt^n} f(t), \omega\right\} = (i\omega)^n \hat{f}(\omega). \quad (1.3)$$

Note that, the generalized fractional derivative is expected to satisfy similar property as Eq. (1.3). Thus, in this thesis, an implicit definition of the fractional derivative is adopted.

The fractional derivative $D_+^\alpha f(t)$ with arbitrary order α is defined via the Fourier transform

$$\mathbb{F}\{D_+^\alpha f(t), \omega\} = (i\omega)^\alpha \hat{f}(\omega), \operatorname{Re} \alpha > 0, \quad (1.4)$$

where

$$(i\omega)^\alpha = \omega^\alpha [\cos(\alpha\pi/2) + i \sin(\alpha\pi/2)]. \quad (1.5)$$

Eq. (1.4) is actually satisfied by different kinds of definition of the fractional derivative.

A more common approach is to directly generalize the integer-order derivative with a fractional number. This is also a quite practical way, especially for a function in the bounded domain or interval. In this context, for a continuous function $f(t), t \in [a, b]$, the integer-order derivatives, if exist, are expressed as

$$f'(t) = \lim_{h \rightarrow 0} \frac{f(t) - f(t-h)}{h}, \quad (1.6)$$

$$f''(t) = \lim_{h \rightarrow 0} \frac{f'(t) - f'(t-h)}{h} = \lim_{h \rightarrow 0} \frac{f(t) - 2f(t-h) + f(t-2h)}{h^2}, \quad (1.7)$$

and, by induction, for a positive integer n ,

$$f^{(n)}(t) = \lim_{h \rightarrow 0} \frac{1}{h^n} \sum_{j=0}^n (-1)^{-j} \binom{n}{j} f(t-jh), \quad (1.8)$$

where

$$\binom{n}{j} = \frac{n(n-1)(n-2)\cdots(n-j+1)}{j!} \quad (1.9)$$

is the binomial coefficient.

Next, attempt to generalize the derivative in Eq. (1.8) for a positive real number α , such

that $n - 1 < \alpha < n$. Take $h = (t - a)/n$, so that when $h \rightarrow 0, n \rightarrow \infty$. Then, a formal generalization from Eq. (1.8) is attained.

$${}^{GL}D_{a+}^{\alpha} f(t) = f^{(\alpha)}(t) = \lim_{h \rightarrow 0+} \frac{1}{h^{\alpha}} \sum_{j=0}^{\lfloor \frac{t-a}{h} \rfloor} (-1)^j \binom{\alpha}{j} f(t - jh), \quad (1.10)$$

where

$$\binom{\alpha}{j} = \frac{(-1)^{j-1} \alpha \Gamma(j - \alpha)}{\Gamma(1 - \alpha) \Gamma(j + 1)}. \quad (1.11)$$

is the generalized binomial coefficient.

Such a derivative is named the Grunwald-Letnikov fractional derivative and is denoted by ${}^{GL}D_{a+}^{\alpha} f(t)$. The Grunwald-Letnikov derivative is quite useful in applications and numerical analysis as it can be calculated by finite difference scheme with proper truncation. That is, choose a small step-size h and remove the limit symbol in Eq. (1.10).

$${}^{GL}D_{a+}^{\alpha} f(t) = \frac{1}{h^{\alpha}} \sum_{j=0}^{\lfloor \frac{t-a}{h} \rfloor} (-1)^j \binom{\alpha}{j} f(t - jh). \quad (1.12)$$

This is a finite difference algorithm that is widely used for the calculation of the fractional derivative.

Note that other definitions and expressions of fractional derivatives and integrals (Monje, Chen, Vinagre, Xue and Feliu-Batlle, 2010) are also commonly used. For example, the Riemann-Liouville integral and derivative are widely used by mathematicians for theoretical analysis. They are defined as,

$${}^{RL}I_{a+}^{\alpha} f(t) = \frac{1}{\Gamma(\alpha)} \int_a^t \frac{f(\tau)}{(t - \tau)^{1-\alpha}} d\tau, \quad \alpha > 0. \quad (1.13)$$

$${}^{RL}D_{a+}^{\alpha} f(t) = \frac{d}{dt} {}^{RL}I_{a+}^{1-\alpha} f(t) = \frac{1}{\Gamma(1-\alpha)} \frac{d}{dt} \int_a^t \frac{f(\tau)}{(t - \tau)^{\alpha}} d\tau, \quad 0 < \alpha < 1, \quad (1.14)$$

and

$${}^{RL}D_{b-}^{\alpha} f(t) = -\frac{1}{\Gamma(1-\alpha)} \frac{d}{dt} \int_t^b \frac{f(\tau)}{(t-\tau)^{\alpha}} d\tau, \quad (1.15)$$

where ${}^{RL}D_{a+}^{\alpha} f(t)$ and ${}^{RL}D_{b-}^{\alpha} f(t)$ are called the left and right Riemann-Liouville fractional derivative respectively.

Caputo derivative is widely used in engineering applications (Rossikhin and Shitikova, 1997, 2000, 2001, 2006, 2010), as it allows the formulation of practical initial conditions for differential equations with a fractional derivative. Specifically,

$${}^c D_{a+}^{\alpha} f(t) = \frac{1}{\Gamma(n-\alpha)} \int_a^t \frac{f^{(n)}(\tau)}{(t-\tau)^{\alpha-n+1}} d\tau. \quad (1.16)$$

Another quite convenient property of the Caputo definition is that the Caputo derivative of a constant is 0, whereas the Riemann-Liouville derivative and Grunwald-Letnikov derivative do not share this property.

$${}^{GL}D_{a+}^{\alpha} 1 = \frac{(t-a)^{-\alpha}}{\Gamma(1-\alpha)}, \quad (1.17)$$

$${}^{RL}D_{a+}^{\alpha} 1 = \frac{(t-a)^{-\alpha}}{\Gamma(1-\alpha)}, \quad (1.18)$$

$${}^c D_{a+}^{\alpha} 1 = 0. \quad (1.19)$$

Note that, the Grunwald-Letnikov, Riemann-Liouville and Caputo derivative all satisfy the Fourier transform property as in Eq. (1.4). More information about different expressions of the fractional derivatives and integrals can be seen in Samko (1993).

In the multi-dimensional case, the theory of the fractional calculus becomes more complex, as there arise partial fractional derivative $\frac{\partial^{\alpha} f}{\partial x_k^{\alpha}}$, and mixed fractional derivative

$$\frac{\partial^{\alpha_1 + \alpha_2} f}{\partial x_1^{\alpha_1} \partial x_2^{\alpha_2}},$$

as well as the corresponding fractional integrals. Another approach is to

introduce the fractional powers $(-\Delta)^{\alpha/2}$ of the Laplace operator that is

$$\Delta = \frac{\partial^2}{\partial x_1^2} + \dots + \frac{\partial^2}{\partial x_n^2}.$$

Such an operator, named the fractional Laplacian or Reisz derivative (Pozrikidis, 2016), is the main topic of this thesis. Same as one-dimensional fractional

derivative, there are different expressions of the fractional Laplacian. In this thesis, the fractional Laplacian of a scalar function $u(\mathbf{x})$, $\mathbf{x} \in \mathbb{R}^d$, is defined also implicitly by Fourier transform. That is,

$$\mathbb{F}\{(-\Delta)^{\alpha/2} u(\mathbf{x}), \boldsymbol{\omega}\} = |\boldsymbol{\omega}|^\alpha \mathbb{F}\{u(\mathbf{x}), \boldsymbol{\omega}\}, \quad (1.20)$$

where $\boldsymbol{\omega} \in \mathbb{R}^d$ are the spatial frequencies, and the Fourier transform is defined as

$$\mathbb{F}\{u(\mathbf{x}), \boldsymbol{\omega}\} = \int_{\mathbb{R}^d} u(\mathbf{x}) e^{-i\mathbf{x}\cdot\boldsymbol{\omega}} d\mathbf{x}. \quad (1.21)$$

Besides the implicit definition of the fractional Laplacian in Eq. (1.20), a number of different representations and definitions of the fractional Laplacian have been introduced from different approaches (Caffarelli and Silvestre, 2007). Most of these definitions contain hyper-singular kernels in the integral representation and hence are difficult to deal with in numerical analysis. Among them, the Caputo-type definition is of great importance in this thesis, as it includes boundary information and eases the hyper-singularity. Thus, such a representation is very suitable for application. More information about the fractional Laplacian will be provided in Chapter 2.

Despite the considerable development of the fractional calculus as mentioned above, this theory has not received much attention in science and engineering until recent decades. One of the reasons is that the fractional derivative is proved to be able to serve as a great instrument to describe the memory and nonlocal properties of various materials and processes (Petráš, 2011). While the integer-order derivatives demonstrate only the local state of the system, the fractional order derivatives depend on the information of a neighborhood. Such a property is called “fading-memory”.

Recall the Grunwald-Letnikov derivative in Eq. (1.8). It is shown that the value of the fractional derivative ${}^{GL}D_{a+}^\alpha f(t_0)$ not only depends on the points in the neighbor of t_0 , but also on the whole interval $[a, t_0]$. Such is called the nonlocal property. Further, the coefficients, by the properties of the generalized binomial coefficients, are

$$GL_j^{(\alpha)} = (-1)^j \binom{\alpha}{j} = \binom{j-\alpha-1}{j} = \frac{\Gamma(j-\alpha)}{\Gamma(-\alpha)\Gamma(j+1)}. \quad (1.22)$$

These coefficients depend only on the order α and number j . As an example, for the order $\alpha = 1.75$, the absolute values of $GL_j^{(\alpha)}$ are plotted in Fig. 1.1.

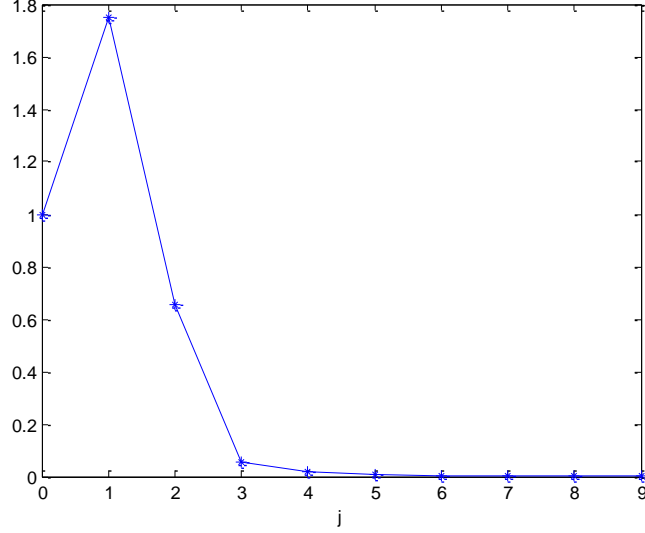


Fig. 1.1. Absolute values of $GL_j^{(\alpha)}$.

It is seen that, independent by the step size h , the coefficient $GL_j^{(\alpha)}$ always concentrates to 0 as j increases. Actually, for any $\alpha > 0$, it can be proved that $GL_j^{(\alpha)} \rightarrow 0$ as $j \rightarrow \infty$. This implies that for large value of t , the coefficients $GL_j^{(\alpha)}$ corresponding to values of the function near the initial point have very little influence in the value of the derivate ${}^{GL}D_{a+}^{\alpha}f(t)$. This fact indicates that the value of the fractional derivative depends mainly on a “recent past”, i.e., the interval $[t_0 - L, t_0]$, where L is the length of “memory”. Hence, the fractional derivative neither shows a local nor a global information of the system, but a non-local information. Such property is called the “fading memory” of the fractional derivative. This is the reason that the fractional derivative is quite suitable for the description of nonlocal properties of various real materials and processes.

Considering the nonlocal property of the fractional Laplacian, take a one-dimensional case as an example. On the interval $[-L, L]$, the fractional Laplacian can be defined in terms of the left and right Riemann-Liouville fractional derivatives (Huang and Oberman, 2014, 2016),

$$(-\Delta)^{\alpha/2} u(x) = \frac{{}^{RL}D_{L-}^{\alpha} u(x) + {}^{RL}D_{-L+}^{\alpha} u(x)}{2 \cos(\alpha\pi/2)}, \alpha \neq 1. \quad (1.23)$$

Thus, the operator also emphasizes a nonlocal information of the system.

New models involving the fractional integrals and derivatives have been developed and applied successfully in many fields of research, including viscoelasticity mechanics (Rossikhin, Shitikova, Chao and Persada, 2008. Rossikhin, Shitikova, and Ngenzi, 2015), electrical engineering and fractional control theory. A detailed survey of applications of the fractional calculus in various fields of science is given in references such as Podlubny (1998). Especially, the fractional Laplacian is widely used in the modelling of various dynamic systems, including nonlocal wave equations (D'Abbicco and Ebert, 2014), nonlocal heat equations, phase transitions, crystal dislocation, and finance problems. The fractional Laplace operator can be seen as the generator of Levy flights, or α -stable processes, and hence is suitable to describe unusual diffusion process when a particle moves randomly in space subjecting to random processes that allow long jumps (Zoja, Rosso and Kardar, 2007). Such nonlocal diffusions, or called anomalous diffusions, which incorporate long range interactions, are phenomena that can be found in a turbulent fluid system (Chen 2006). Another example exhibiting anomalous diffusion is cell migration (Turner, Wick, Hanel, Sedivy and Huber, 2003). Several experiments about anomalous diffusion can be found in Vlahos, Isliker, Kominis and Hizanidis (2008), where the Continuous Time Random Walk (CTRW) was discussed as a model for anomalous diffusion. The fractional diffusion equation was then derived from the CTRW equation. In this regard, note that Abe and Turner (2005) have revisited Einstein's theory of Brownian motion in the context of anomalous diffusion, and have shown how the fractional Laplacian can be introduced in the generalized theory.

Corresponding to the application of the fractional calculus, many researches have been reported on the numerical analysis of the differential equation with the fractional derivative, i.e., the fractional differential equation. Nonlinear random vibration of a single-degree-of-freedom system with damping modeled by a fractional derivative was investigated by Huang and Jin (2009) via a stochastic averaging procedure. Spanos and

Malara (2014) proposed a statistical linearization method for analysis of the nonlinear random vibrations of beams with fractional derivative element. However, most of the recent works have focused on the time-fractional derivatives, while fewer reports have been provided on the space-fractional derivatives. Perhaps, one of the reasons for this trend is that many existing definitions and analysis theories are only feasible for one-dimensional case and will become quite complicated and time-consuming for the multi-dimensional problem. The space-fractional derivative, especially the fractional Laplacian, due to the multiple variables in the system and nonlocal property, are always much challenging for numerical analysis.

Huang and Oberman (2014) derived a finite difference/quadrature evaluation for the fractional Laplacian. The method works for both bounded and unbounded domain, but only in one-dimension. Varlamov (1999) investigated the existence and uniqueness of the solution of a nonlinear fractional heat equation. Vazquez (2014) explained the general existence and uniqueness theory of the fractional porous medium equation. Chen and Pang (2016) introduced an implicit definition of the fractional Laplacian, and applied the Singular Boundary Method to a fractional Laplace equation. On a bounded domain, the study of the fractional Laplacian becomes more complicated. In contrast to the standard Laplace operator, the probabilistic and physical interpretation of the boundary condition of the system containing the fractional Laplacian has not been well established. This is especially true for the numerical methods, where truncation of the operator in a bounded domain is always required. Clearly different representations may lead to different results. Guan and Ma (2005) studied the boundary value problem for the Schrodinger type equation with a fractional Laplacian. Given that a general analytic solution, to the author's knowledge, is not available, the need of numerical algorithm of dynamic system with the fractional Laplacian is clear.

Following the directions of the existing methods for numerical analysis of time-fractional differential equation, the Boundary Element Method (Katsikadelis, 1990, 1991, 1994. Katsikadelis and Sapountzakis, 1991. Sapountzakis and Katsikadelis, 1999, 2000)) and the statistical linearization methods (Roberts and Spanos, 2003) are generalized for

dynamic systems endowed with the fractional Laplacian in this thesis.

Developed by Bezine, Stern, Katsikadelis and many other authors, the Boundary Element Method (BEM) is one of the most popular computational method in engineering applications with considerable effectiveness and accuracy. It is a technique to analyze the behavior of the various systems subjected to external loads. The BEM requires the fundamental solution of the governing equation and uses an integral representation of the solution as a continuous mathematical expression. For certain problems, discretization in the BEM procedure involves only the boundary, which makes the numerical computation easier. Based on the BEM, the Analog Equation Method (AEM) is developed (Katsikadelis and Nerantzaki, 1994, 1996). According to this method, the actual problem, whose fundamental solution is not available, is converted into an equivalent linear problem with a simple fundamental solution. Then, the integral representation of the solution is conveniently established. In the equivalent problem, the geometry of the domain and the boundary conditions are conserved, whereas the unknown term to be evaluated numerically involves on algorithm. Recently, the BEM has been implemented in conjunction with Grunwald-Letnikov algorithm and Newmark numerical integration scheme for approximating the response of systems with time-fractional derivative, by Spanos and Malara (2014, 2017). In this thesis, a BEM-based approach is proposed to determine the response of a system governed by the fractional diffusion equation.

In the classical partial differential equation theories, separation of variables is often considered as an effective way to solve the system. The same strategy is considered for analysis of partial differential equation with the fractional Laplacian. A spectral decomposition definition of the fractional Laplace operator was investigated and applied in a time-space fractional diffusion equation in two dimensions with Dirichlet boundary conditions by Yang, Liu and Turner (2011), and Yang, Turner, Liu and Ilic (2011). However, note that such a representation does not satisfies the Fourier transform property. Therefore, it is different from the implicit definition of the fractional Laplacian used in this thesis. If the separation of variables, namely modal expansion can be introduced in a nonlinear stochastic system, the method of statistical linearization can be proved to be a

quite useful approximate technique. As mentioned before, the statistical linearization method has already been applied to estimate the response statistics for fractional partial differential equations with time-fractional derivatives. The nonlinear response of a single-degree-of-freedom system was investigated by Spanos and Evangelatos (2010). Malara and Spanos (2017) considered the problem of determining the response of a plate endowed with fractional derivative element via a statistical linearization procedure. In this thesis, a modal expansion of the fractional Laplacian is first introduced. Then, based on this expression, a simplified approximation and complete statistical linearization method have been proposed, which allow calculating approximately the response statistics.

1.2 Thesis Outline

This thesis has 6 chapters related to numerical analysis of dynamic system endowed with fractional Laplacian. The main contributions are: Boundary Element methods for the dynamic systems endowed with the fractional Laplacian based on the Riesz-Marchaud definition and Caputo-type definition, a method to obtain modal expansion of the fractional Laplacian, and statistical linearization for frequency domain analysis of the dynamic systems with the fractional Laplacian.

Chapter 1 provides a perspective and outline of the thesis.

Chapter 2 introduces the mathematical background of the fractional Laplacian and the algorithms that can be generalized and implemented to dynamic systems endowed with the fractional Laplacian in the context. A brief review about the progress of fractional diffusion and application of the fractional Laplacian is provided first. Next, different representations of the fractional Laplacian and the examples are discussed. Different from the standard Laplace operator that involves the summation of all the second derivatives of the variables, and hence from certain directions, in this thesis, the fractional Laplacian is defined via the Fourier transform. While different representation of the operator in the space domain are presented and illustrated, the Caputo-type representation is significant

as it includes naturally the boundary conditions. Such properties make it useful in the application of a bounded domain problem. Calculation of the Riesz-Marchaud and Caputo-type representation of the fractional Laplacian is provided. Then, the BEM and the statistical linearization method are briefly illustrated, for the dynamic systems with time-fractional derivatives, as they will be further developed for the fractional Laplacian in the following chapters.

In Chapter 3, a Boundary Element Method-based algorithm (BEM_{rm}) is introduced to approximate the response of dynamic systems with the fractional Laplacian. The algorithm is constructed by utilizing the integral representation of the fractional Poisson equation solution, as the analog equation, in which the unknown constants are determined by the BEM. The value of the fractional Laplacian of the response can then be updated progressively. Different examples are presented to demonstrate the proposed algorithm.

In Chapter 4, first the limitation of the Caputo-type fractional Laplacian when the order of the operator tends to 2 is considered. A proof is given to show that the limit of the fractional Laplacian is just the standard Laplace operator, which is a property that is expected as the fractional Laplacian is considered as generalization of the Laplace operator. Then, based on such kind of representation, a BEM-based algorithm (BEM_c) is developed for the dynamic systems with the fractional Laplacian. The difference of BEM_c from BEM_{rm} is that, instead of the fractional Poisson equation, the standard Poisson equation is chosen as the analog equation. The algorithm itself emphasizes the nonlocal property of the fractional Laplacian.

Chapter 5 proposes a method to obtain modal expansion of the fractional Laplacian. The expansion is established using the Caputo-type representation of the fractional Laplacian, and hence includes the information of the boundary conditions. The non-orthogonal eigenfunctions of the fractional Laplacian are transformed from the linear modes of classical diffusion equation solution. Based on the novel modal expansion, frequency domain analysis of fractional differential equation is available. Further, statistical linearization based approaches are proposed for determining the response statistics of a

nonlinear fractional diffusion/heat equation. The new representation allows deriving a system of nonlinear fractional ordinary differential equations, which is linearized in a stochastic mean square sense. Then, the response statistics and power spectral density are calculated by an iterative procedure. For a smaller order, to ensure the accuracy, the non-orthogonality must be considered. The methods proposed, even though it provides symbolic expressions, require discretization of the domain. It is also pointed out that, although the proposed eigenfunctions are not orthogonal to each other in theory, in the numerical implementation, they can be assumed to be orthogonal so that the numerical calculation would consume less time. Further, the proposed algorithms based on the Caputo-type fractional Laplacian are applied to linear and nonlinear fractional diffusion equation with different boundary conditions. Numerical results are presented to demonstrate the efficiency of the methods, as well as detail process of an example. Comparisons and parameter studies are provided for elucidating the influence of the order of the fractional Laplacian.

Chapter 6 provides concluding remarks and concepts of future work. Based on the Caputo-type representation of the fractional Laplacian and on the non-orthogonal modal expansion, other numerical methods, such as deterministic linearization, may be available for the analysis of the dynamic systems with the fractional operator. It is noted that the proposed methods can also be implemented for different kinds of fractional partial differential equations, such as the fractional Porous Medium Equation and the fractional wave equation.

Chapter 2

Mathematical Background

2.1 Preliminary Remark

This chapter introduces requisite mathematical background on the fractional Laplacian and the algorithm that can be further developed and generalized in the following chapters. One of the applications of the fractional Laplacian is to model the anomalous diffusion process. A brief progress of the theory about the fractional diffusion is first provided. Replacing the standard Laplace operator in the heat/diffusion equation with the fractional Laplacian, the fractional heat/diffusion recently has received attention both in mathematic theory and engineering. Such a system is a generalization of the classical diffusion equation (Luchko, 2015). Determining the response of a dynamic system with the fractional Laplacian is a daunting task, as analytical solutions, to the authors' knowledge, are not available. Compared with the partial differential equation endowed with time-fractional derivative, the fractional diffusion equation is more challenging for the numerical analysis, due to the multiple spatial variables and nonlocal properties of the fractional Laplacian operator.

Next, some widely used expressions on the fractional Laplacian are discussed, amongst which the Caputo-type operator receives particular attention. It simplifies the kernel function in the singular integral representation and includes the boundary conditions and hence is of great value in application.

In Section 2.4 and 2.5, two techniques that have been proposed for determining the dynamic systems with fractional derivative operator are briefly discussed that involve the Boundary Element Method (BEM) based Monte Carlo simulation and statistical linearization. In the later chapters, these two techniques are further generalized for the dynamic system with the fractional Laplacian element. Katsikadelis and Tsiatas (2003,

2004), Spanos and Malara (2014) have made contributions to the BEM of the dynamic systems with time-fractional derivative. The key to such an algorithm is to find a proper analog equation (Katsikadelis and Babouskos, 2007, 2009, 2010) that will be convenient for numerical analysis by the BEM. The statistical linearization method is explained for one kind of fractional partial differential equations. Such method, developed by Spanos and Malara (2014, 2017), is to recast the governing equation, through a modal expansion, into a set of ordinary differential equations, where the statistical linearization method is applied to estimate the statistics of the response. The BEM and statistical linearization method are briefly described, and details can be seen in the reference. The time-fractional derivatives in this chapter are all defined on the positive real axis and is calculated by the Grunwald-Letnikov algorithm.

2.2 Fractional Diffusion

The mathematical models of heat conduction and diffusion play important roles not only in theory but also in physics and engineering (Bayazıtıođlu and Özişik, 1988). They also have made great progress in biology, economics and social sciences. Recently, in many natural systems, diffusion processes, which do not follow the classical theory have been observed. Such a phenomenon is referred as anomalous diffusion, where the space scale of the propagation of the distribution is not proportional to $t^{1/2}$ as in the Brownian motion, because of the diffusion being either faster or slower.

Anomalous diffusion is exhibited in the motion of tracer particles in turbulent flows, where particles may stay for a long time in a relatively small area, and there are particles that are carried over large distances very quickly. Such phenomenon can also be found in cell migration, chaotic dynamics and porous glasses (Stapf, Kimmich and Seitter, 1995). Solomon, Weeks and Swinney (1994) and Weeks, Urbach and Swinney (1996) used the experiment of a highly turbulent rotating annulus to illustrate the difference between normal and anomalous diffusion. Details of the experiment can be found in Vlahos, Isliker, Kominis and Hizanidis (2008).

In the last decade, there has been a number of works focusing on the use of the fractional Laplacian to replace the standard Laplace operator in order to model anomalous diffusion (D'Elia and Gunzburger, 2013). Abe and Thurner (2005) revisited Einstein's theory of Brownian motion in the context of anomalous diffusion and showed how the fractional Laplacian is introduced in the generalized diffusion equation:

$$\dot{u} + (-\Delta)^{\alpha/2} u = 0. \quad (2.1)$$

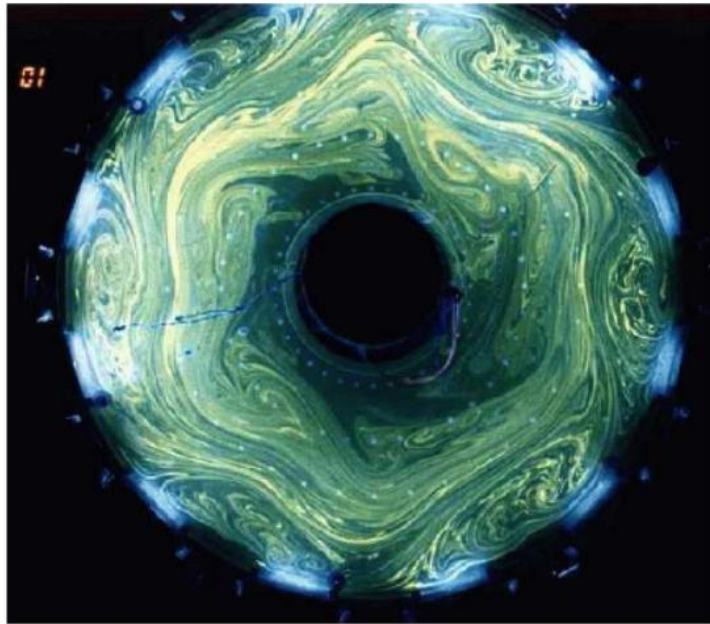


Fig. 2.1. The experiment of the rotating annulus to illustrate the anomalous diffusion. (From Vlahos, Isliker, Kominis and Hizanidis (2008))

In the work of Vlahos and Isliker, etc., it is also shown how fractional diffusion equations is derived starting from random walk models. Some researches indicate that the fractional Laplacian is actually the infinitesimal generator of Levy process that includes jumps and long-distances interactions. Therefore, the fractional diffusion equation is suitable to be used to model such unusual diffusion process where a particle can move randomly in the space subjecting to a random process that allows long jumps.

Starting from the linear fractional diffusion equation, Vazquez (2012, 2014, 2017) contributes a lot to the combination of the anomalous and nonlinear diffusion equation.

The Fractional Porous Medium Equation (del Teso, 2014) is hence introduced,

$$\dot{u} + (-\Delta)^{\alpha/2} (u^m) = 0, \quad (2.2)$$

as well as the fractional reaction-diffusion equation

$$\dot{u} + (-\Delta)^{\alpha/2} u = f(u). \quad (2.3)$$

Utilizing the nonlocal property of the operator, the fractional Laplacian is also applied in the wave model (Oh and Tzvetkov, 2017. Treeby and Cox, 2010), crystal dislocation and nonlocal phase transition. More notes about application of the fractional Laplacian can be found in Bucur and Valdinoci (2016).

2.3 The Fractional Laplacian

Denoted by $(-\Delta)^{\alpha/2}$, the fractional Laplacian is a spatial integro-differential operator that can describe the spatial nonlocality and power law behaviors of mathematics and engineering problems. It is a generalization of the standard Laplace operator $\Delta = \frac{\partial^2}{\partial x_1^2} + \dots + \frac{\partial^2}{\partial x_n^2}$. It is well known that the Laplace operator of a scalar function $u(\mathbf{x})$, $\mathbf{x} \in \mathbb{R}^d$ satisfies the following Fourier transform:

$$\mathbb{F}\{-\Delta u(\mathbf{x}), \boldsymbol{\omega}\} = |\boldsymbol{\omega}|^2 \mathbb{F}\{u(\mathbf{x}), \boldsymbol{\omega}\} = |\boldsymbol{\omega}|^2 \hat{u}(\boldsymbol{\omega}), \quad (2.4)$$

where $\boldsymbol{\omega} \in \mathbb{R}^d$ are the spatial frequencies, and $|\cdot|$ denotes the norm of $\boldsymbol{\omega}$. The Fourier transform is defined as:

$$\hat{u}(\boldsymbol{\omega}) = \mathbb{F}\{u(\mathbf{x}), \boldsymbol{\omega}\} = \int_{\mathbb{R}^d} u(\mathbf{x}) e^{-i\mathbf{x}\cdot\boldsymbol{\omega}} d\mathbf{x}. \quad (2.5)$$

To ensure the similar property of the generalized operator, the fractional Laplacian $(-\Delta)^{\alpha/2}$ is defined implicitly via Fourier transform. That is,

$$\mathbb{F}\{(-\Delta)^{\alpha/2} u(\mathbf{x}), \boldsymbol{\omega}\} = |\boldsymbol{\omega}|^\alpha \hat{u}(\boldsymbol{\omega}). \quad (2.6)$$

Besides the implicit definition, there are many different explicit expressions of the fractional Laplacian listed below. One of the most used expression for the theoretical study is given by a singular integral, sometimes called the Riesz-Marchaud type

definition,

$$(-\Delta)^{\alpha/2} u(\mathbf{x}) = C_1(d, \alpha) \int_{\mathbb{R}^d} \frac{u(\mathbf{x}) - u(\mathbf{y})}{|\mathbf{x} - \mathbf{y}|^{d+\alpha}} d\mathbf{y}, \quad 0 < \alpha < 2, \quad (2.7)$$

where $C_1(d, \alpha)$ is a constant dependent on the order α and dimension d , and $|\cdot|$ denotes the norm of $(\mathbf{x} - \mathbf{y})$. However, in the kernel function, the denominator is a power function with the power $(d + \alpha)$ greater than the dimension d , which makes it a “hypersingular” kernel.

Another representation of the operation $(-\Delta)^{\alpha/2}$ can also be given by a hypersingular integral, as well as finite difference operator. Specifically,

$$(-\Delta)^{\alpha/2} u(\mathbf{x}) = C_2(d, \alpha) \int_{\mathbb{R}^d} \frac{\Delta_{\mathbf{y}}^l u(\mathbf{x})}{|\mathbf{y}|^{d+\alpha}} d\mathbf{y}, \quad 0 < \alpha < l, \quad (2.8)$$

where $C_2(d, \alpha)$ is a constant and $\Delta_{\mathbf{y}}^l u(\mathbf{x}) = \sum_{k=0}^l (-1)^k \binom{l}{k} u(\mathbf{x} - k\mathbf{y})$.

These versions are defined for the operator acts in \mathbb{R}^d . In a bounded domain, however, the so-called restricted fractional Laplacian is considered in this thesis, which acts on the functions defined in the bounded domain Ω and extended by zero to the complement. Thus, such operators are just the fractional Laplacian defined in the whole space and equal to 0 outside Ω .

As a special case, for one-dimensional function $u(x)$ in the interval $[-L, L]$, a representation of the fractional Laplacian can be derived,

$$(-\Delta)^{\alpha/2} u(x) = \frac{D_{L-}^{\alpha} u(x) + D_{-L+}^{\alpha} u(x)}{2 \cos(\alpha\pi/2)}, \quad \alpha \neq 1. \quad (2.9)$$

Note that, through the Grunwald-Letnikov fractional derivative, a finite difference method (Huang and Oberman, 2014) can be established for the calculation of such an expression. Further, it is an expression that can be applied for real problems in a bounded domain. However, despite the convenience of the formula, this expression is restricted in one dimension.

It is worth noting that the spectral fractional Laplacian, also defined in a bounded domain, is not considered in this thesis, as it does not satisfy the implicit definition in the thesis. The spectral decomposition is to define the fractional Laplacian in a bounded domain $\Omega \in \mathbb{R}^d$. Let (λ_k, ϕ_k) be the eigenpairs of the negative Laplace operator:

$$-\Delta \phi_k = \lambda_k \phi_k. \quad (2.10)$$

Subject to appropriate boundary condition, which ensure that all the λ_k are non-negative and that $\{\phi_k\}$ is a complete orthonormal basis. Then if $u(\mathbf{x}) = \sum_{k=1}^{\infty} C_k \phi_k(\mathbf{x})$, the fractional Laplacian is defined as

$$(-\Delta)^{\alpha/2} u(\mathbf{x}) = \sum_{k=1}^{\infty} C_k \lambda_k^{\alpha/2} \phi_k(\mathbf{x}). \quad (2.11)$$

Note that, this decomposition does not satisfy the Fourier transform Eq. (2.3). In this regard, consider a simple counterexample.

Let $f(x) = \phi_1(x)$, i.e. $C_1 = 1, C_k = 0$ for all $k \neq 1$. Then,

$$-\Delta f = -\Delta \phi_1 = \lambda_1 \phi_1. \quad (2.12)$$

Take the Fourier transform of the standard Laplace operator and the spectral decomposition expression of Eq. (2.8),

$$\mathbb{F}\{-\Delta f(x), \omega\} = |\omega|^2 \mathbb{F}\{f(x), \omega\} = |\omega|^2 \hat{f}(\omega). \quad (2.13)$$

Further, note that

$$\begin{aligned} \mathbb{F}\{(-\Delta)^{\alpha/2} f(x), \omega\} &= \mathbb{F}\{\lambda_1^{\alpha/2} \phi_1, \omega\} \\ &= \mathbb{F}\{\lambda_1^{\alpha/2-1} \lambda_1 \phi_1, \omega\} = \mathbb{F}\{\lambda_1^{\alpha/2-1} (-\Delta f), \omega\} \\ &= \lambda_1^{\alpha/2-1} \mathbb{F}\{-\Delta f, \omega\} = \lambda_1^{\alpha/2-1} |\omega|^2 \hat{f}(\omega), \end{aligned} \quad (2.14)$$

which is different to the Eq. (2.3). Thus, this decomposition is not the fractional Laplacian discussed in this thesis. Instead, a new expansion will be derived in Chapter 5.

In 2004, Chen and Holm introduced an operator as a composition of the Riesz potentials and Laplacian which is critical in this thesis. Specifically, the operator is defined as

$$(-\Delta)^{\alpha/2} u(\mathbf{x}) = I_d^{2-\alpha} (-\Delta u(\mathbf{x})), 1 < \alpha < 2. \quad (2.15)$$

The Riesz potential on a bounded convex domain Ω in \mathbb{R}^d is defined as

$$I_d^{2-\alpha} \varphi(\mathbf{x}) = c(\alpha) \int_{\Omega} \frac{\varphi(\xi)}{|\mathbf{x}-\xi|^{d+\alpha-2}} d\xi, \quad (2.16)$$

where ξ is the coordinate in the domain Ω and

$$c(\alpha) = \frac{\Gamma[(d-2+\alpha)/2]}{\pi^{d/2} 2^{2-\alpha} \Gamma((2-\alpha)/2)}. \quad (2.17)$$

Such a representation is called the Caputo-type fractional Laplacian. Note that the Riesz potential works as the inverse operator of the fractional Laplacian. In the case of sufficiently smooth functions $f(\mathbf{x})$ defined in \mathbb{R}^d (if the function is defined on a bounded domain Ω , set $u(\mathbf{x}) = 0, \mathbf{x} \in \mathbb{R}^d \setminus \Omega$), the Fourier transform of the Riesz potential is

$$\mathbb{F}\{I_d^s f(\mathbf{x}), \boldsymbol{\omega}\} = |\boldsymbol{\omega}|^{-s} \hat{f}(\boldsymbol{\omega}). \quad (2.18)$$

Then, based on the Fourier transform of the Riesz potential and of the standard Laplace operator one finds that

$$\mathbb{F}\{I_d^{2-\alpha} [-\Delta u(\mathbf{x})], \boldsymbol{\omega}\} = |\boldsymbol{\omega}|^{\alpha-2} \mathbb{F}\{-\Delta u(\mathbf{x})\} = |\boldsymbol{\omega}|^{\alpha} \hat{u}(\boldsymbol{\omega}), \quad (2.19)$$

which satisfies the implicit definition. Next an example are provided to demonstrate the computation of the Caputo-type fractional Laplacian.

Example 2.1 The first example involves the function $u(x) = e^{-x^2}, x \in \mathbb{R}$. The fractional Laplacian of u at $x = 0$ can be obtained directly from the inverse Fourier transform, since

$$\mathbb{F}\{u(x), \omega\} = \sqrt{\pi} e^{-\frac{\omega^2}{4}}. \quad (2.20)$$

By the implicit definition Eq. (2.6),

$$\begin{aligned}
(-\Delta)^{\alpha/2} u(0) &= \frac{1}{2\pi} \int_{-\infty}^{+\infty} |\omega|^\alpha \sqrt{\pi} e^{-\frac{\omega^2}{4}} d\omega \\
&= \frac{1}{\sqrt{\pi}} \int_0^{+\infty} \omega^\alpha e^{-\frac{\omega^2}{4}} d\omega = 2^\alpha \Gamma\left(\frac{1+\alpha}{2}\right) / \sqrt{\pi}. \tag{2.21}
\end{aligned}$$

And by the Caputo-type representation Eq. (2.15), same value can be obtained.

$$\begin{aligned}
(-\Delta)^{\alpha/2} u(0) &= I_1^{2-\alpha} (-\Delta u(y)) \Big|_{y=0} \\
&= c(\alpha) \int_{-\infty}^{+\infty} \frac{-u_{xx}(x)}{|0-x|^{\alpha-1}} dx \\
&= c(\alpha) \int_{-\infty}^{+\infty} \frac{2e^{-x^2} - 4x^2 e^{-x^2}}{|0-x|^{\alpha-1}} dx \\
&= 2c(\alpha) \left[2 \int_0^{+\infty} x^{1-\alpha} e^{-x^2} dx - 4 \int_0^{+\infty} x^{3-\alpha} e^{-x^2} dx \right] \\
&= 2c(\alpha) \left[2 \frac{1}{2} \Gamma\left(\frac{2-\alpha}{2}\right) - 4 \frac{1}{2} \Gamma\left(\frac{4-\alpha}{2}\right) \right] \\
&= 2 \frac{\Gamma[(\alpha-1)/2]}{\pi^{1/2} 2^{2-\alpha} \Gamma((2-\alpha)/2)} (\alpha-1) \Gamma\left(\frac{2-\alpha}{2}\right) \\
&= \frac{2^2}{\pi^{1/2} 2^{2-\alpha}} \left(\frac{\alpha-1}{2}\right) \Gamma\left(\frac{\alpha-1}{2}\right) \\
&= 2^\alpha \Gamma\left(\frac{1+\alpha}{2}\right) / \sqrt{\pi}, \tag{2.22}
\end{aligned}$$

which is the same solution as Eq. (2.21).

As mentioned, different representations may give different results in a bounded domain, while they are equal in the infinite domain. Thus, a conjecture is that as the domain is enlarged, evaluations of the fractional Laplacian based on different representation may become closer.

Example 2.2 The second example involves computation of two different expressions for the fractional Laplacian of the function $u(x) = (1+x^2)^{-(1-\alpha)/2}$ in the interval $[-L, L]$. In this regard the finite difference-quadrature approach proposed by Huang and Oberman (2014) is applied to calculate the Riesz-Marchaud type definition. The Caputo-type representation is calculated by adaptive quadrature (Shampine, 2008). For $\alpha = 1.5$, the finite difference-quadrature results and Caputo-type representation results are presented in Fig. 2.2.

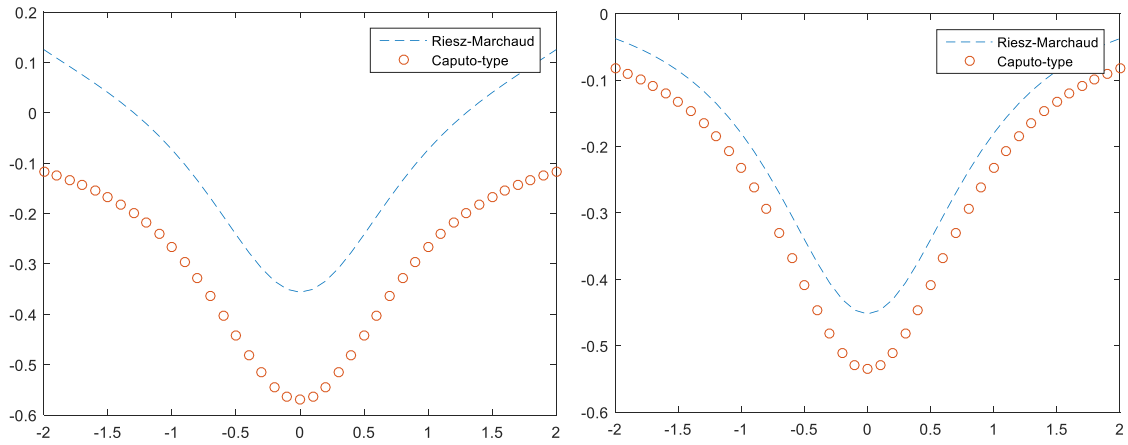


Fig. 2.2. Evaluation of the fractional Laplacian based on Riesz-Marchaud and Caputo-type definition with $L=4$ (left) and $L=8$ (right).

The exact fractional Laplacian of the function in the whole axis $(-\infty, +\infty)$ is

$$(-\Delta)^{\alpha/2} u(x) = 2^\alpha \Gamma\left(\frac{1+\alpha}{2}\right) \Gamma\left(\frac{1-\alpha}{2}\right)^{-1} (1+x^2)^{-(1+\alpha)/2}. \quad (2.23)$$

It is shown that as L increase, the results calculated by the Riesz-Marchaud and Caputo-type definition become closer. Later in Chapter 4, it is shown that the limit of the Caputo-type fractional Laplacian is the classical Laplacian:

$$\lim_{\alpha \rightarrow 2^-} (-\Delta)^{\alpha/2} u(\mathbf{x}) = -\Delta u(\mathbf{x}). \quad (2.24)$$

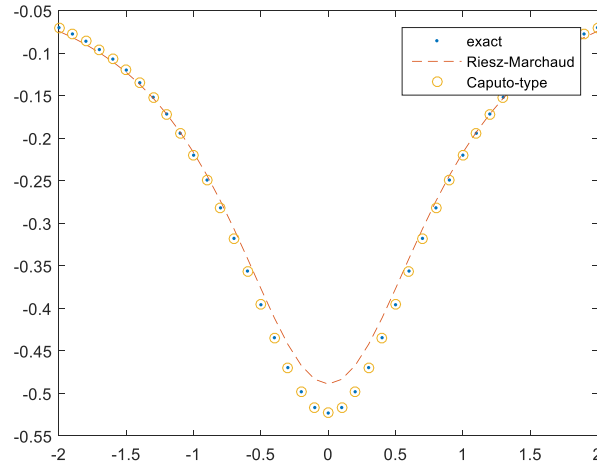


Fig. 2.3. Evaluation of the fractional Laplacian based on Riesz-Marchaud and Caputo-type definition on the whole axis $(-\infty, +\infty)$.

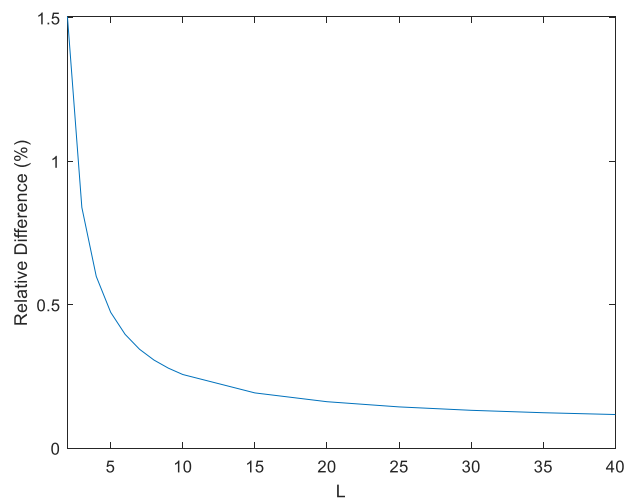


Fig. 2.4. Relative difference of the evaluated fractional Laplacian at the point $x=0$.

The Caputo-type representation of the fractional Laplacian is of importance in this thesis, as in Eq. (2.15), for multidimension $d \geq 2 > \alpha$, the denominator in the integrand is still singular, but not hypersingular, which makes it much more convenient for numerical treatment. Further, it includes the information of the boundary conditions, and thus it is suitable to be applied to the bounded problems. Such good properties lead to the modal expansion and the statistical linearization method that will be proposed in Chapter 5.

2.4 The Boundary Element Method

The Boundary Element Method (BEM) is one of the most popular computational methods in engineering applications with good effectiveness and accuracy. The Analog Equation Method (Babouskos and Katsikadelis, 2010), a BEM-based algorithm, can be employed to the analysis nonlinear dynamic systems. Recently, in conjunction with the Grunwald-Letnikov algorithm, the BEM (Katsikadelis, 2002, 2006, 2008) has been implemented for determining the response of systems with time-fractional derivative. Linear fractional-order system was investigated by Agrawal (2001) and Di Paola, Failla, et al. (2012). Nonlinear fractional ordinary differential equation was investigated by Spanos and Evangelatos (2010), while nonlinear partial differential equation was discussed by Spanos and Malara (2014, 2017).

A nonlinear continuous system can be described via a partial differential equations of the form

$$D[u] = q, \quad (2.25)$$

where u is the unknown response of the system, $D[\cdot]$ is a nonlinear differential operator, and q is the known load.

The basic objective of the BEM is to select an appropriate linear partial differential equation

$$L[u] = b, \quad (2.26)$$

with $L[\cdot]$ being a linear differential operator, and b being the unknown load. Eq. (2.26) is called the analog equation. An integral representation of the solution of this system is then discretized to determine the response as

$$u = \mathbf{G} \cdot \mathbf{b}, \quad (2.27)$$

where \mathbf{G} is a known matrix and \mathbf{b} is the unknown source vector. Finally, the unknown source term \mathbf{b} is calculated by collocating Eq. (2.25) in each element of the continuum so that the equation

$$\mathbf{B}[\mathbf{b}] = \mathbf{q} \quad (2.28)$$

is obtained. Eq. (2.25) is a system of nonlinear ordinary differential equations involving

fractional derivatives that can be solved in the time domain by a numerical integration scheme. Thus, the load \mathbf{b} is obtained, and the system response can be computed via Eq. (2.24). This procedure is then repeated many times to derive Monte Carlo simulation for the response statistics.

An example in Katsikadelis and Tsiatas (2003) , for a nonlinear fractional partial differential equation governing the vibration of a beam

$$\rho A \ddot{u} + EI \frac{\partial^4 u(x,t)}{\partial x^4} + c D_t^\alpha u + F(u) = q(x,t) \quad (2.29)$$

is considered. In this regard, the analog equation

$$\frac{\partial^4 u(x,t)}{\partial x^4} = b(x,t) \quad (2.30)$$

is first established. The integral representation of the solution is written as

$$u(x,t) = c_0 + c_1 x + c_2 x^2 + c_3 x^3 + \int_0^L G(x,\xi) b(\xi,t) d\xi, \quad (2.31)$$

with $c_i(t), i = 0,1,2,3$ being time-dependent functions depending on the boundary conditions, and

$$G(x,\xi) = \frac{1}{12} |x-\xi| (x-\xi)^2. \quad (2.32)$$

Discretizing the beam into N elements and assuming that $b(x,t)$ is constant on each element, the discretized representation of Eq. (2.31) is

$$\mathbf{u} = c_0 + c_1 \mathbf{x}_1 + c_2 \mathbf{x}_2 + c_3 \mathbf{x}_3 + \mathbf{G} \mathbf{b}(t), \quad (2.33)$$

where \mathbf{x}_k are vectors containing the k -th power of the coordinates x^k of the nodal point in each element

Substituting Eq. (2.33) into Eq. (2.29)

$$\rho A \mathbf{G} \ddot{\mathbf{b}}(t) + c \mathbf{G} D_t^\alpha \mathbf{b}(t) + E \mathbf{I} \mathbf{b}(t) + \mathbf{F}(\mathbf{b}(t), \mathbf{G}) = \mathbf{q}(t), \quad (2.34)$$

the set of equations is obtained, where $\mathbf{F}(\mathbf{b}, \mathbf{G})$ is the nonlinear vector function and $\mathbf{q}(t)$

is the vector containing the excitation value on each element. Eq. (2.34) is then solved via the numerical integration scheme and the Grunwald-Letnikov algorithm presented in Chapter 1. Details about this problem can be found in Katsikadelis, Tsiatas (2003) and Spanos, Malara (2014).

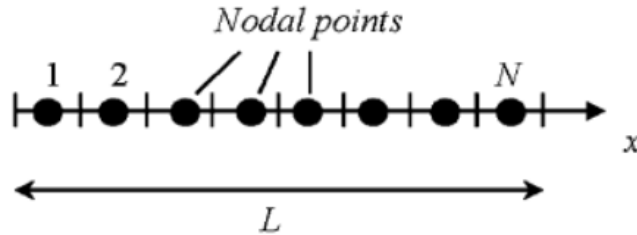


Fig. 2.5. Discretization of the beam into N equal elements. (From Spanos and Malara, 2014)

2.5 Statistical Linearization

Statistical linearization is a method that has been applied to the time-fractional differential equation involving stochastic excitation. The nonlinear response of a single-degree-of-freedom system was investigated by Spanos and Evangelatos (2010). Further, Malara and Spanos (2014, 2017) considered the problem of determining the response of a beam or a plate endowed with fractional derivative element under stochastic excitation via a statistical linearization procedure.

The method is to replace the nonlinear differential equation

$$D[u] = q, \quad (2.25')$$

by an equivalent linear system, in which the system parameters are determined by minimizing a mean square error between the two systems. Its application to a partial differential equation is based on an expansion of the system response. Such an expansion is used to rewrite the system as a system of nonlinear ordinary differential equations

$$D_{nl}[w] = Q. \quad (2.35)$$

Such nonlinear system is then replaced by an equivalent linear system,

$$D_{eq}[w] = Q. \quad (2.36)$$

The parameters in Eq. (2.36) are determined by minimizing the mean square error

$$\varepsilon = E \left\{ \left(D_{nl} [w] - D_{eq} [w] \right)^2 \right\}. \quad (2.37)$$

Specifically, as an example in Malara and Spanos (2017), consider the transverse displacement $u(x, y, t)$ of a rectangular plate of sides a and b ,

$$\rho h \frac{\partial^2 u}{\partial t^2} + c \partial_t^\alpha u + D \nabla^4 u + F(u) = q, \quad (2.38)$$

where $F(u(x, y, t))$ is the nonlinear function of $u(x, y, t)$, and ρ , h , c , α , D are parameters. The transverse load $q(x, y, t)$ is assumed to be separable. That is,

$$q(x, y, t) = p(x, y) f(t), \quad (2.39)$$

where $p(x, y)$ is a deterministic spatial function, and $f(t)$ is a random process with a given power spectral density $S(\omega)$ and zero mean. ∇^4 is the biharmonic operator

$$\nabla^4 = \frac{\partial^4}{\partial x^4} + \frac{\partial^4}{\partial y^4} + 2 \frac{\partial^4}{\partial x^2 \partial y^2}. \quad (2.40)$$

First, the response of the system is represented by expansion of spatial functions and time-dependent amplitudes.

$$u(x, y, t) = \sum_{m,n=1}^{\infty} w_{mn}(t) U_{mn}(x, y). \quad (2.41)$$

Substituting Eq. (2.41) into Eq. (2.38) and taking into account of the orthogonal properties of the eigenfunctions, a set of ordinary differential equations can be derived.

$$\ddot{w}_{mn} + \frac{c}{\rho h} \partial_t^\alpha w_{mn} + \omega_{mn}^2 w_{mn} + g(\mathbf{w}) = \frac{4}{ab\rho h} P_{mn} f(t), \text{ for } m, n = 1, 2, \dots, \quad (2.42)$$

where \mathbf{w} is the vector containing all w_{mn} , and

$$P_{mn} = \iint_{\Omega} p(x, y) U_{mn} d\Omega, \quad (2.43)$$

with $g(\mathbf{w})$ being the nonlinear function of all w_{mn} , which means that Eq. (2.42) is a coupled system. However, in the statistical linearization method, an approximate solution of Eq. (2.42) is sought by the decoupled equivalent linear system

$$\ddot{w}_{mn} + \frac{c}{\rho h} \partial_t^\alpha w_{mn} + \omega_{eq,mn}^2 w_{mn} = \frac{4}{ab\rho h} P_{mn} f(t). \quad (2.44)$$

Note that the frequencies $\omega_{eq,mn}$ are determined by minimizing the error between the nonlinear and linear equations in a mean square sense. That is, requiring

$$\frac{\partial}{\partial (\omega_{eq,mn}^2)} \langle \varepsilon_{mn}^2 \rangle = 0, \quad (2.45)$$

with ε being the error,

$$\varepsilon_{mn} = \omega_{mn}^2 w_{mn} + g(\mathbf{w}) - \omega_{eq,mn}^2 w_{mn}. \quad (2.46)$$

Once Eq. (2.45) is treated and $\omega_{eq,mn}$ is obtained, the response statistics of the linear system Eq. (2.44) can be determined by input-output relations via the transfer function

$$H_{mn}(i\omega) = \frac{1}{-\omega^2 + \frac{c}{\rho h} (i\omega)^\alpha + \omega_{eq,mn}^2}, \quad (2.47)$$

which is an estimation of the response statistics of the original system Eq. (2.38). Normally, $\omega_{eq,mn}$ cannot be solved directly. An iterative method is always applied until $\omega_{eq,mn}$ converges to a reasonable value. Details about this problem can be seen in Malara and Spanos (2017).

Chapter 3

The Boundary Element Method (Riesz-Marchaud) for Dynamic Systems with the Fractional Laplacian

3.1 Preliminary Remark

In this chapter, a BEM-based algorithm (BEMrm) is proposed for the fractional differential equation. The algorithm is based on the Riesz-Marchaud definition of the fractional Laplacian. First, the algorithm is applied for approximation of the fractional Laplace/Poisson equation. Based on the fractional Poisson equation as the analog equation, the algorithm is generalized for the fractional diffusion equation.

3.2 The Boundary Element Method Based Algorithm (BEMrm) for Static Problem

Consider a two-dimensional differential equation with the fractional Laplacian

$$(-\Delta)^{\alpha/2} u(x, y) = q(x, y), 1 < \alpha < 2. \quad (3.1)$$

The boundary condition is

$$\beta_1 u + \beta_2 \frac{\partial u}{\partial n} = \beta_3 \text{ on } \Gamma, \quad (3.2)$$

where $\beta_1, \beta_2, \beta_3$ are known values given on the boundary Γ . When $\alpha=2$, it corresponds to the standard Laplace/Poisson equation.

The fundamental solution of this problem is given by Bucur (2015),

$$\Phi_r(P, Q) = \frac{\Gamma((2-\alpha)/2)}{2^\alpha \pi \Gamma(\alpha/2)} \frac{1}{|P-Q|^{2-\alpha}}, \quad (3.3)$$

where $P = (x_P, y_P)$ and $Q = (x_Q, y_Q)$ are two points in the domain Ω or on the boundary Γ , and

$$|P-Q| = \sqrt{(x_P - x_Q)^2 + (y_P - y_Q)^2}. \quad (3.4)$$

Assume that the solution is represented by the integration. That is,

$$\begin{aligned} \rho u(P) = & - \int_{\Gamma} \left(\Phi_r(P, Q) \frac{\partial u(Q)}{\partial n} - u(Q) \frac{\partial \Phi_r(P, Q)}{\partial n} \right) dS(Q) \\ & + \int_{\Omega} \Phi_r(P, Q) q(Q) d\Omega(Q), \end{aligned} \quad (3.5)$$

where $\rho = 1$ or $1/2$ depending on the position of point P , inside the domain Ω or on the boundary Γ , respectively. q is the load in Eq. (3.1).

Discretize the domain into N_1 elements, and the boundary into N_2 elements. Further, assume that the load is constant over each element. The values of the response u are supposed to be constant over each domain element and boundary element. Those values are calculated at fixed nodes in each element. The normal derivative $\partial u / \partial n$ is also assumed to be constant over each boundary element and equals to its value at a fixed node in the element.

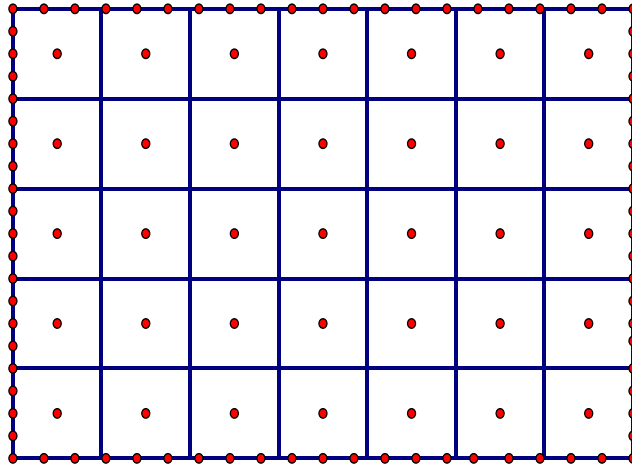


Fig. 3.1. Discretization of the domain.

Then, for a given point P_i on Γ , the discretized form of Eq. (3.5) is expressed as

$$\begin{aligned} \frac{1}{2}u(P_i) &= \sum_{j=1}^{N_1} \int_{\Omega_j} \Phi_r(P_i, Q) q(Q) d\Omega(Q) \\ &\quad - \sum_{j=1}^{N_2} \int_{\Gamma_j} \Phi_r(P_i, Q) \frac{\partial u(Q)}{\partial n} dS(Q) + \sum_{j=1}^{N_2} \int_{\Gamma_j} u(Q) \frac{\partial \Phi_r(P_i, Q)}{\partial n} dS(Q), \end{aligned} \quad (3.6)$$

where Γ_j is the segment on which the j -th node is located and over which integration is carried out, and P_i is the nodal point of the i -th element. For constant elements, the boundary is smooth at the nodal points, hence $\rho = 1/2$. Denote by u^j and u_n^j the values of u and $\partial u / \partial n$, respectively, on the j -th element. Eq. (3.6) can be written as

$$\begin{aligned} \frac{1}{2}u^i &= \sum_{j=1}^{N_1} q^j \int_{\Omega_j} \Phi_r(P_i, Q) d\Omega(Q) \\ &\quad - \sum_{j=1}^{N_2} u_n^j \int_{\Gamma_j} \Phi_r(P_i, Q) dS(Q) + \sum_{j=1}^{N_2} u^j \int_{\Gamma_j} \frac{\partial \Phi_r(P_i, Q)}{\partial n} dS(Q) \end{aligned} \quad (3.7)$$

Define the coefficient matrices as

$$\mathbf{G}_b(i, j) = \int_{\Omega_j} \Phi_r(P_i, Q) d\Omega(Q), \quad P_i \in \Gamma, \quad (3.8)$$

$$\mathbf{L}_b(i, j) = \int_{\Gamma_j} \Phi_r(P_i, Q) dS(Q), \quad P_i \in \Gamma, \quad (3.9)$$

and

$$\mathbf{H}_b(i, j) = \int_{\Gamma_j} \frac{\partial \Phi_r(P_i, Q)}{\partial n} dS(Q), \quad P_i \in \Gamma, \quad (3.10)$$

where the point P_i remains fixed point (reference point), while the point Q varies over the j -th boundary element (integration point). Introduce the notation (3.8), (3.9) and (3.10) into Eq. (3.7),

$$\frac{1}{2}u^i = \sum_{j=1}^{N_1} \mathbf{G}_b(i, j) q^j - \sum_{j=1}^{N_2} \mathbf{L}_b(i, j) u_n^j + \sum_{j=1}^{N_2} \mathbf{H}_b(i, j) u^j. \quad (3.11)$$

Moreover, set

$$\hat{\mathbf{H}}_b(i, j) = \mathbf{H}_b(i, j) - \frac{1}{2} \delta_{ij}, \quad (3.12)$$

where δ_{ij} is the Kronecker delta function. Eq. (3.11) is then written as

$$\sum_{j=1}^{N_1} \mathbf{G}_b(i, j) q^j + \sum_{j=1}^{N_2} \hat{\mathbf{H}}_b(i, j) u^j = \sum_{j=1}^{N_2} \mathbf{L}_b(i, j) u_n^j. \quad (3.13)$$

Eq. (3.13) is applied consecutively for all the nodes $P_i, i = 1, 2, \dots, N_2$, yielding a system of N_2 linear algebraic equations which are arranged in matrix form

$$\mathbf{G}_b \mathbf{q} + \hat{\mathbf{H}}_b \mathbf{u}_b = \mathbf{L}_b \mathbf{u}_{n|b}, \quad (3.14)$$

where \mathbf{q} is the vector containing the values of the load at nodes, and \mathbf{u}_b and $\mathbf{u}_{n|b}$ are vectors containing the solution u and their directional derivative at the nodes on the boundary, respectively. Further, \mathbf{G}_b is $N_2 \times N_1$ matrix, $\hat{\mathbf{H}}_b$ and \mathbf{L}_b are $N_2 \times N_2$ square matrices, \mathbf{q} is a vector of dimension N_1 , while \mathbf{u}_b and $\mathbf{u}_{n|b}$ are vectors of dimension N_2 .

Eq. (3.14) can be used to estimate the unknown boundary quantities by introducing the boundary condition. Assume mixed boundary conditions as in Eq. (3.2). Further, suppose that the part Γ_1' of the boundary on which u is described and the part Γ_2' on which u_n is described, are discretized into N_{21} and N_{22} constant elements respectively ($\Gamma_1' \cup \Gamma_2' = \Gamma, N_{21} + N_{22} = N_2$). Furthermore, partition the matrices $\hat{\mathbf{H}}_b$ and \mathbf{L}_b by an appropriate rearrangement of columns. Thus Eq. (3.14) can be written as

$$\begin{bmatrix} \hat{\mathbf{H}}_{b11} & \hat{\mathbf{H}}_{b12} \end{bmatrix} \begin{Bmatrix} \bar{\mathbf{u}}_{b1} \\ \mathbf{u}_{b2} \end{Bmatrix} + \mathbf{G}_b \mathbf{q} = \begin{bmatrix} \mathbf{L}_{b11} & \mathbf{L}_{b12} \end{bmatrix} \begin{Bmatrix} \mathbf{u}_{n|b1} \\ \bar{\mathbf{u}}_{n|b2} \end{Bmatrix}, \quad (3.15)$$

where $\bar{\mathbf{u}}_{b1}$ and $\bar{\mathbf{u}}_{n|b2}$ denote the known quantities respectively, while \mathbf{u}_{b2} and $\mathbf{u}_{n|b1}$ denote the corresponding unknown ones. The unknown vectors can then be described by the vector of \mathbf{q} , that is,

$$\begin{bmatrix} -\mathbf{L}_{b11} & \hat{\mathbf{H}}_{b12} \end{bmatrix} \begin{Bmatrix} \mathbf{u}_{n|b1} \\ \mathbf{u}_{b2} \end{Bmatrix} = \begin{bmatrix} -\hat{\mathbf{H}}_{b11} & \mathbf{L}_{b12} \end{bmatrix} \begin{Bmatrix} \bar{\mathbf{u}}_{b1} \\ \bar{\mathbf{u}}_{n|b2} \end{Bmatrix} - \mathbf{G}_b \mathbf{q}. \quad (3.16)$$

Therefore, all the boundary quantities are then obtained or represented by \mathbf{q} .

Upon obtaining the representation of \mathbf{u}_b and $\mathbf{u}_{n|b}$, similar to Eq. (3.6) and (3.7), for a given point P_i in Ω , the discretized form of Eq. (3.5) is expressed as

$$u^i = \sum_{j=1}^{N_1} q^j \int_{\Omega_j} \Phi_r(P_i, Q) d\Omega(Q) - \sum_{j=1}^{N_2} u_n^j \int_{\Gamma_j} \Phi_r(P_i, Q) dS(Q) + \sum_{j=1}^{N_2} u^j \int_{\Gamma_j} \frac{\partial \Phi_r(P_i, Q)}{\partial n} dS(Q). \quad (3.17)$$

Define the similar coefficient matrices as

$$\mathbf{G}_d(i, j) = \int_{\Omega_j} \Phi_r(P_i, Q) d\Omega(Q), \quad P_i \in \Omega, \quad (3.18)$$

$$\mathbf{L}_d(i, j) = \int_{\Gamma_j} \Phi_r(P_i, Q) dS(Q), \quad P_i \in \Omega, \quad (3.19)$$

and

$$\mathbf{H}_d(i, j) = \int_{\Gamma_j} \frac{\partial \Phi_r(P_i, Q)}{\partial n} dS(Q), \quad P_i \in \Omega. \quad (3.20)$$

Introduce the notation (3.18), (3.19) and (3.20) into Eq. (3.17),

$$u^i = \sum_{j=1}^{N_1} \mathbf{G}_d(i, j) q^j - \sum_{j=1}^{N_2} \mathbf{L}_d(i, j) u_n^j + \sum_{j=1}^{N_2} \mathbf{H}_d(i, j) u^j. \quad (3.21)$$

Eq. (3.21) is applied consecutively for all the nodes $P_i, i = 1, 2, \dots, N_1$, yielding a system of N_1 linear algebraic equations, which are arranged in the matrix form

$$\mathbf{u} = \mathbf{G}_d \mathbf{q} - \mathbf{L}_d \mathbf{u}_{n|b} + \mathbf{H}_d \mathbf{u}_b, \quad (3.22)$$

where \mathbf{u} is the N_1 -dimensional vector containing values of the response u in each domain, \mathbf{G}_d is $N_1 \times N_1$ square matrix, and \mathbf{H}_d and \mathbf{L}_d are $N_1 \times N_2$ matrices.

Note that all the values in vector \mathbf{u}_b and $\mathbf{u}_{n|b}$ are known or represented by \mathbf{q} as in Eq. (3.35), and \mathbf{G}_d , \mathbf{H}_d and \mathbf{L}_d are all known matrices. Therefore, via Eq. (3.22), the vector \mathbf{u} is also represented by \mathbf{q} , that is,

$$\mathbf{u} = \mathbf{M} \mathbf{q} + \mathbf{e}, \quad (3.23)$$

where \mathbf{M} and \mathbf{e} are known matrix and vector that is calculated from $\mathbf{G}_d, \mathbf{G}_b, \mathbf{H}_d, \mathbf{H}_c, \mathbf{L}_d$ and \mathbf{L}_b .

Example 3.1 Consider the two-dimensional problem (Ros-Oton and Serra, 2014)

$$(-\Delta)^{\alpha/2} u = 1, \text{ in } B_r(\mathbf{x}_0), \quad (3.24)$$

where $B_r(\mathbf{x}_0) = \{\mathbf{x} \in \mathbb{R}^2 \mid |\mathbf{x} - \mathbf{x}_0|^2 < r\}$. The boundary condition is

$$u = 0, \text{ on } \Gamma. \quad (3.25)$$

The explicit solution is given by Gettoor (1961),

$$u(\mathbf{x}) = \frac{1}{2^\alpha (\Gamma(1 + \alpha/2))^2} \left(r^2 - |\mathbf{x} - \mathbf{x}_0|^2 \right)^{\alpha/2}. \quad (3.26)$$

Apply BEMrm on this problem with $r = 1$ and $\mathbf{x}_0 = (0, 0)$ and different orders. The results are shown in Fig. 3.2. It shows that BEMrm gives good approximation of the solution.

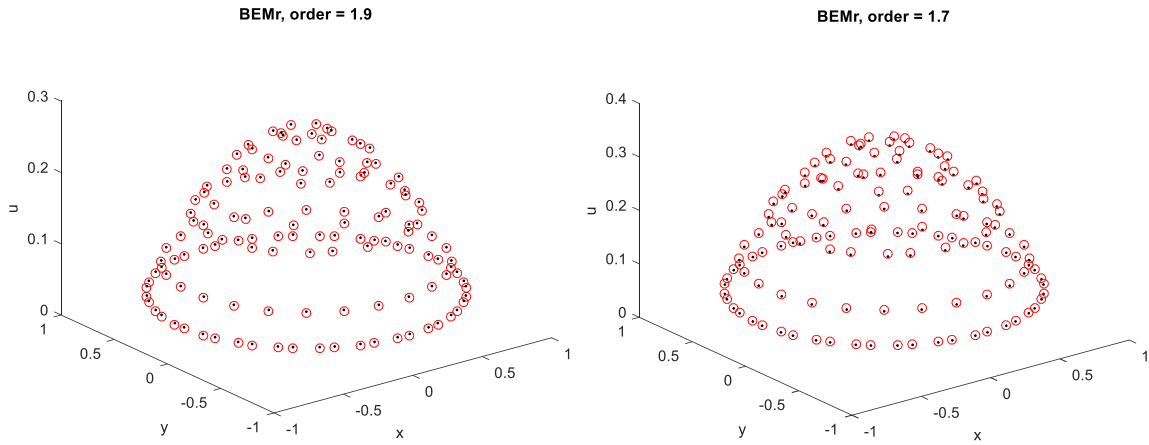


Fig. 3.2. The exact solution (dots) and BEMrm solution (circles) of Eq. (3.24) with order $\alpha = 1.9$ (left) and $\alpha = 1.7$ (right).

Example 3.2 Consider the Dirichlet boundary problem of the fractional Laplace equation in a square domain

$$\begin{cases} (-\Delta)^{\alpha/2} u = 0, & \text{in } \Omega, \\ u = u_b, & \text{on } \Gamma. \end{cases} \quad (3.27)$$

The boundary conditions are specified by

$$u_b(x, y) = 100(1 + x + 0.5). \quad (3.28)$$

SBM introduced by Chen and Pang (2016) is also applied to the problem. Results from two methods for fractional order 1.9 and 1.5 are given in Table 3.1 and Table 3.2, using 400 boundary elements.

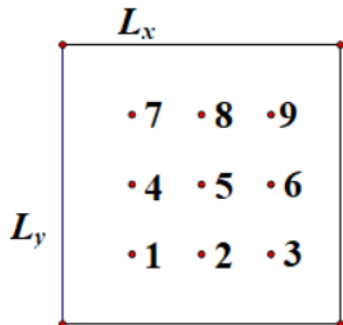


Fig. 3.3. Square Domain and internal points of Example 3.2.

Table 3.1. Internal values computed by SBM and BEMrm when $\alpha = 1.9$.

Node	SBM	BEMrm	Error (%)
1	125.5229	120.4276	4.0593
2	125.5344	120.5218	3.9930
3	125.5229	120.4276	4.0593
4	149.5250	143.9508	3.7279
5	149.4447	143.9475	3.6784
6	149.5250	143.9508	3.7279
7	173.6342	167.4782	3.5454
8	173.5155	167.3797	3.5362
9	173.6342	167.4782	3.5454

Table 3.2. Internal values computed by SBM and BEMrm when $\alpha = 1.5$.

Node	SBM	BEMrm	Error (%)
1	115.1553	113.3835	1.5386
2	114.1440	113.6093	0.4684
3	115.1553	113.3835	1.5386
4	131.4541	134.0266	1.9570
5	129.5744	133.9520	3.3784
6	131.4541	134.0266	1.9570
7	150.3618	154.7713	2.9326
8	148.7642	154.4439	3.8179
9	150.3618	154.7713	2.9326

3.3 BEMrm for Fractional Diffusion Equation

In this section, BEMrm is applied to the fractional diffusion equation, leading to a set of ordinary diffusion equations.

Consider the two-dimensional diffusion equation with the fractional Laplacian:

$$\dot{u} + (-\Delta)^{\alpha/2} u + F(u) = q(x, y, t), 1 < \alpha < 2. \quad (3.29)$$

The boundary condition is

$$\beta_1 u + \beta_2 \frac{\partial u}{\partial n} = \beta_3 \text{ on } \Gamma, \quad (3.30)$$

and the initial condition is

$$u(t=0) = u_0(x, y), \quad (3.31)$$

where $\beta_1, \beta_2, \beta_3$ are known functions defined on the boundary Γ . When $\alpha=2$, it corresponds to the standard diffusion, while the case $1 < \alpha < 2$ corresponds to the anomalous diffusion.

The standard Poisson equation is first chosen as the analog equation

$$(-\Delta)^{\alpha/2} u = b, \quad (3.32)$$

where $b(x, y)$ is to be constructed later. Apply the algorithm BEMrm as introduced in Section 3.2 to solve Eq. (3.32). The following matrix equations are derived.

$$\mathbf{u} = \mathbf{G}_d \mathbf{b} - \mathbf{L}_d \mathbf{u}_n + \mathbf{H}_d \mathbf{u}_b, \text{ in the domain} \quad (3.33)$$

and

$$\frac{1}{2} \mathbf{u}_b = \mathbf{G}_b \mathbf{b} - \mathbf{L}_b \mathbf{u}_n + \mathbf{H}_b \mathbf{u}_b, \text{ on the boundary} \quad (3.34)$$

where $\mathbf{b}(t)$ is the vector containing the values of the unknown load at nodes, \mathbf{u} contains the values of the response u at the nodes in the domain, and \mathbf{u}_b and \mathbf{u}_n are response and its directional derivative at the nodes on the boundary. The matrices are defined as in Section 3.3.

By Eq. (3.34), all the boundary quantities are represented by $\mathbf{b}(t)$. Substituting the values of the known matrices and vectors to Eq. (3.33) yields

$$\mathbf{u} = \mathbf{M} \mathbf{b} + \mathbf{e}, \quad (3.35)$$

where \mathbf{M} is a known matrix and \mathbf{e} is a known vector. Substituting Eq. (3.32) and (3.35) to the original system Eq. (3.29), a matrix nonlinear ordinary differential equation is obtained

$$\mathbf{M}_2 \dot{\mathbf{b}} + \mathbf{b} + \mathbf{F}(\mathbf{b}, \mathbf{M}_1) = \mathbf{q}. \quad (3.36)$$

This ordinary differential equation can be solved numerically. After Eq. (3.36) is solved, substitute $\mathbf{b}(t)$ into Eq. (3.35) and the values of the unknown response \mathbf{u} are obtained.

Example 3.3 Consider a stochastic fractional diffusion equation on a rectangular plate ($-5 \leq x \leq 5, -2.5 \leq y \leq 2.5$),

$$\dot{u} + (-\Delta)^{\alpha/2} u + ku^3 = p(x, y)f(t), \quad (3.37)$$

with Dirichlet boundary condition

$$u = 0 \text{ on } \Gamma, \quad (3.38)$$

and initial condition

$$u(x, y, t = 0) = 0. \quad (3.39)$$

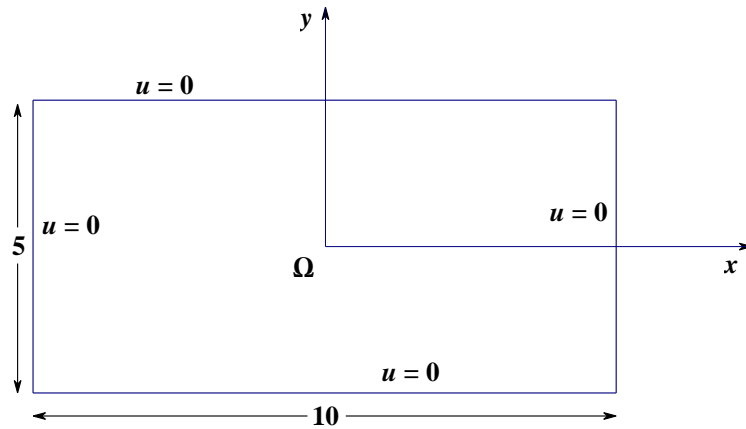


Fig. 3.4. The rectangular domain with Dirichlet boundary condition.

The time-dependent part $f(t)$ of the source term is white noise, while the determinant spatial part is a constant, $p(x, y) = 1$. The algorithm proposed by Shinozuka and Deodatis (1991) is applied to generate excitation. Specifically, for a given power spectral density $S(\omega)$, the load $f(t)$ is represented by a truncated infinite series,

$$f(t) = \sqrt{2} \sum_{n=0}^{N-1} A_n \cos(\omega_n t + \phi_n), \quad (3.40)$$

where

$$A_n = \sqrt{2S(\omega_n)\Delta\omega}, \quad (n = 0, 1, 2, \dots, N-1), \quad (3.41)$$

$$\omega_n = n\Delta\omega, \quad \Delta\omega = \frac{\omega_c}{N}, \quad (3.42)$$

and

$$A_0 = 0 \text{ or } S(\omega_0 = 0) = 0. \quad (3.43)$$

In Eq. (3.40), ϕ_n is uniformly distributed over the interval $(0, 2\pi)$ and ω_c is the cut-off frequency of the target spectrum. It is worth mentioning that, as expressed in Eq. (3.43), the power spectral density of the generated random process $f(t)$ this method is always zero at 0 frequency. Therefore, in order to simulate white noise, a broad-band noise is generated with the spectral density $S(\omega = 0) = 0$.

Apply BEMrm to this problem with different parameters for simulation. A broad-band noise is generated with the power spectral density of the white noise being $S(\omega) = 1$ for $0 < \omega \leq 10\pi$ and $S(\omega = 0) = 0$. The domain is meshed into 75 elements while the boundary into 200 elements. The results are shown in Fig. 3.5 and Fig. 3.6.

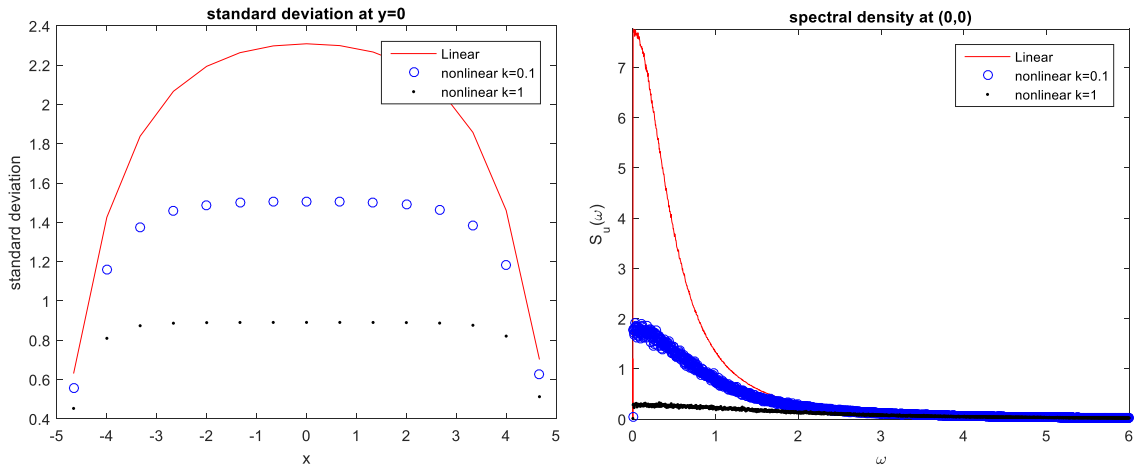


Fig. 3.5. Standard deviation of the response u along the line $y=0$ and the power spectral density of u at the point $(0,0)$ with white noise input and fractional order 1.9. The values of coefficient of the nonlinear term are: $k=0$ linear (continuous line); $k=0.1$ (circles); $k=1$ (dotted line).

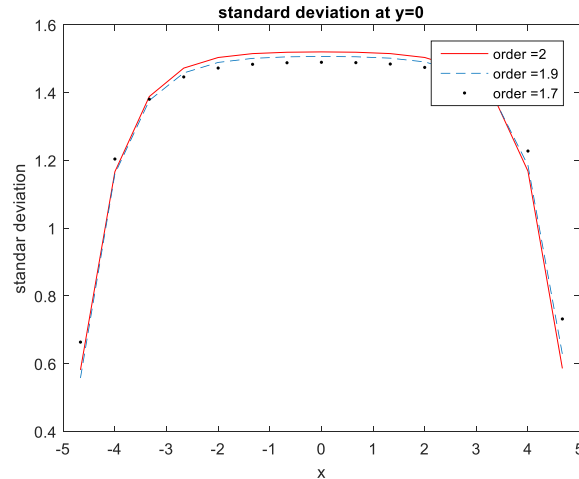


Fig. 3.6. Standard deviation of the response u along the line $y=0$ with white noise input and coefficient of the nonlinear term $k=0.1$. The values of fractional orders are: $\alpha = 2$ classical Laplacian (continuous line); $\alpha = 1.9$ (dashed line); $\alpha = 1.7$ (dotted line).

Fig. 3.5 and Fig. 3.6 show the boundary element method-based simulation results with different nonlinear parameter and fractional Laplacian order. The left panel of Fig. 3.4 shows values of response standard deviation calculated by the proposed algorithm and the right panel is the spectrum of the response.

3.4 Synopsis

In this Chapter, a BEM-based algorithm was developed for the fractional Poisson equation first. Different examples are provided to compare the results from BEMrm with the exact solution and SBM solution. Next, for the fractional diffusion equation, the analog equation was first established with the unknown load being calculated by the boundary element method. The value of the fractional Laplacian of the response was updated progressively. Numerical results pertaining to a system exposed to white noise input were presented to demonstrate the method.

Chapter 4

The Caputo-type Fractional Laplacian and the Boundary Element Method (Caputo)

4.1 Preliminary Remark

In this chapter, the limit of the Caputo-type fractional Laplacian when the order α tends to 2 is first discussed. It is shown that the limit is just the standard Laplace operator, which is a complementation of the theory about the Caputo-type fractional Laplacian. Then, based on such representation, a BEM-based algorithm is proposed for the diffusion equation with the fractional Laplacian. Such a system is a generalization of the classical diffusion equation involving the fractional Laplacian of the unknown system response. Determining the response of a dynamic system with the fractional Laplacian is a daunting task, as analytical solutions, to the authors' knowledge, are not available. Therefore, a new BEM-based numerical algorithm is developed for time domain simulation of the response. The algorithm is constructed by utilizing the integral representation of the classical Poisson equation solution, in which unknown constants are determined by the BEM. Then, based on the Caputo-type representation, the value of the fractional Laplacian of the response is updated progressively by matrix transformation of these constants

4.2 Property of the Caputo-type Fractional Laplacian

Recall the Caputo-type fractional Laplacian, which is represented as a composition of the Riesz potential and Laplace operator. Specifically,

$$(-\Delta)^{\alpha/2} u(\mathbf{x}) = I_d^{2-\alpha} [-\Delta u(\mathbf{x})], 1 < \alpha < 2. \quad (4.1)$$

The Riesz potential on a bounded convex domain $\Omega \subset \mathbb{R}^d$ is defined as

$$I_d^{2-\alpha} \varphi(\mathbf{x}) = c(\alpha) \int_{\Omega} \frac{\varphi(\xi)}{|\mathbf{x} - \xi|^\alpha} d\xi, \quad (4.2)$$

where ξ is the coordinate in the domain Ω and

$$c(\alpha) = \frac{\Gamma[(d-2+\alpha)/2]}{\pi^{d/2} 2^{2-\alpha} \Gamma((2-\alpha)/2)}. \quad (4.3)$$

Next seek to prove that in the bounded domain Ω , the following equation holds

$$\lim_{\alpha \rightarrow 2^-} (-\Delta)^{\alpha/2} u(\mathbf{x}) = -\Delta u(\mathbf{x}). \quad (4.4)$$

Clearly, Eq. (4.4) is equivalent to

$$\lim_{\alpha \rightarrow 2^-} I_2^{2-\alpha} u = u \Leftrightarrow \lim_{\alpha \rightarrow 0^+} I_2^\alpha u = u. \quad (4.5)$$

The following given proof is given in two-dimension. Obviously, it can be readily generalized to the three-dimensional system.

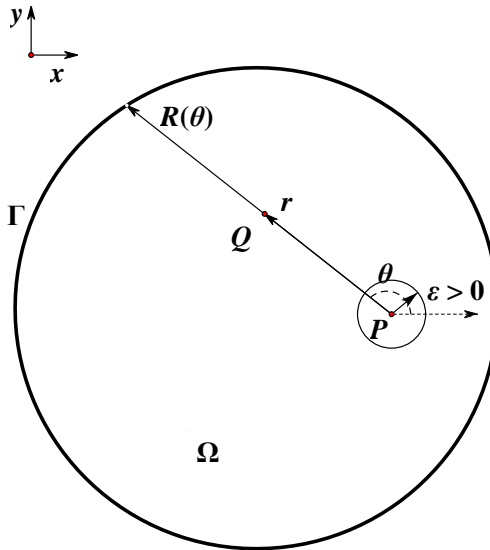


Fig. 4.1. The coordinates on the considered domain.

Consider two points $P = (x_P, y_P)$ and $Q = (x_Q, y_Q)$ in the domain Ω or on the boundary Γ . The distance of the two points is

$$|P-Q| = \sqrt{(x_P - x_Q)^2 + (y_P - y_Q)^2}. \quad (4.6)$$

Set $u(x_P, y_P) = u(P)$ and assume $u(P) = 0$ for $P \notin \bar{\Omega}$. Then,

$$-\Delta u(P) = 0, \text{ for } P \notin \bar{\Omega}, \quad (4.7)$$

and hence

$$I_2^{2-\alpha}(-\Delta u(P)) = 0, \text{ for } P \notin \bar{\Omega}. \quad (4.8)$$

Use the polar coordinates as shown in Fig. 4.1, to express the vector from point P to Q ,

$$P-Q = (r \cos \theta, r \sin \theta), \quad (4.9)$$

where

$$|P-Q| = r. \quad (4.10)$$

Denote $\sigma = (\cos \theta, \sin \theta)$. Then, the vector $(P-Q)$ can be expressed as

$$P-Q = r\sigma, \quad Q = P - r\sigma. \quad (4.11)$$

Hence,

$$\begin{aligned} I_2^\alpha u(P) &= c(2-\alpha) \int_{\Omega} \frac{\varphi(Q)}{|P-Q|^{2-\alpha}} d\Omega(Q) \\ &= c(2-\alpha) \int_0^{2\pi} \int_0^{R(\theta)} r^{\alpha-2} u(P-r\sigma) r dr d\theta \\ &= c(2-\alpha) \int_0^{2\pi} \left[\int_0^\varepsilon r^{\alpha-1} u(P-r\sigma) dr + \int_\varepsilon^{R(\theta)} r^{\alpha-1} u(P-r\sigma) dr \right] d\theta, \end{aligned} \quad (4.12)$$

where the radius of the neighbor circle of the point P is a small value $\varepsilon > 0$. $R(\theta)$ is the length of the line segment starting from point P to the boundary along the angle θ . The angular coordinate $\theta \in [0, 2\pi)$.

Note that the constant in Eq. (3.12) is

$$c(2-\alpha) = \frac{\Gamma[(2-\alpha)/2]}{\pi 2^\alpha \Gamma(\alpha/2)}. \quad (4.13)$$

As $\alpha \rightarrow 0+$, $2^\alpha \rightarrow 1$, $\Gamma((2-\alpha)/2) \rightarrow 1$, and $\Gamma(\alpha/2) \rightarrow +\infty$. Hence, $c(2-\alpha) \rightarrow 0$.

And in Eq. (4.12), the value of the non-singular integral $\int_\varepsilon^{R(\theta)} r^{\alpha-1} u(P-r\sigma) dr$ is always limited. Thus,

$$\lim_{\alpha \rightarrow 0^+} c(2-\alpha) \int_0^{2\pi} \int_{\varepsilon}^{R(\theta)} r^{\alpha-1} u(P-r\sigma) dr d\theta = 0. \quad (4.14)$$

Next consider the other integral in Eq. (3.12), which contains a singular integrand

$\int_0^{\varepsilon} r^{\alpha-1} u(P-r\sigma) dr$, when $\alpha \rightarrow 0^+$. Algebraic manipulations lead to

$$\begin{aligned} & c(2-\alpha) \int_0^{2\pi} \int_0^{\varepsilon} r^{\alpha-1} u(P-r\sigma) dr d\theta \\ &= c(2-\alpha) \int_0^{2\pi} d\theta \left[\frac{1}{\alpha} \int_0^{\varepsilon} u(P-r\sigma) dr^{\alpha} \right] \\ &= \frac{c(2-\alpha)}{\alpha} \int_0^{2\pi} d\theta \left[r^{\alpha} u(P-r\sigma) \Big|_0^{\varepsilon} - \int_0^{\varepsilon} r^{\alpha} du(P-r\sigma) \right] \\ &= \frac{c(2-\alpha)}{\alpha} \int_0^{2\pi} d\theta \left[\varepsilon^{\alpha} u(P-\varepsilon\sigma) - \int_0^{\varepsilon} r^{\alpha} du(P-r\sigma) \right]. \end{aligned} \quad (4.15)$$

Note that when $\alpha \rightarrow 0^+$, $\varepsilon^{\alpha} \rightarrow 1$, $r^{\alpha} \rightarrow 1$, and

$$\begin{aligned} \frac{c(2-\alpha)}{\alpha} &= \frac{\Gamma(1-\alpha/2)}{2^{\alpha} \pi \Gamma(\alpha/2) \alpha} \\ &= \frac{\Gamma(1-\alpha/2)}{2^{\alpha+1} \pi \Gamma(1+\alpha/2)} \rightarrow \frac{1}{2\pi}. \end{aligned} \quad (4.16)$$

Thus,

$$\begin{aligned} I_2^{\alpha} u(P) &\rightarrow \frac{1}{2\pi} \int_0^{2\pi} d\theta \left[u(P-\varepsilon\sigma) - \int_0^{\varepsilon} du(P-r\sigma) \right] \\ &= \frac{1}{2\pi} \int_0^{2\pi} d\theta \left[u(P-\varepsilon\sigma) - u(P-\varepsilon\sigma) + u(P) \right] \\ &= \frac{1}{2\pi} 2\pi u(P) = u(P). \end{aligned} \quad (4.17)$$

Hence,

$$\lim_{\alpha \rightarrow 0^+} I_2^{\alpha} u = u. \quad (4.18)$$

Therefore,

$$\lim_{\alpha \rightarrow 2^-} (-\Delta)^{\alpha/2} u(\mathbf{x}) = -\Delta u(\mathbf{x}), \quad (4.4')$$

and Eq. (4.4) is recovered. The limit of the Caputo-type fractional Laplacian is the standard Laplace operator when the order $\alpha \rightarrow 2^-$. An analogous proof holds in three dimensions.

4.3 The Boundary Element Method Based Approach (BEMc) for Fractional Diffusion Equation

In this section a BEM-based algorithm (BEMc) is developed for numerical treatment of a dynamic system endowed with the fractional Laplacian. A fractional diffusion/heat equation is considered for example. The key to the algorithm is to find a proper analog equation, which is the classical Poisson equation in the proposed method. The solution of the analog equation is constructed by utilizing the integral, in which unknown constants are determined by the BEM (Katsikadelis, 2009, 2011, 2014). Based on the Caputo-type representation of the fractional Laplacian operator, the value of the fractional Laplacian of the response can then be updated progressively (Jiao, Malara and Spanos, 2018).

Consider the two-dimensional diffusion equation with the fractional Laplacian:

$$\dot{u} + (-\Delta)^{\alpha/2} u = 0, 1 < \alpha < 2, \quad (4.19)$$

The boundary condition is

$$\beta_1 u + \beta_2 \frac{\partial u}{\partial n} = \beta_3 \text{ on } \Gamma, \quad (4.20)$$

and the initial condition is

$$u(t=0) = u_0(x, y), \quad (4.21)$$

where $\beta_1, \beta_2, \beta_3$ are known functions defined on the boundary Γ . When $\alpha=2$, it corresponds to the standard diffusion, while the case $1 < \alpha < 2$ corresponds to the anomalous diffusion.

A BEM-based solution of the system is sought by considering the solution of the linear equation

$$\Delta u = b, \quad (4.22)$$

where $b(x, y, t)$ is a load to be constructed later.

A singular particular solution of

$$\Delta\Phi = \delta(P-Q), \quad (4.23)$$

where $\delta(\cdot)$ is the delta function, is called the fundamental solution of the potential equation (4.22). The fundamental solution of Eq. (4.22) is

$$\Phi_c(P, Q) = \frac{1}{2\pi} \log|P-Q|, \quad (4.24)$$

where $P = (x_P, y_P)$ and $Q = (x_Q, y_Q)$ are two points in the domain Ω or on the boundary Γ , and

$$|P-Q| = \sqrt{(x_P - x_Q)^2 + (y_P - y_Q)^2}. \quad (4.25)$$

Recall the Green's identity

$$\int_{\Omega} (v\Delta u - u\Delta v) d\Omega = \int_{\Gamma} \left(v \frac{\partial u}{\partial n} - u \frac{\partial v}{\partial n} \right) dS. \quad (4.26)$$

Applying the Green's identity with functions u and Φ_c , the solution of Eq. (4.22) can be represented by the integral equation

$$\begin{aligned} \rho u(P) = & - \int_{\Gamma} \left(\Phi_c(P, Q) \frac{\partial u(Q)}{\partial n} - u(Q) \frac{\partial \Phi_c(P, Q)}{\partial n} \right) dS(Q) \\ & + \int_{\Omega} \Phi_c(P, Q) b(Q) d\Omega(Q), \end{aligned} \quad (4.27)$$

where $\rho = 1$ or $1/2$ depending on the position of point P , inside the domain Ω or on the boundary Γ .

Following the similar process in Chapter 3, discretize the domain into N_1 elements, and the boundary into N_2 elements. Further, assume that the load is constant over each element. The values of the response u and the normal derivative $\partial u / \partial n$ is also assumed to be constant over each boundary element and equal to its value at a fixed node in the element. The integral representation of the solution can be recast in the matrix form

$$\mathbf{u} = \mathbf{G}_d \mathbf{b} - \mathbf{L}_d \mathbf{u}_n + \mathbf{H}_d \mathbf{u}_b, \quad \text{in the domain} \quad (4.28)$$

and

$$\frac{1}{2} \mathbf{u}_b = \mathbf{G}_b \mathbf{b} - \mathbf{L}_b \mathbf{u}_n + \mathbf{H}_b \mathbf{u}_b, \quad \text{in the boundary} \quad (4.29)$$

where $\mathbf{b}(t)$ is the vector containing the values of the unknown load at nodes, \mathbf{u} contains the values of the response u at the nodes in the domain, and \mathbf{u}_b and \mathbf{u}_n are response and its directional derivative at the nodes on the boundary. The matrices are defined as:

$$\mathbf{G}_b(i, j) = \int_{\Omega_j} \Phi_c(P_i, Q) d\Omega(Q), \quad P_i \in \Gamma, \quad (4.30)$$

$$\mathbf{G}_d(i, j) = \int_{\Omega_j} \Phi_c(P_i, Q) d\Omega(Q), \quad P_i \in \Omega, \quad (4.31)$$

$$\mathbf{L}_b(i, j) = \int_{\Gamma_j} \Phi_c(P_i, Q) dS(Q), \quad P_i \in \Gamma, \quad (4.32)$$

$$\mathbf{L}_d(i, j) = \int_{\Gamma_j} \Phi_c(P_i, Q) dS(Q), \quad P_i \in \Omega, \quad (4.33)$$

$$\mathbf{H}_b(i, j) = \int_{\Gamma_j} \frac{\partial \Phi_c(P_i, Q)}{\partial n} dS(Q), \quad P_i \in \Gamma, \quad (4.34)$$

and

$$\mathbf{H}_d(i, j) = \int_{\Gamma_j} \frac{\partial \Phi_c(P_i, Q)}{\partial n} dS(Q), \quad P_i \in \Omega. \quad (4.35)$$

Then Eq. (4.29) can be used to estimate the unknown boundary quantities by introducing the boundary condition Eq. (4.20). Therefore, all the boundary quantities are represented by $\mathbf{b}(t)$. Substituting equations (4.30) - (4.35) into Eq. (4.28) yields

$$\mathbf{u} = \mathbf{M}_1 \mathbf{b} + \mathbf{e}, \quad (4.36)$$

where \mathbf{M}_1 is a known matrix and \mathbf{e} is a known vector. Differentiating Eq. (4.36) with respect to time and taking into account that the vector \mathbf{e} is a constant vector,

$$\dot{\mathbf{u}} = \mathbf{M}_1 \dot{\mathbf{b}}. \quad (4.37)$$

The fractional Laplacian of u is estimated by the Caputo-type representation. Collocate the source vector \mathbf{b} in each element. That is,

$$\begin{aligned}
(-\Delta)^{\alpha/2} u(P_i) &= c(\alpha) \int_{\Omega} \frac{-\Delta u(Q)}{|P_i - Q|^{d+\alpha-2}} d\Omega \\
&= c(\alpha) \sum_{j=1}^{N_1} b_j \int_{\Omega_j} \frac{-1}{|P_i - Q|^{d+\alpha-2}} d\Omega.
\end{aligned} \tag{4.38}$$

Define

$$\mathbf{M}_2(i, j) = c(\alpha) \int_{\Omega_j} \frac{1}{|P_i - Q|^{d+\alpha-2}} d\Omega. \tag{4.39}$$

Then,

$$(-\Delta)^{\alpha/2} \mathbf{u} = -\mathbf{M}_2 \mathbf{b}. \tag{4.40}$$

By substitute the proposed representations (4.37) and (4.40) into the original system Eq. (4.19), the ordinary differential equation

$$\mathbf{M}_1 \dot{\mathbf{b}} - \mathbf{M}_2 \mathbf{b} = 0 \tag{4.41}$$

is obtained. Taking the boundary conditions Eq. (4.20) and initial condition Eq. (4.21) into consideration, Eq. (4.41) can be solved numerically. After Eq. (4.41) is solved, substitute $\mathbf{b}(t)$ into Eq. (4.36) and the values of the response \mathbf{u} are obtained.

In this BEM-based procedure, \mathbf{M}_2 is a large non-sparse matrix, while in the problem with a classical Laplace operator, \mathbf{M}_2 is merely an identity matrix. Thus, due to the existence of the fractional Laplacian, $\mathbf{M}_2 \mathbf{b}(i)$ is a linear combination of $(b_j, j = 1, 2, \dots)$. It suggests that the load on the j -th ($j \neq i$) elements will influence the i -th element, which represents the nonlocal property of the fractional Laplacian.

Another influence of the nonlocal property is that, although the system is a homogenous equation (4.19), in order to calculate the value of a point in the domain, the whole domain need to be meshed and the response at each node is required. On the contrary, for a standard homogenous heat/diffusion equation, only the boundary needs to be meshed in the BEM. Such complication is introduced due to the nonlocality of the fractional Laplacian, as the response at different nodes contribute to each other.

Next consider a more general model, which is a nonhomogeneous nonlinear fractional diffusion equation,

$$\dot{u} + (-\Delta)^{\alpha/2} u + F(u) = q, \quad (4.42)$$

where $F(u)$ is a nonlinear function of $u(x, y, t)$, and $q(x, y, t)$ is the load, deterministic or stochastic.

The proposed BEMc is applied in the same way to this system, leading to a nonlinear ordinary differential equation

$$\mathbf{M}_1 \dot{\mathbf{b}} - \mathbf{M}_2 \mathbf{b} + \mathbf{F}(\mathbf{b}, \mathbf{M}_1, \mathbf{e}) = \mathbf{q}, \quad (4.43)$$

where $\mathbf{F}(\mathbf{b}, \mathbf{M}_1, \mathbf{e})$ is a nonlinear vector function encapsulating the nonlinear terms of the original equation, and \mathbf{q} is the vector containing the load at each node. After Eq. (4.43) is solved numerically, the values of the response \mathbf{u} can be obtained by Eq. (4.36).

Note that in Eq. (4.39) the calculation of \mathbf{M}_2 may involve singular integrals for the diagonal terms $\mathbf{M}_2(i, i)$, i.e. when P_i is in the element Ω_i . In this context, the method of Chen and Pang (2016) is applied for the evaluation of these entries. This will be discussed in the next section.

4.4 Evaluation of the Singular Integrals in the BEM discretization

The method in this section is given by Chen and Pang (2016) that can be used to calculate the singular integral entries in the contribution matrix $\mathbf{M}_2(i, i)$ defined in Eq. (4.39).

In the discretization step in the proposed BEM, assume a domain element that is quadrilateral with four vertices A , B , C and D , as in Fig. 4.2. The element can be partitioned into four triangles $P_i AB$, $P_i BC$, $P_i CD$ and $P_i DA$. Then,

$$\begin{aligned} \mathbf{M}_f(i, i) &= c(\alpha) \int_{\Omega_j} \frac{1}{|P_i - Q|^{d+\alpha-2}} d\Omega \\ &= c(\alpha) \left(\int_{P_i AB} + \int_{P_i BC} + \int_{P_i CD} + \int_{P_i DA} \right) \frac{1}{|P_i - Q|^\alpha} d\Omega(Q). \end{aligned} \quad (4.44)$$

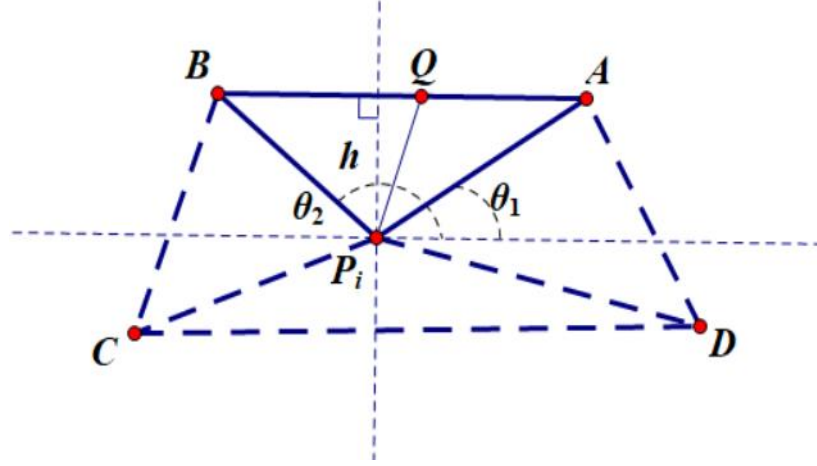


Fig. 4.2. The element and local coordinate.

Next consider the integral over the triangle P_iAB as an instance. Transform the Cartesian coordinates to the polar coordinates and rewrite the surface integral as

$$\int_{P_iAB} \frac{1}{|P_i - Q|^\alpha} d\Omega(Q) = \int_{\theta_1}^{\theta_2} \int_0^{R(\theta)} \frac{1}{r^\alpha} r dr d\theta, \quad (4.45)$$

where θ_1 and θ_2 are the angular coordinates of the points A and B respectively. Further, $R(\theta)$ is the length of the line segment P_iQ that the integration point $x(r, \theta)$ lies in,

$$R(\theta) = \frac{h}{\sin(\theta)}. \quad (4.46)$$

Then, the integral in Eq. (4.45) can be computed as

$$\int_{P_iAB} \frac{1}{|P_i - Q|^\alpha} d\Omega(Q) = \frac{h^{2-\alpha}}{2-\alpha} \int_{\theta_1}^{\theta_2} (\sin \theta)^{\alpha-2} d\theta. \quad (4.47)$$

Note that $0 < \theta_1 < \theta_2 < \pi$, the integral in the right-hand side of Eq. (4.47) is regular and can be evaluated by numerical integration methods such as Gauss quadrature. After the integrals in the four triangles are solved, $\mathbf{M}_2(i, i)$ can be evaluated by Eq. (4.44).

4.5 Examples

In this section, BEMc is applied to fractional diffusion equation with periodic and

stochastic excitations.

Example 4.1 Consider a linear fractional diffusion equation on a rectangular plate $(-5 \leq x \leq 5, -2.5 \leq y \leq 2.5)$

$$\dot{u} + (-\Delta)^{\alpha/2} u = p(x, y) f(t), \quad (4.48)$$

with Dirichlet boundary condition

$$u = 0 \text{ on } \Gamma, \quad (4.49)$$

and initial condition

$$u(x, y, t = 0) = 0, \quad (4.50)$$

where $f(t) = \sin(t)$, and $p(x, y) = 1$.

Apply BEMc and BEMrm to this problem with different fractional order and nonlinear coefficient. The results are shown in Fig. 4.3. It shows that BEMc and BEMrm give close results for a higher order. While for a lower order, there is a difference in the peak in each period.

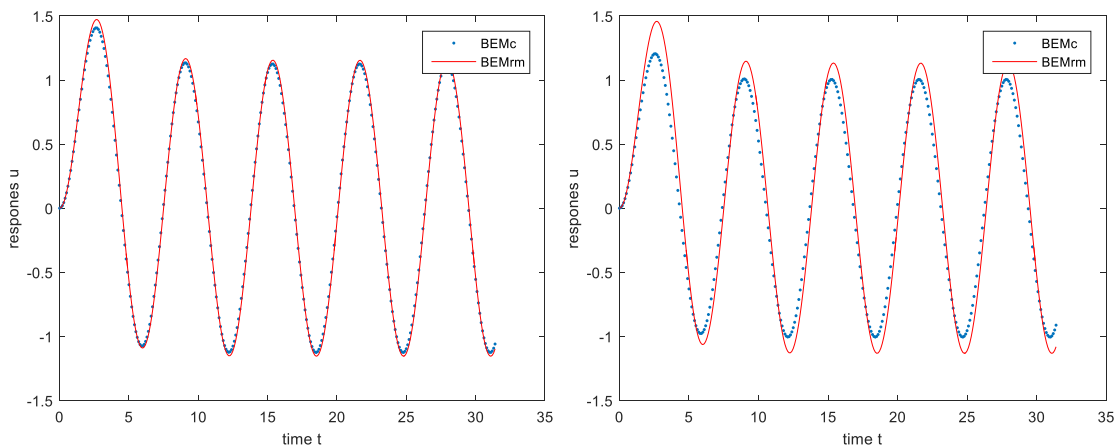


Fig. 4.3. Response calculated by BEMc and BEMrm with order $\alpha = 1.9$ (left) and $\alpha = 1.7$ (right) on a 10×5 rectangular plate.

Note that BEMc is derived from the Caputo-type representation, while BEMrm is based on the Riesz-Marchaud representation. As discussed in Chapter 2, a conjecture is that, as the domain is enlarged, numerical results calculated by BEMc and BEMrm may become

closer.

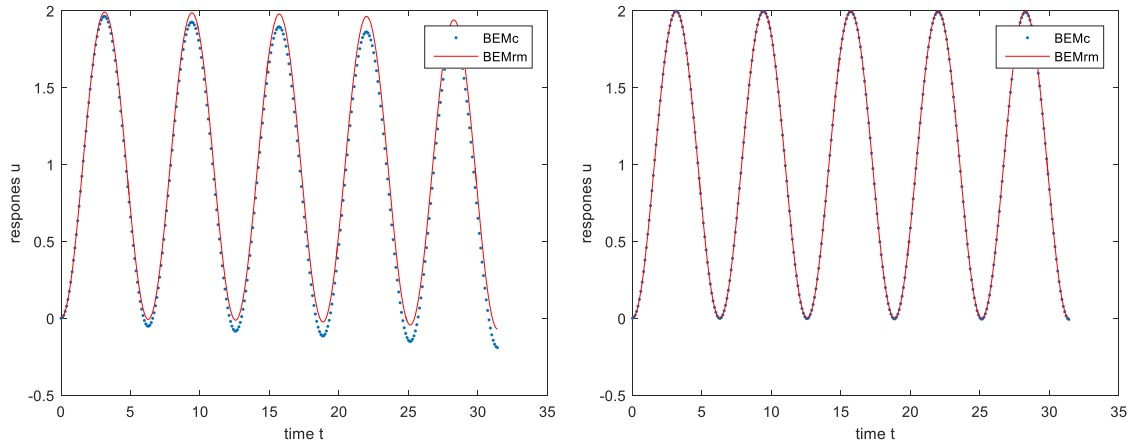


Fig. 4.4. Response calculated by BEMc and BEMrm with $\alpha = 1.7$ on a 100×50 rectangular plate (left) and a 1000×500 rectangular plate (right).

It is shown that numerical results calculated by BEMc and BEMrm are closer as the domain size increases.

Example 4.2 Consider a stochastic fractional diffusion equation on a rectangular plate with same boundary and initial condition,

$$\dot{u} + (-\Delta)^{\alpha/2} u = p(x, y) f(t). \quad (4.51)$$

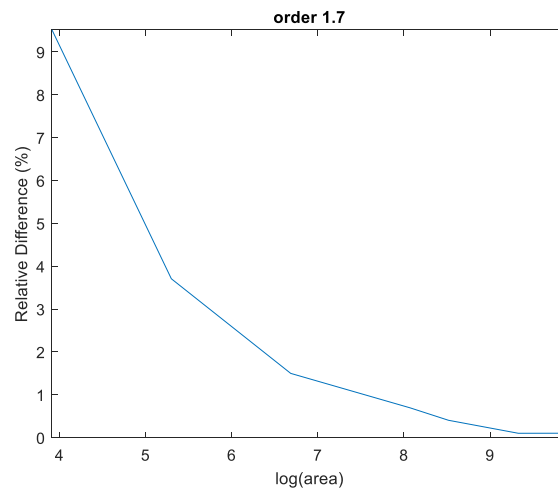


Fig. 4.5. Relative difference of the variance of the response calculated by BEMc and BEMrm with $\alpha = 1.7$.

$f(t)$ is a broad-band noise that is generated with the power spectral density $S(\omega)=1$ for $0 < \omega \leq 10\pi$, $S(\omega = 0) = 0$, and $p(x, y)=1$. The domain is meshed into 75 elements while the boundary into 200 elements. Compute the variance of the response at the point (0, 0) by BEMrm and BEMc with different area of the plate. The relative error of the results from two methods are in Fig. 4.5.

4.6 Synopsis

In this Chapter, first, a proof was given to show that the Caputo-type fractional Laplacian converges to the standard Laplace operator as the fractional order tends to 2. This part supplies the theory about the Caputo-type representation introduced by Chen and Holm in 2004. Next, a BEM-based algorithms was developed for the fractional Poisson equation. In BEMc, the analog equation is first established with the unknown load being calculated by the boundary element method. The Caputo-type representation of the fractional Laplacian of the response was then calculated. Compared with the standard problem, there is an additional non-diagonal matrix to construct in the algorithm, which renders the nonlocal property of the fractional Laplacian operator. Although the theory and the numerical method were discussed in two-dimension, it was pointed out that it is can also be applied in three-dimensional cases.

Chapter 5

Modal Expansion and Statistical Linearization Methods for Fractional Diffusion Equation

5.1 Preliminary Remark

A modal expansion of the fractional Laplacian and the statistical linearization method are developed in this chapter. These methods are applied to a fractional diffusion. They can be used for frequency-domain analysis of the dynamic systems with the fractional Laplacian. The proposed method allows calculating approximately, albeit iteratively, the response statistics.

First, based on the Caputo-type representation, a new non-orthogonal mode expansion of the fractional Laplacian is proposed, which accounts the boundary conditions information. A domain mesh is required for the numerical evaluation of the eigenfunctions. The first method, in which the constructed matrix is assumed to be diagonal, leads to an uncoupled system of nonlinear fractional ordinary differential equations. Such a system is derived from the original problem by applying the proposed expansion and is then linearized in a stochastic mean square sense. Further, a more general and accurate method is considered without requiring the modal orthogonality assumption, leading to a matrix ordinary differentiation equation. In both methods, the response statistics and the power spectral density are determined by an iterative procedure. Numerical results are provided to demonstrate the proposed methods. All values and variables in the examples are dimensionless, and the programming software packages are MATLAB and Mathematica.

5.2 The Non-Orthogonal Modal Expansion

Consider the two-dimensional fractional diffusion equation,

$$\dot{u}(x, y, t) + (-\Delta)^{\alpha/2} u(x, y, t) = p(x, y) f(t), \quad (5.1)$$

with proper boundary and initial conditions. When $\alpha = 2$, it corresponds to the “standard diffusion”, while the case $1 < \alpha < 2$ corresponds the “anomalous diffusion”.

This section seeks the proper eigenfunctions, or mode shapes, $z_{mn}(x, y)$, such that the fractional Laplacian in Eq. (5.1) can be represented by the series

$$(-\Delta)^{\alpha/2} u(x, y, t) = \sum_{m=1}^{\infty} \sum_{n=1}^{\infty} \lambda_{mn} w_{mn}(t) z_{mn}(x, y), \quad (5.2)$$

where $z_{mn}(x, y)$ are related to the boundary condition, and λ_{mn} are constants and $w_{mn}(t)$ are time-dependent amplitudes.

To find the proper eigenfunctions, first consider a standard heat equation. That is, suppose $\alpha = 2$ in Eq. (5.1). That is,

$$\dot{u} - \Delta u = 0. \quad (5.3)$$

The separation of variables method starts from assuming that the system response is represented as the product of two functions (Beck, Wright, Haji-Sheikh, Cole, and Amos, 2008). That is,

$$u(x, y, t) = w(t)v(x, y). \quad (5.4)$$

Substitute Eq. (5.4) into Eq. (5.3) yielding

$$\dot{w}v = w\Delta v. \quad (5.5)$$

Eq. (5.5) can then be recast as

$$\frac{\dot{w}}{w} = \frac{\Delta v}{v} = -\lambda, \quad (5.6)$$

where λ is a positive constant. From Eq. (5.6) it is seen that the eigenfunctions satisfy the equation

$$-\Delta v(x, y) = \lambda v(x, y). \quad (5.7)$$

Provided with proper boundary condition, Eq. (5.7) can be solved and the eigenfunctions can be determined. For example, consider the homogenous Dirichlet boundary condition for a rectangular plate. That is,

$$\begin{cases} u(-a, y, t) = u(a, y, t) = 0 \\ u(x, -b, t) = u(x, b, t) = 0 \end{cases} \quad (5.8)$$

Then, from the expansion Eq. (5.4),

$$\begin{cases} v(-a, y) = v(a, y) = 0 \\ v(x, -b) = v(x, b) = 0 \end{cases} \quad (5.9)$$

From the governing equation (5.7) and the boundary condition (5.9), a set of solution is found. That is,

$$v_{mn}(x, y) = \sin\left(\frac{m\pi(x+a)}{2a}\right) \sin\left(\frac{n\pi(y+b)}{2b}\right), \quad (5.10)$$

with

$$\lambda_{mn}(x, y) = \left(\frac{m\pi}{2a}\right)^2 + \left(\frac{n\pi}{2b}\right)^2, \quad (5.11)$$

where $m, n = 1, 2, 3, \dots$ Further, it is noted that the eigenfunctions are orthogonal. Without loss of generality, such orthogonality can be expressed by the equation

$$\int_{-b}^b \int_{-a}^a v_{st} v_{mn} dx dy = C \delta_{ms} \delta_{nl}, \quad (5.12)$$

with δ_{ms} denoting the Kronecker delta, and C being a constant. For the homogenous Dirichlet boundary condition, $C = ab$.

Thus, the solution of Eq. (5.3) can be expanded as

$$u(x, y, t) = \sum_{m=1}^{\infty} \sum_{n=1}^{\infty} w_{mn}(t) v_{mn}(x, y), \quad (5.13)$$

with the functions $w_{mn}(t)$ to be determined. Further the expansion of the negative standard Laplace operator is simply derived as

$$-\Delta u(x, y, t) = \sum_{m=1}^{\infty} \sum_{n=1}^{\infty} \lambda_{mn} w_{mn}(t) v_{mn}(x, y). \quad (5.14)$$

Starting from the eigenfunctions of the standard homogenous heat equation, next consider the fractional diffusion equation (5.1). Recall the two-dimensional Caputo-type fractional Laplacian with the order $1 < \alpha < 2$,

$$(-\Delta)^{\alpha/2} u(x, y) = I_2^{2-\alpha} [-\Delta u(x, y)], \quad (5.15)$$

where

$$I_2^{2-\alpha} \varphi(x, y) = c(\alpha) \int_{\Omega} \frac{\varphi(\xi, \eta)}{\sqrt{(x-\xi)^2 + (y-\eta)^2}^{\alpha}} d\xi d\eta. \quad (5.16)$$

Introduce next the function $z_{mn}(x, y)$ as

$$z_{mn}(x, y) = I_2^{2-\alpha} (v_{mn}(x, y)). \quad (5.17)$$

Then, from Eq. (5.7) and (5.15), it is clear that

$$\begin{aligned} (-\Delta)^{\alpha/2} v_{mn}(x, y) &= I_2^{2-\alpha} (-\Delta v_{mn}(x, y)) \\ &= I_2^{2-\alpha} (\lambda_{mn} v_{mn}(x, y)) \\ &= \lambda_{mn} I_2^{2-\alpha} (v_{mn}(x, y)) \\ &= \lambda_{mn} z_{mn}(x, y). \end{aligned} \quad (5.18)$$

Thus, the fractional Laplacian is represented by the expansion

$$(-\Delta)^{\alpha/2} u = \sum_{m=1}^{\infty} \sum_{n=1}^{\infty} \lambda_{mn} w_{mn}(t) z_{mn}(x, y). \quad (5.19)$$

Note the difference between Eq. (5.14) and (5.19). The mode functions of the standard Laplace operator v_{mn} 's only depend on the position of the point (x, y) , while the modes of the fractional Laplacian z_{mn} 's are defined in the integral form, which means that their values depend on the entire domain. This demonstrates the nonlocality of the fractional Laplacian. Further, the proposed eigenfunctions z_{mn} 's are not orthogonal.

5.3 Simplified Statistical Linearization Approximation

In this section the proposed expansion of the fractional Laplacian is applied to a stochastic nonlinear fractional diffusion equation. The simplified statistical linearization approximation (SL-1) is then introduced for determining the response statistics of such a system. The new representation of the fractional Laplacian allows deriving a system of nonlinear fractional ordinary differential equations which is linearized in a stochastic mean square sense. Then, the response statistics and the power spectral density are calculated by an iterative procedure.

Consider a two-dimensional fractional nonlinear diffusion equation on a rectangular plate $(-a \leq x \leq a, -b \leq y \leq b)$. That is,

$$\dot{u} + (-\Delta)^{\alpha/2} u + ku^3 = q(x, y, t), 1 < \alpha < 2. \quad (5.20)$$

The source term $q(x, y, t)$ is assumed to have the separable form

$$q(x, y, t) = p(x, y) f(t), \quad (5.21)$$

where $p(x, y)$ is deterministic and $f(t)$ is a stationary Gaussian process with given power spectral density and zero mean. The boundary condition is

$$\beta_1 u + \beta_2 \frac{\partial u}{\partial n} = \beta_3 \text{ on } \Gamma, \quad (5.22)$$

and the initial condition is

$$u(t=0) = u_0(x, y), \quad (5.23)$$

where $\beta_1, \beta_2, \beta_3$ are known functions defined on the boundary Γ . The nonlinear term is merely an example, and the proposed method is suitable for several nonlinear systems.

The eigenfunctions $z_{mn}(x, y)$ of the fractional Laplacian are defined by Eq. (5.17), which depend on the eigenfunction $v_{mn}(x, y)$ of the solution of the linear standard heat equation. Assume that approximately the orthogonality holds. That is,

$$\int_{\Omega} v_{mn} z_{sl} d\Omega = \gamma_{mn} \delta_{ms} \delta_{nl}, \quad (5.24)$$

where γ_{mn} 's are constants. Then, the values of these constants are estimated numerically by discretizing the domain, as in the proposed BEM in Chapter 3, and assuming that v_{mn} is constant in each element. Denote by $P = (x_P, y_P)$ and $Q = (x_Q, y_Q)$ two points in the domain Ω . Further, the norm is

$$|P - Q| = \sqrt{(x_P - x_Q)^2 + (y_P - y_Q)^2}. \quad (5.25)$$

Given the boundary condition (5.22), the value of $v_{mn}(x_i, y_i)$ at nodes (x_i, y_i) in i -th element can be determined by the procedure described in Section 5.2. Then the vector $\mathbf{z}_{mn} = \{z_{mn}\}$ can be calculated from the vector $\mathbf{v}_{mn} = \{v_{mn}\}$. That is,

$$\mathbf{z}_{mn} = \mathbf{M} \mathbf{v}_{mn}, \quad (5.26)$$

where the matrix \mathbf{M} is defined as the introduced matrix in the proposed BEM in Chapter 3. Specifically,

$$\mathbf{M}(i, j) = c(\alpha) \int_{\Omega_j} \frac{1}{|P_i - Q|^\alpha} d\Omega, \quad (5.27)$$

where P_i is kept constant and Q varies over the j -th element in the domain. Hence, a domain mesh is required for the evaluation of the matrix. Further, the value of γ_{mn} 's in Eq. (5.24) is estimated by numerical integration. That is,

$$\gamma_{mn} = \int_{\Omega} v_{mn} z_{mn} d\Omega. \quad (5.28)$$

Next, based on Eq. (5.13) and the propose expansion one derives

$$(-\Delta)^{\alpha/2} u = \sum_{m=1}^{\infty} \sum_{n=1}^{\infty} \omega_{mn}^2 w_{mn}(t) z_{mn}(x, y), \quad (5.29)$$

and the original equation (5.20) is recast as

$$\sum_{m,n} \dot{w}_{mn} v_{mn} + \sum_{m,n} \omega_{mn}^2 w_{mn} z_{mn} + ku^3 = pf, \quad (5.30)$$

where

$$u^3 = \left(\sum_{k_1, l_1} w_{k_1 l_1} v_{k_1 l_1} \right) \left(\sum_{k_2, l_2} w_{k_2 l_2} v_{k_2 l_2} \right) \left(\sum_{k_3, l_3} w_{k_3 l_3} v_{k_3 l_3} \right), \quad (5.31)$$

and $\omega_{mn}^2 = \lambda_{mn}$ in Eq. (5.2).

Introduce the constants

$$p_{mn} = \int_{\Omega} v_{mn} p d\Omega, \quad (5.32)$$

and

$$I(m, n, k_1, l_1, k_2, l_2, k_3, l_3) = \int_{\Omega} v_{mn} v_{k_1 l_1} v_{k_2 l_2} v_{k_3 l_3} d\Omega, \quad (5.33)$$

so that

$$\begin{aligned} \int_{\Omega} v_{mn} u^3 d\Omega &= \int_{\Omega} v_{mn} \left(\sum_{k_1, l_1} w_{k_1 l_1} v_{k_1 l_1} \right) \left(\sum_{k_2, l_2} w_{k_2 l_2} v_{k_2 l_2} \right) \left(\sum_{k_3, l_3} w_{k_3 l_3} v_{k_3 l_3} \right) d\Omega \\ &= \sum_{k_1, l_1} \sum_{k_2, l_2} \sum_{k_3, l_3} I(m, n, k_1, l_1, k_2, l_2, k_3, l_3) w_{k_1 l_1} w_{k_2 l_2} w_{k_3 l_3}. \end{aligned} \quad (5.34)$$

Integrate both sides of Eq. (5.30) by function v_{mn} . Then, based on the assumption of orthogonality (Eq. (5.12) and (5.24)), the equation

$$\dot{w}_{mn} + \bar{\omega}_{mn}^2 w_{mn} + \frac{k}{ab} \sum_{k_1, l_1} \sum_{k_2, l_2} \sum_{k_3, l_3} I(m, n, k_1, l_1, k_2, l_2, k_3, l_3) w_{k_1 l_1} w_{k_2 l_2} w_{k_3 l_3} = \frac{p_{mn}}{ab} f \quad (5.35)$$

is obtained, where the constants are

$$\bar{\omega}_{mn}^2 = \frac{\gamma_{mn} \omega_{mn}^2}{ab}. \quad (5.36)$$

Apply the statistical linearization method, where the equivalent linearized equation is expected to be

$$\dot{w}_{mn} + \omega_{eq,mn}^2 w_{mn} = \frac{P_{mn}}{ab} f. \quad (5.37)$$

The quantity $\omega_{eq,mn}^2$ is determined by minimizing the error between the nonlinear and linear equations in mean square sense. That is,

$$\frac{d}{d(\omega_{eq,mn}^2)} \langle \varepsilon_{mn}^2 \rangle = 0, \quad (5.38)$$

with ε_{mn} being the error,

$$\begin{aligned} \varepsilon_{mn} &= \omega_{eq,mn}^2 w_{mn} - \bar{\omega}_{mn}^2 w_{mn} \\ &+ \frac{k}{ab} \sum_{k_1, l_1} \sum_{k_2, l_2} \sum_{k_3, l_3} I(m, n, k_1, l_1, k_2, l_2, k_3, l_3) w_{k_1 l_1} w_{k_2 l_2} w_{k_3 l_3}. \end{aligned} \quad (5.39)$$

Note that Eq. (5.35) is a coupled system, while Eq. (5.37) is decoupled. This theory is given by Elishakoff and Fang in 1995.

Substituting Eq. (5.39) into Eq. (5.38), and after some algebra manipulation, the equation

$$\begin{aligned} \frac{d}{d(\omega_{eq,mn}^2)} \langle \varepsilon_{mn}^2 \rangle &= 2\omega_{eq,mn}^2 \langle w_{mn}^2 \rangle - 2\bar{\omega}_{mn}^2 \langle w_{mn}^2 \rangle \\ &- \frac{2k}{ab} \sum_{k_1, l_1} \sum_{k_2, l_2} \sum_{k_3, l_3} I(m, n, k_1, l_1, k_2, l_2, k_3, l_3) \langle w_{mn} w_{k_1 l_1} w_{k_2 l_2} w_{k_3 l_3} \rangle \\ &= 0 \end{aligned} \quad (5.40)$$

is obtained. Thus,

$$\omega_{eq,mn}^2 = \bar{\omega}_{mn}^2 + \frac{k}{ab} \frac{1}{\langle w_{mn}^2 \rangle} \sum_{k_1, l_1} \sum_{k_2, l_2} \sum_{k_3, l_3} I(m, n, k_1, l_1, k_2, l_2, k_3, l_3) \langle w_{mn} w_{k_1 l_1} w_{k_2 l_2} w_{k_3 l_3} \rangle. \quad (5.41)$$

From Eq. (5.41), the quantity $\omega_{eq,mn}^2$ cannot be calculated explicitly. Hence an iterative method is applied. Define

$$S_{mns} = \int_{-\infty}^{\infty} H_{mn}(i\omega) S_f(\omega) H_{sl}(-i\omega) d\omega, \quad (5.42)$$

where S_f is the given power spectral density of $f(t)$ with the transfer function represented as

$$H_{mn}(i\omega) = \frac{1}{i\omega + \omega_{eq,mn}^2}. \quad (5.43)$$

Then, based on the property of normal distribution, the following equality is given by Seide (1976).

$$\begin{aligned} & \langle f(t-\tau_1) f(t-\tau_2) f(t-\tau_3) f(t-\tau_4) \rangle \\ &= \langle f(t-\tau_1) f(t-\tau_2) \rangle \langle f(t-\tau_3) f(t-\tau_4) \rangle \\ &+ \langle f(t-\tau_1) f(t-\tau_3) \rangle \langle f(t-\tau_2) f(t-\tau_4) \rangle \\ &+ \langle f(t-\tau_1) f(t-\tau_4) \rangle \langle f(t-\tau_2) f(t-\tau_3) \rangle. \end{aligned} \quad (5.44)$$

Thus, the related expected values in Eq. (5.41) are determined by the following equations:

$$\langle w_{mn}^2 \rangle = \left(\frac{p_{mn}}{ab} \right)^2 S_{mmmm}, \quad (5.45)$$

and

$$\begin{aligned} & \langle w_{mn} w_{k_1 l_1} w_{k_2 l_2} w_{k_3 l_3} \rangle \\ &= \frac{P_{mn} P_{k_1 l_1} P_{k_2 l_2} P_{k_3 l_3}}{(ab)^4} (S_{mnk_1 l_1} S_{k_2 l_2 k_3 l_3} + S_{mnk_2 l_2} S_{k_1 l_1 k_3 l_3} + S_{mnk_3 l_3} S_{k_1 l_1 k_2 l_2}). \end{aligned} \quad (5.46)$$

Hence,

$$\begin{aligned} \omega_{eq,mn}^2 &= \bar{\omega}_{mn}^2 \\ &+ \frac{k}{(ab)^3} \frac{1}{P_{mn} S_{mmmm}} \sum_{k_1, l_1} \sum_{k_2, l_2} \sum_{k_3, l_3} I(m, n, k_1, l_1, k_2, l_2, k_3, l_3) P_{k_1 l_1} P_{k_2 l_2} P_{k_3 l_3} (S_{mnk_1 l_1} S_{k_2 l_2 k_3 l_3} \\ &+ S_{mnk_2 l_2} S_{k_1 l_1 k_3 l_3} + S_{mnk_3 l_3} S_{k_1 l_1 k_2 l_2}). \end{aligned} \quad (5.47)$$

Then from Eq. (5.47), (5.42) and (5.43), the value of $\omega_{eq,mn}^2$ can be determined by the iterative method. The algorithm involves, starting from an initial value of $\omega_{eq,mn}^2 = \bar{\omega}_{mn}^2$,

calculating $H_{mn}(i\omega)$ and S_{mns} , and obtaining a new value of $\omega_{eq,mn}^2$ from Eq. (5.47). Clearly, iterations are required until convergence to a reasonable value is reached.

The second-order statistic of the response is estimated via the equivalent linear system Eq. (5.37), that is,

$$\begin{aligned}\sigma_u^2(x, y) &= \langle u^2(x, y, t) \rangle \\ &= \frac{1}{(ab)^2} \sum_{m,n} \sum_{s,l} p_{mn} p_{sl} v_{mn} v_{sl} \int_{-\infty}^{\infty} H_{mn}(i\omega) S_f(\omega) H_{sl}(-i\omega) d\omega.\end{aligned}\quad (5.48)$$

Further, the spectral density of the response is evaluated by

$$S_u(x, y, \omega) = \frac{1}{(ab)^2} S_f(\omega) \sum_{m,n} \sum_{s,l} p_{mn} p_{sl} v_{mn} v_{sl} H_{mn}(i\omega) H_{sl}(-i\omega).\quad (5.49)$$

Note that the matrix \mathbf{M} in Eq. (5.30) may involve singular integrals for the diagonal terms, i.e. when P_i is in the element Ω_i . For their evaluation, the method of Chen and Pang (2016) is applied, which is shown in Chapter 3.

5.4 Complete Statistical Linearization Method

Compared with SL-1, the complete statistical linearization method (SL-2) proposed in this section requires more computations and numerical integrations but is strictly derived from the non-orthogonal eigenfunctions. Next the idea to remove the orthogonality assumption of the eigenfunctions of the fractional Laplacian is pursued (Malara, Jiao and Spanos, 2018).

Consider the same system as in Eq. (5.20). The eigenfunctions z_{mn} and v_{mn} are calculated by discretization of the domain as in Section 5.3, as well as the constants ω_{mn}^2 . In this regard, introduce the quantities

$$\gamma_{mn,sl} = \int_{\Omega} v_{mn} z_{sl} d\Omega,\quad (5.50)$$

and

$$\beta_{mn,sl} = \frac{\omega_{sl}^2 \gamma_{mn,sl}}{ab}. \quad (5.51)$$

Note that the difference between Eq. (5.50) and Eq. (5.25), for the orthogonality does not exist and there are more constants to be calculated. Similarly, $\gamma_{mn,sl}$ is calculated numerically based on the discretization of the domain.

Substituting the proposed expansion of Eq. (5.26) into Eq. (5.20) and integrating both sides with v_{mn} , the nonlinear ordinary differential equations

$$\dot{w}_{mn} + \sum_{s,l} \beta_{mn,sl} w_{sl} + \frac{k}{ab} \int_{\Omega} v_{mn} \left(\sum_{s,l} w_{sl} v_{sl} \right)^3 d\Omega = \frac{p_{mn}}{ab} f(t), \quad (5.52)$$

are obtained for $m, n = 1, 2, \dots, \infty$, which describes the time variation of $w_{mn}(t)$.

Note that Eq. (5.52) is different from Eq. (5.34) because of the existence of summation $\sum_{s,l} \beta_{mn,sl} w_{sl}$. Thus, Eq. (5.52) constitutes a system of nonlinear fractional differential equations. In matrix form, they can be written as

$$\mathbf{I}\dot{\mathbf{w}} + \mathbf{K}\mathbf{w} + \mathbf{g}(\mathbf{w}) = \mathbf{q}, \quad (5.53)$$

where \mathbf{w} is the vector containing w_{mn} and \mathbf{I} is the identity matrix and

$$\mathbf{K}(i, j) = \beta_{i,j} = \beta_{mn,sl}, \quad (5.54)$$

To simplify the algebraic expression, denote the index by $i = (m, n), j = (s, l)$. Further, in Eq. (5.53), the vector functions are defined as

$$g_i = \frac{k}{ab} \int_{\Omega} v_{mn} \left(\sum_{s,l} w_{sl} v_{sl} \right) d\Omega, \quad (5.55)$$

and

$$q_i = \frac{p_i}{ab} f(t). \quad (5.56)$$

An approximate solution of Eq. (5.53) can then be sought by statistical linearization, involving replacing it with the equivalent linear system

$$\mathbf{I}\dot{\mathbf{w}} + (\mathbf{K} + \mathbf{K}_{eq})\mathbf{w} = \mathbf{q}. \quad (5.57)$$

The optimal equivalent matrix \mathbf{K}_{eq} is determined by minimizing the difference between the nonlinear and linear system

$$\langle \boldsymbol{\varepsilon}^T \boldsymbol{\varepsilon} \rangle = \text{minimum}, \quad (5.58)$$

where the difference is defined as

$$\boldsymbol{\varepsilon} = \mathbf{g}(\mathbf{w}) - \mathbf{K}_{\text{eq}} \mathbf{w} = \left\{ \mathbf{g}_i - \sum_j K_{ij}^e w_j \right\} = \{\varepsilon_i\}. \quad (5.59)$$

The necessary conditions for this minimization problem are

$$\frac{\partial}{\partial K_{ij}^e} \langle \boldsymbol{\varepsilon}^T \boldsymbol{\varepsilon} \rangle = 0, \quad (5.60)$$

where K_{ij}^e is the (i, j) element of \mathbf{K}_{eq} .

Note that the excitation \mathbf{q} in Eq. (5.53) and (5.57) is a Gaussian random vector. Thus, combining Gaussian approximation of the response and Eq. (5.60) yields

$$K_{ij}^e = \left\langle \frac{\partial g_i}{\partial w_j} \right\rangle. \quad (5.61)$$

Substituting Eq. (5.55) into Eq. (5.61), \mathbf{K}_{eq} can be determined by the equation

$$K_{ij}^e = \frac{3k}{ab} I_{i,j,j,j} \langle w_j^2 \rangle + \frac{6k}{ab} \sum_{l \neq j} I_{i,j,j,l} \langle w_j w_l \rangle + \frac{3k}{ab} \sum_{l_1 \neq j} \sum_{l_2 \neq j} I_{i,j,l_1,l_2} \langle w_{l_1} w_{l_2} \rangle, \quad (5.62)$$

where

$$I_{i,l_1,l_2,l_3} = \int_{\Omega} v_i v_{l_1} v_{l_2} v_{l_3} d\Omega. \quad (5.63)$$

Since $f(t)$ is a stationary Gaussian process with given spectrum, if the first n modes are considered, the spectral density matrix of \mathbf{q} can be represented by

$$\mathbf{S}_q(\omega) = \begin{bmatrix} S_{q_1 q_1}(\omega) & \cdots & S_{q_1 q_n}(\omega) \\ \vdots & \ddots & \vdots \\ S_{q_n q_1}(\omega) & \cdots & S_{q_n q_n}(\omega) \end{bmatrix}. \quad (5.64)$$

Then, the spectral density matrix of the response \mathbf{w} in Eq. (5.57) is

$$\begin{aligned} \mathbf{S}_w(\omega) &= \begin{bmatrix} S_{w_1 w_1}(\omega) & \cdots & S_{w_1 w_n}(\omega) \\ \vdots & \ddots & \vdots \\ S_{w_n w_1}(\omega) & \cdots & S_{w_n w_n}(\omega) \end{bmatrix} \\ &= \mathbf{H}(i\omega) \mathbf{S}_q(\omega) \mathbf{H}^{T*}(i\omega), \end{aligned} \quad (5.65)$$

where $\mathbf{H}(i\omega)$ is the of frequency response matrix

$$\mathbf{H}(i\omega) = \left[i\omega \mathbf{I} + (\mathbf{K} + \mathbf{K}_{\text{eq}}) \right]^{-1}. \quad (5.66)$$

Thus, from Eq. (5.62) and input-output relationship, \mathbf{K}_{eq} is computed as

$$K_{ij}^e = \frac{3k}{ab} I_{i,j,j,j} S_{w_j w_j} + \frac{6k}{ab} \sum_{l \neq j} I_{i,j,j,l} S_{w_j w_l} + \frac{3k}{ab} \sum_{l_1 \neq j} \sum_{l_2 \neq j} I_{i,j,l_1,l_2} S_{w_{l_1} w_{l_2}}. \quad (5.67)$$

The numerical calculation of the equivalent matrix \mathbf{K}_{eq} can be pursued by an iterative method based on Eq. (5.65), (5.66) and (5.67). Then, via the equivalent linear system, the variance of the response in the original system Eq. (5.20) is estimated by the equation

$$\sigma_u^2(x, y) = \sum_{i=1} \sum_{j=1} v_i v_j \int_{-\infty}^{\infty} S_{w_i w_j}(\omega) d\omega, \quad (5.68)$$

and the power spectral density of the response at a certain point is

$$S_u(x, y, \omega) = \sum_{i=1} \sum_{j=1} v_i v_j S_{w_i w_j}(\omega). \quad (5.69)$$

5.5 Examples

Example 5.1 Consider a linear stochastic fractional diffusion equation on a rectangular plate ($-5 \leq x \leq 5, -2.5 \leq y \leq 2.5$),

$$\dot{u} + (-\Delta)^{\alpha/2} u = p(x, y) f(t), \quad (5.70)$$

with Dirichlet boundary condition

$$u = 0 \text{ on } \Gamma, \quad (5.71)$$

and initial condition

$$u(x, y, t = 0) = 0. \quad (5.72)$$

The time-dependent part $f(t)$ of the load is white noise, while the determinant spatial part is a constant, $p(x, y) = 1$.

The BEMc and modal expansion are applied to compute the variance and spectral density of the response. In the simulation, based on the algorithm in Chapter 3, a broad-band noise is generated with the power spectral density of the white noise is $S(\omega) = 0.5$ for $0 < \omega \leq 20\pi$ and $S(\omega = 0) = 0$. The domain is meshed into 75 elements while the boundary into 200 elements. For this Dirichlet boundary condition, the eigenfunctions and eigenvalues in the expansion of the response are given in Eq. (5.10) and (5.11). In this example, the first 81 eigenfunctions are used in calculation.

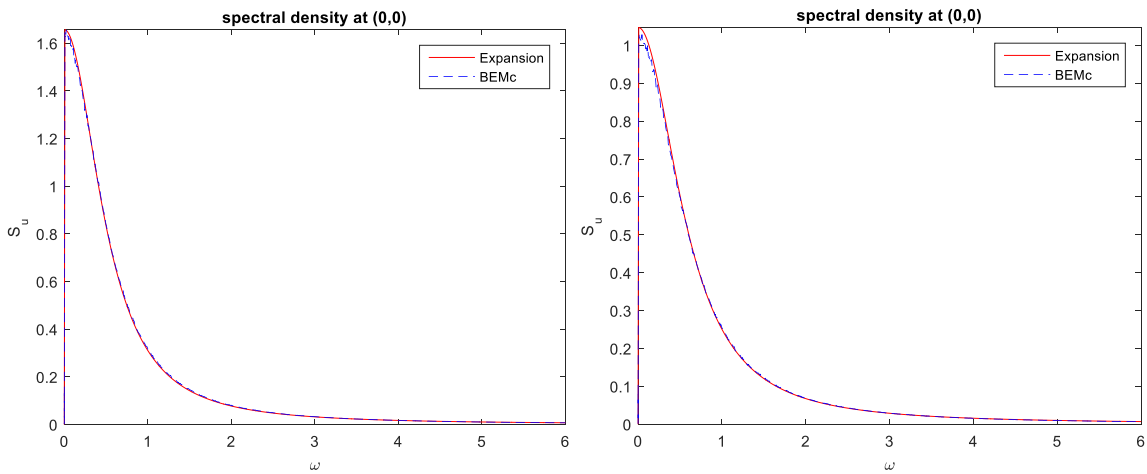


Fig. 5.1. Power spectral density of the response when $\alpha = 1.9$ (left) and $\alpha = 1.7$ (right).

Fig. 5.1 shows the spectrum of the response at the point (0,0), calculated by non-orthogonal expansion and BEMc, with fractional order 1.9 and 1.7 of the fractional Laplacian. As shown, the numerical results match well. It can be seen that the power spectral densities calculated by the proposed expansion and Monte Carlo simulation based on the BEMc are very close.

Example 5.2 Consider a stochastic nonlinear fractional diffusion equation with same boundary and initial conditions,

$$\dot{u} + (-\Delta)^{\alpha/2} u + ku^3 = p(x, y) f(t). \quad (5.73)$$

The time-dependent part of the input is white noise $f(t)$. The proposed method SL-1 and SL-2 are applied to the system.

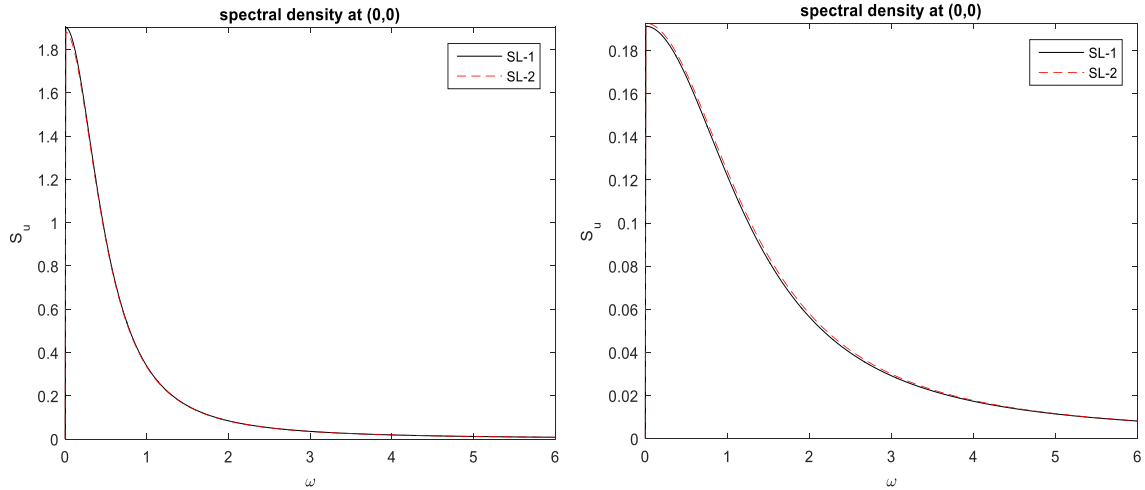


Fig. 5.2. Power spectral density of the response calculated by SL-1 and SL-2 (36 mode shapes) with $k = 0, \alpha = 1.95$ (left) and $k = 1, \alpha = 1.9$ (right).

It is seen that two statistical linearization algorithms give close results. In SL-1, there is less numerical calculation, while in SL-2, the non-orthogonality of the eigenfunctions are taken into consideration.

Next, apply BEMc to this problem with different parameters. The results are shown in Fig. 5.3 and Fig. 5.4.

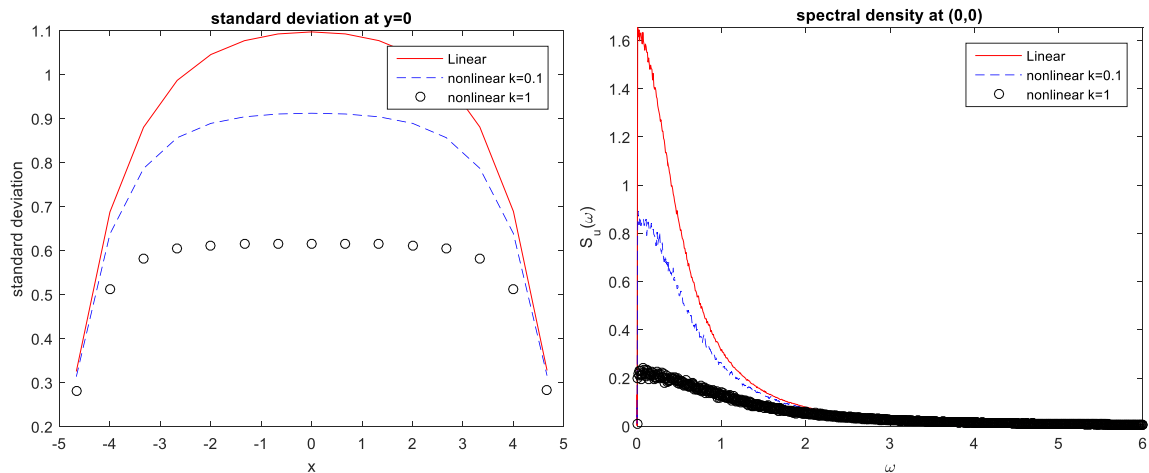


Fig. 5.3. Standard deviation of the response u along the line $y=0$ and the power spectral density of u at the point $(0,0)$ with white noise input and fractional order 1.9. The values of coefficient of the nonlinear term are: $k=0$ linear (continuous line); $k=0.1$ (dashed line); $k=1$ (circles).

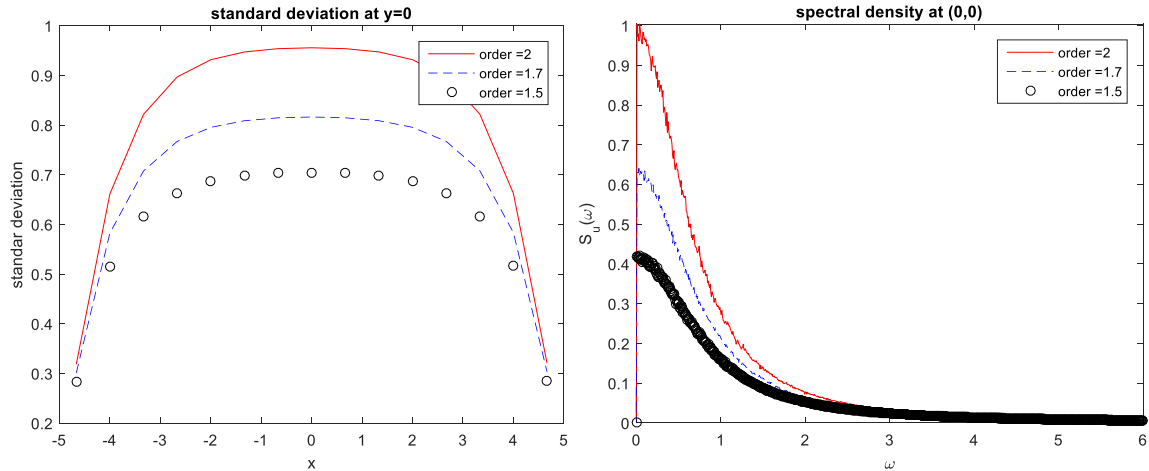


Fig. 5.4. Standard deviation of the response u along the line $y=0$ and the power spectral density of u at the point $(0,0)$ with white noise input and coefficient of the nonlinear term $k=0.1$. The values of fractional orders are: $\alpha = 2$ classical Laplacian (continuous line); $\alpha = 1.7$ (dashed line); $\alpha = 1.5$ (circles).

Fig. 5.3 and Fig. 5.4 show the BEMc-based simulation results with different nonlinear parameter and fractional Laplacian order. The left panel of each figure shows values of response standard deviation calculated by the proposed algorithm and the right panel is the spectrum of the response. The statistics of the response is well captured with different nonlinear coefficient and fractional Laplacian order.

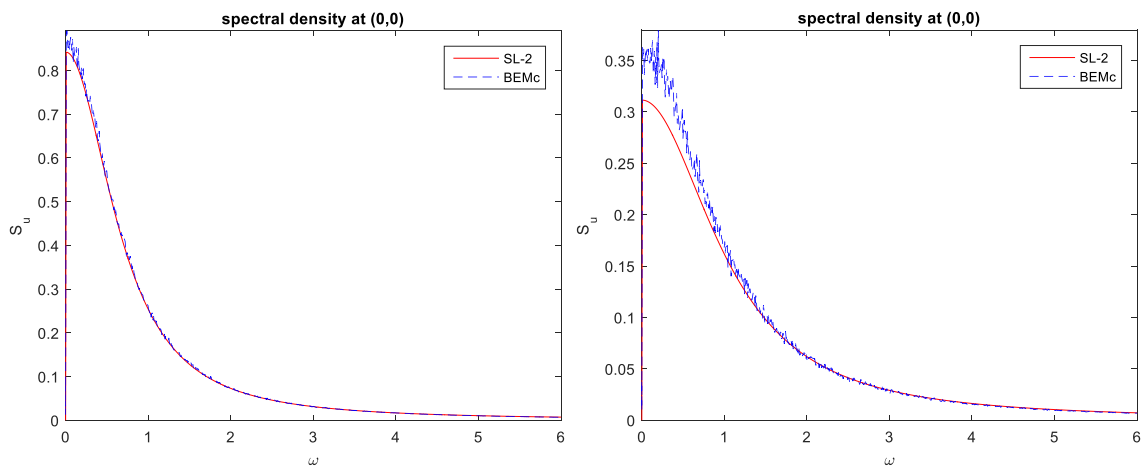


Fig. 5.5. Power spectrum of u at the point $(0,0)$ calculated by BEMc simulation and SL-2 (with 81 mode shapes) when $\alpha=1.9$. Nonlinear parameter $k = 0.1$ (left) and $k = 0.5$ (right).

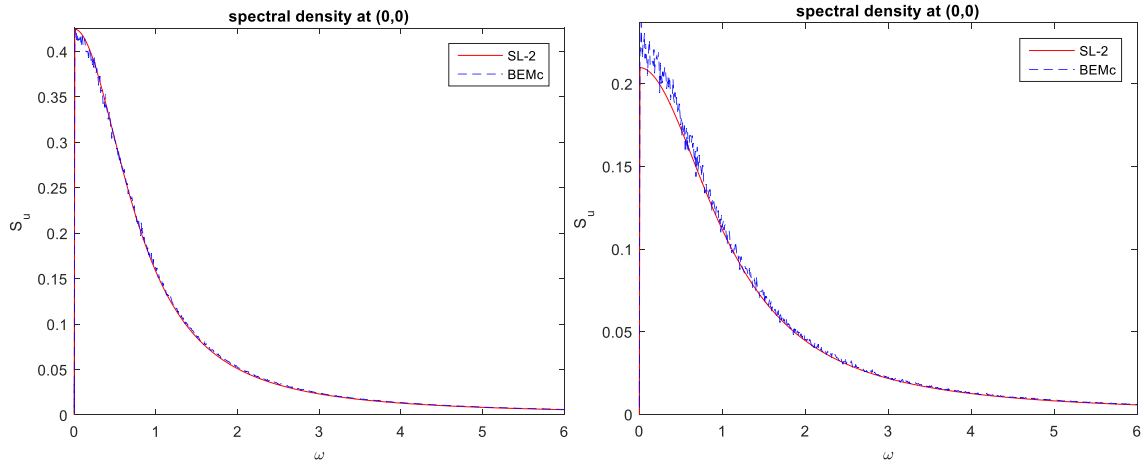


Fig. 5.6. Power spectrum calculated of u at the point $(0,0)$ by BEMc simulation and SL-2 (with 121 mode shapes) when $\alpha=1.5$. Nonlinear parameter $k = 0.1$ (left) and $k = 0.5$ (right).

Fig. 5.5 and Fig. 5.6 show a comparison of the power spectral densities calculated by SL-2 and BEMc simulation. It is seen that, for weak nonlinearity, the statistical linearization is in agreement with the numerical solution, while for a relatively strong nonlinear system ($k=0.5$), there is a small difference in the maximum value of the spectral density.

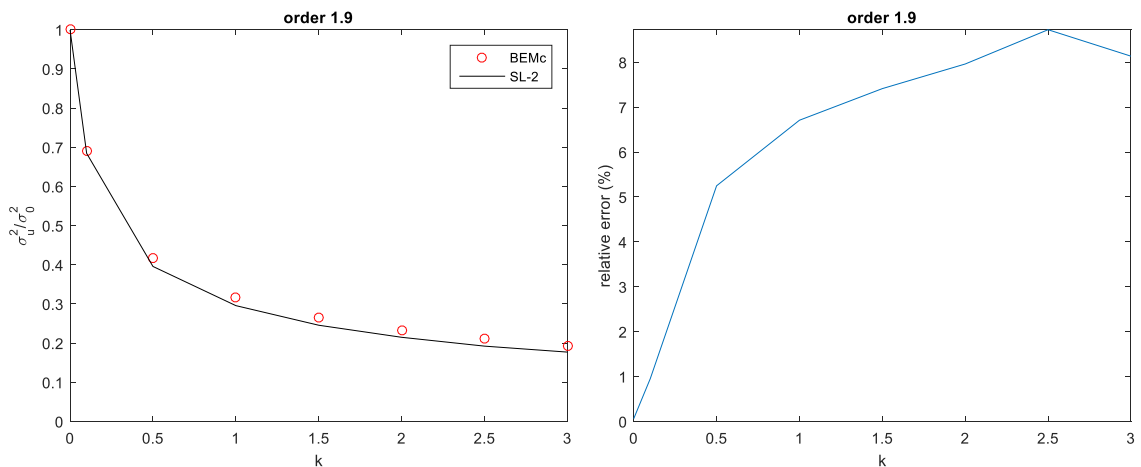


Fig. 5.7. Variance of u at the point $(0,0)$ by BEMc simulation and SL-2 (with 81 mode shapes) when $\alpha = 1.9$ (left) and relative error (right).

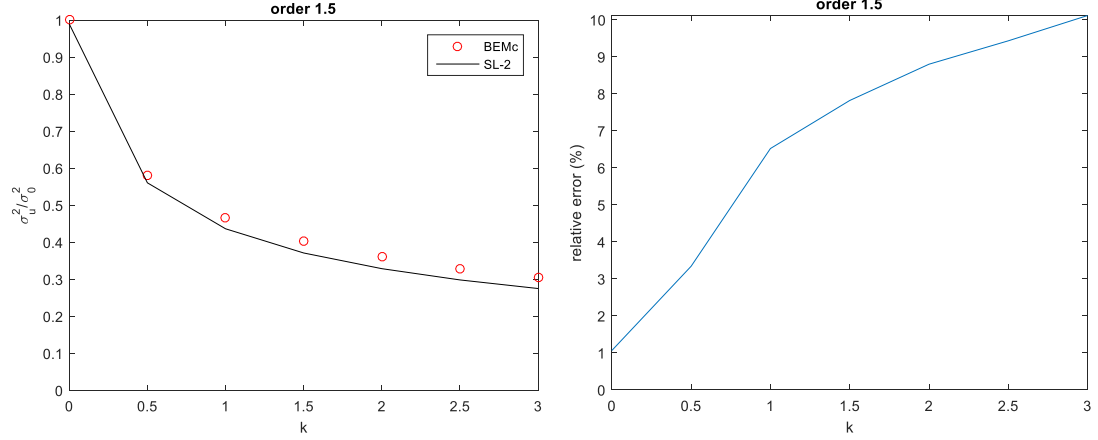


Fig. 5.8. Variance of u at the point $(0,0)$ by BEMc simulation and SL-2 (with 121 mode shapes) when $\alpha = 1.5$ (left) and relative error (right).

Fig. 5.7 and Fig. 5.8 show the variance computed by the BEMc simulation and statistical linearization-2, and the relative error of the results. σ_0^2 is the variance of the linear response calculated by the simulation. As shown in the figures, the relative error is less than 9% for $\alpha = 1.9$ and less than 11% for $\alpha = 1.5$, when the coefficient of nonlinear term $k=3$.

Example 5.3 Consider a stochastic linear fractional diffusion equation with same Dirichlet boundary condition, zero initial conditions and colored noise as part of the source term

$$\dot{u} + (-\Delta)^{\alpha/2} u + ku^3 = p(x, y) f(t). \quad (5.74)$$

The spectrum of $f(t)$ is

$$\hat{S}(w) = \frac{Cw^4}{\left[(w^2 - k_1)^2 + (c_1 w)^2 \right] \left[(w^2 - k_2)^2 + (c_2 w)^2 \right]}. \quad (5.75)$$

The parameters are set as $C = 0.46, k_1 = 0.97, c_1 = 0.20, k_2 = 3.44, c_2 = 2.32$, and $w = \omega/\omega_p$ (ω_p is the peak frequency of the spectrum). The standard deviation is 0.8 and the peak period ω_p is 5.

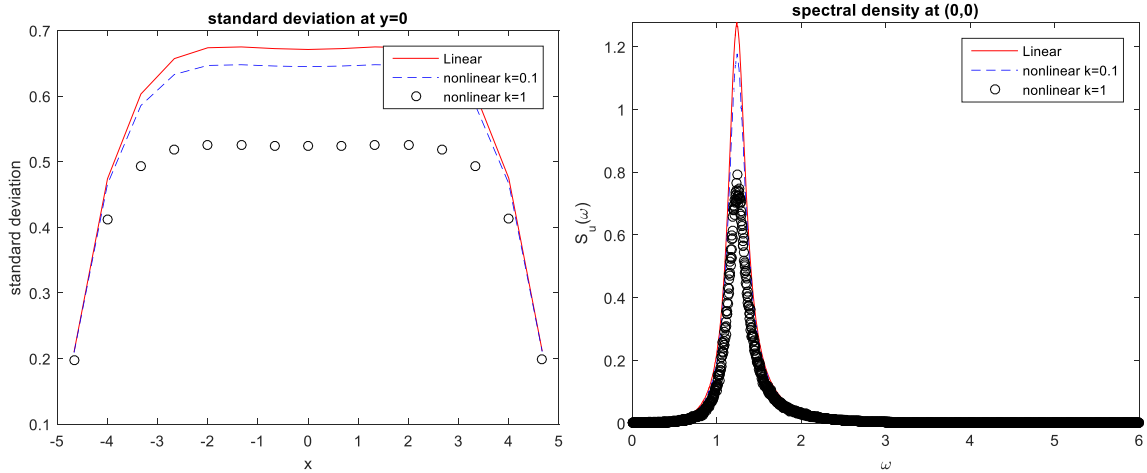


Fig. 5.9. Standard deviation of the response u along the line $y=0$ and the power spectral density of u at the point $(0,0)$ with fractional order 1.9 . The values of coefficient of the nonlinear term are: $k=0$ linear (continuous line); $k=0.1$ (dashed line); $k=1$ (circles).

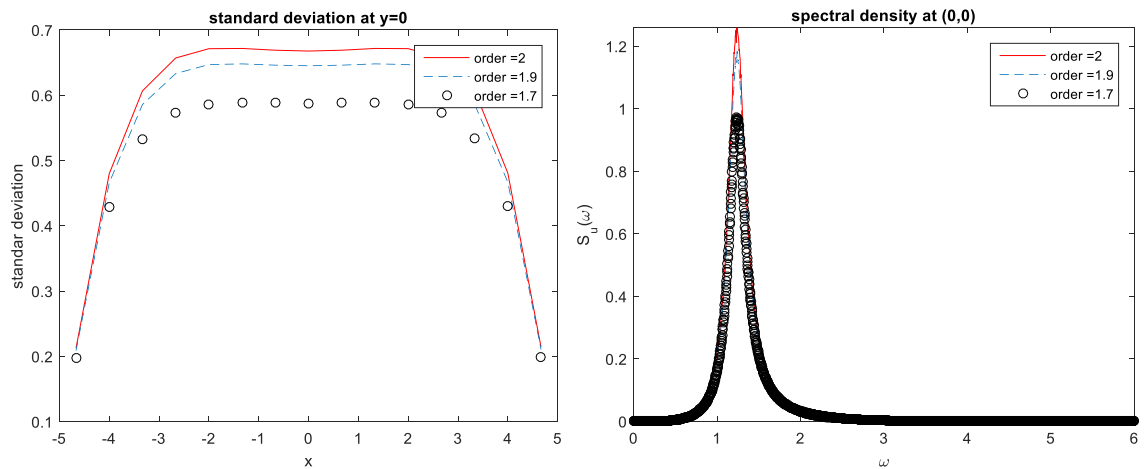


Fig. 5.10. Standard deviation of the response u along the line $y=0$ and the power spectral density of u at the point $(0,0)$ with coefficient of the nonlinear term $k=0.1$. The values of fractional orders are: $\alpha=2$ classical Laplacian (continuous line); $\alpha=1.9$ (dashed line); $\alpha=1.7$ (circles).

The BEMc-based Monte Carlo simulation result of the response spectra of the nonlinear system (5.73) given different nonlinear parameters and fractional orders are shown in Fig. 5.9 and 5.10.

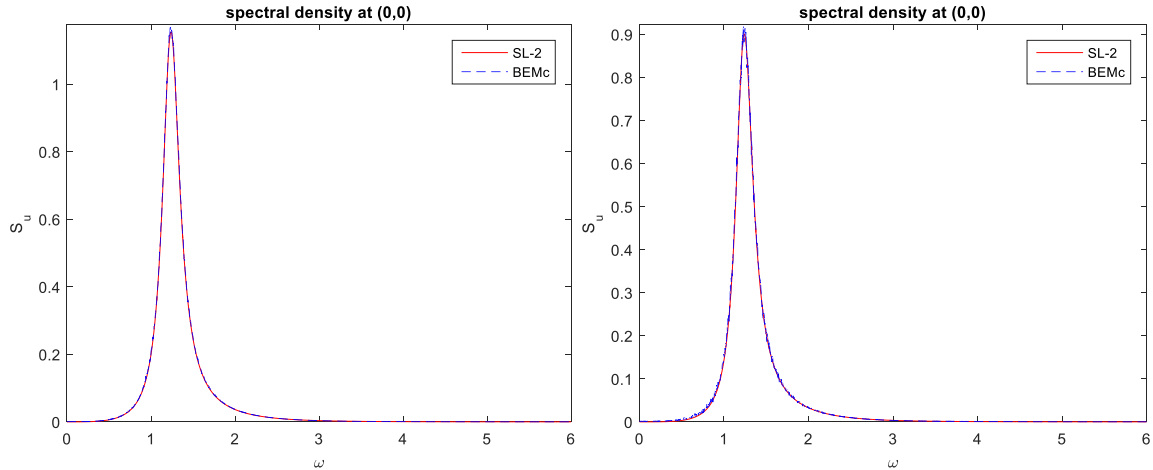


Fig. 5.11. Power spectrum of u at the point $(0,0)$ calculated by BEMc and SL-2 (with 81 mode shapes) when $\alpha=1.9$. Nonlinear parameter $k = 0.1$ (left) and $k = 0.5$ (right).

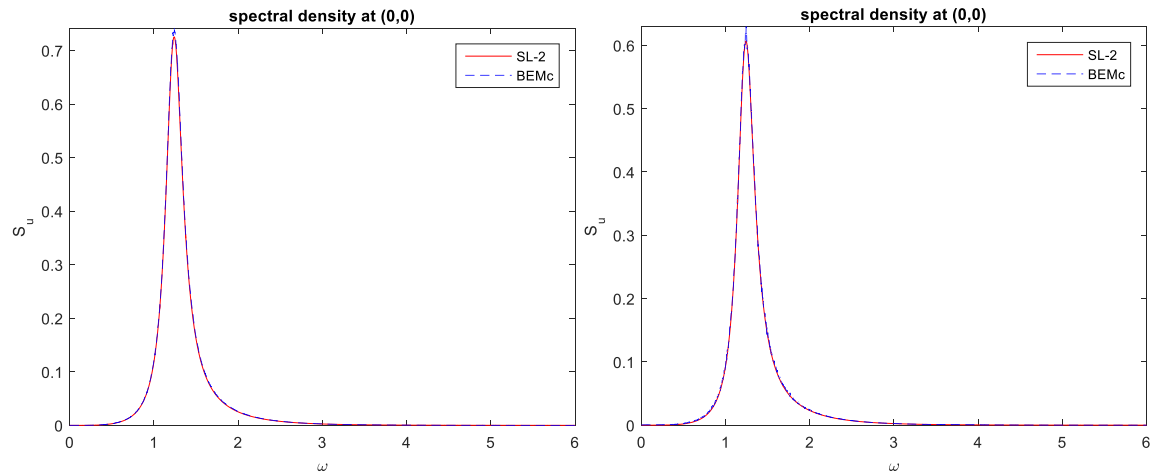


Fig. 5.12. Power spectrum calculated of u at the point $(0,0)$ by BEMc and SL-2 (with 121 mode shapes) when $\alpha=1.5$. Nonlinear parameter $k = 0.1$ (left) and $k = 0.5$ (right).

Fig. 5.11 and 5.12 show the comparison of the power spectral density of the nonlinear response calculated by the BEMc simulation and statistical linearization-2. The results are very close.

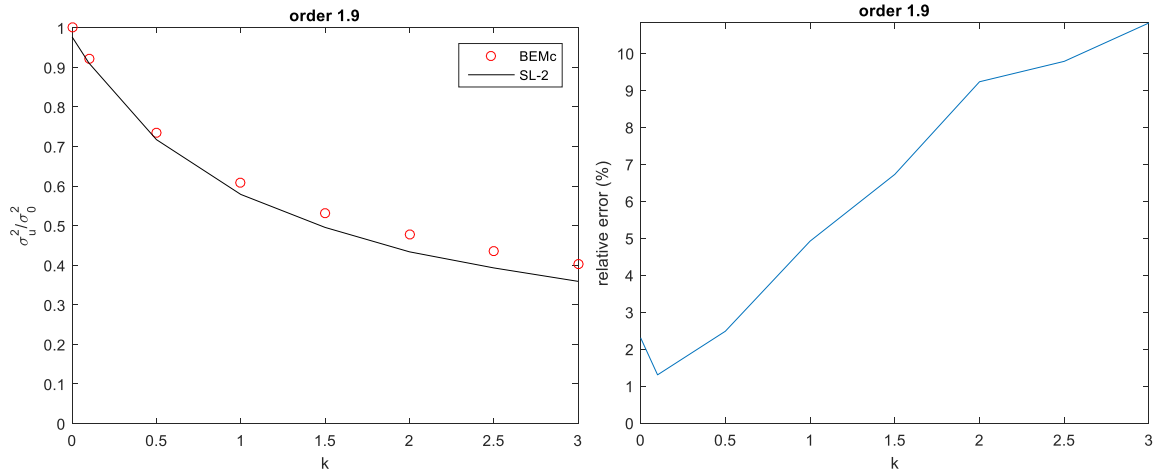


Fig. 5.13. Variance of u at the point $(0,0)$ by BEMc simulation and SL-2 (with 81 mode shapes) when $\alpha=1.9$ (left) and relative error (right).

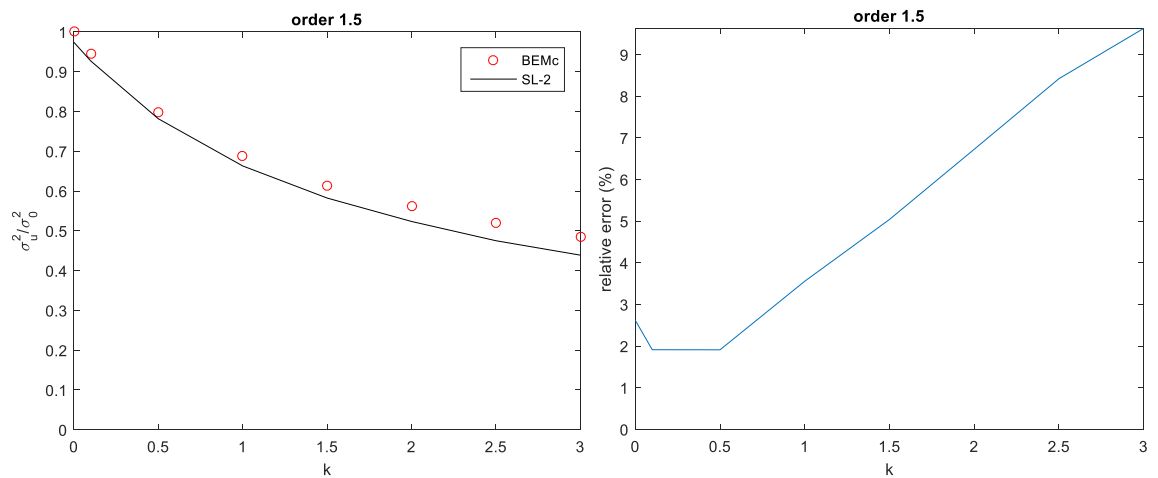


Fig. 5.14. Variance of u at the point $(0,0)$ by BEMc simulation and SL-2 (with 121 mode shapes) when $\alpha=1.5$ (left) and relative error (right).

Fig. 5.13 and Fig. 5.14 show the variance computed by BEMc simulation and statistical linearization-2, and the relative error of the results. As shown in the figures, the relative error is less than 11% for $\alpha = 1.9$ and less than 10% for $\alpha = 1.5$, when the coefficient of nonlinear term $k=3$. As the examples showed, the proposed numerical methods work well for both linear and nonlinear systems with white or colored noise.

Example 5.4 Consider the stochastic nonlinear fractional diffusion equation

$$\dot{u} + (-\Delta)^{\alpha/2} u + ku^3 = p(x, y) f(t). \quad (5.76)$$

with mixed boundary condition:

$$\frac{\partial u}{\partial n}(-a, y, t) = 0 = \frac{\partial u}{\partial n}(a, y, t), \quad (5.77)$$

$$u(x, -b, t) = 0 = u(x, b, t), \quad (5.78)$$

and initial condition

$$u(x, y, t = 0) = 0. \quad (5.79)$$

The time-dependent part $f(t)$ of the load is white noise, while the determinant spatial part is a constant, $p(x, y) = 1$. An illustration of the domain and mixed boundary conditions is provided in Fig. 5.15.

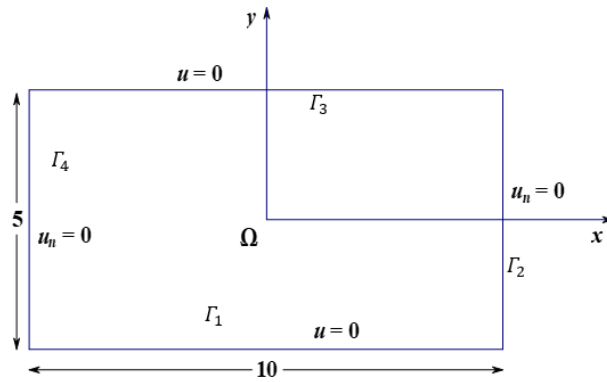


Fig. 5.15. Rectangular domain with mixed boundary condition.

The eigenfunctions of the response and fractional Laplacian are obtained by the same way introduced in Section 5.2. That is, assume

$$u(x, y, t) = w(t)v(x, y). \quad (5.80)$$

Substitute Eq. (5.79) into

$$\dot{u} - \Delta u = 0, \quad (5.81)$$

to obtain the following equation

$$\frac{\dot{w}}{w} = \frac{\Delta v}{v} = -\lambda, \quad (5.82)$$

where λ is a positive eigenvalue. Eq. (5.81) can be recast as

$$-\Delta v(x, y) = \lambda v(x, y). \quad (5.83)$$

The boundary condition (5.76), (5.77) and Eq. (5.82) lead to the equations

$$\begin{cases} v_x(-a, y) = v_x(a, y) = 0 \\ v(x, -b) = v(x, b) = 0 \end{cases}. \quad (5.84)$$

From the governing equation (5.76) and the boundary condition (5.77), (5.78), a set of solution is obtained,

$$v_{mn}(x, y) = \cos\left(\frac{m\pi(x+a)}{2a}\right) \sin\left(\frac{n\pi(y+b)}{2b}\right), \quad (5.85)$$

and

$$\lambda_{mn}(x, y) = \left(\frac{m\pi}{2a}\right)^2 + \left(\frac{n\pi}{2b}\right)^2, \quad (5.86)$$

where $m = 0, 1, 2, \dots$, $n = 1, 2, 3, \dots$

The eigenfunctions v_{mn} satisfy the orthogonality property

$$\int_{-b}^b \int_{-a}^a v_{0l} v_{0l} dx dy = 2ab, \quad (5.87)$$

$$\int_{-b}^b \int_{-a}^a v_{mn} v_{mn} dx dy = ab, \quad m \geq 1, \quad (5.88)$$

and

$$\int_{-b}^b \int_{-a}^a v_{sl} v_{mn} dx dy = 0, \quad \text{if } s \neq m \text{ or } l \neq n. \quad (5.89)$$

Next, from the eigenfunctions v_{mn} , the non-orthogonal expansion of the fractional Laplacian is obtained,

$$(-\Delta)^{\alpha/2} u(x, y, t) = \sum_{m=1}^{\infty} \sum_{n=1}^{\infty} \lambda_{mn} w_{mn}(t) z_{mn}(x, y), \quad (5.90)$$

where

$$z_{mn}(x, y) = I_2^{2-\alpha} (v_{mn}(x, y)). \quad (5.91)$$

To evaluate the eigenfunctions z_{mn} , discretization of the domain is required.

If the eigenfunctions $z_{sl}, s = 0, 1, \dots, m, l = 1, 2, \dots, n$, are incorporated in the calculation, following the second statistical linearization method, the matrix equation is obtained

$$\mathbf{C}\dot{\mathbf{w}} + \mathbf{K}\mathbf{w} + \mathbf{g}(\mathbf{w}) = \mathbf{q}, \quad (5.92)$$

where the matrices \mathbf{K} and vector \mathbf{g} are defined in Eq. (5.53) and (5.54), respectively.

$$\mathbf{C} = \begin{bmatrix} 2\mathbf{I}_1 & \mathbf{0} \\ \mathbf{0} & \mathbf{I}_2 \end{bmatrix}, \quad (5.93)$$

where \mathbf{I}_1 and \mathbf{I}_2 are the n -dimensional and $(m-1)n$ -dimensional identity matrices, respectively.

From Eq. (5.92), the equivalent linearized equation is obtained from the statistical linearization procedure. That is,

$$\mathbf{C}\dot{\mathbf{w}} + (\mathbf{K} + \mathbf{K}_{\text{eq}})\mathbf{w} = \mathbf{q}, \quad (5.94)$$

from where the response statistics of the response can be calculated.

In the BEM, the matrix representation of the unknown boundary value by the vector to be constructed is a little complicated than the above problems with Dirichlet boundary conditions which is based on the equation.

$$\mathbf{G}_b \mathbf{b} + \hat{\mathbf{H}}_b \mathbf{u}_b = \mathbf{L}_b \mathbf{u}_{nb}. \quad (5.95)$$

Denote the four boundaries as $\Gamma_1, \Gamma_2, \Gamma_3$ and Γ_4 as shown in Fig. 5.15. On the boundary Γ_1 and Γ_3 , the value u is provided as 0, while on Γ_2 and Γ_4 , $u_n = 0$. Denote the vectors $\bar{\mathbf{u}}_{b1}$, $\bar{\mathbf{u}}_{n|b2}$, $\bar{\mathbf{u}}_{b3}$ and $\bar{\mathbf{u}}_{n|b4}$, which contain the known quantities at the nodes on the four boundaries respectively, while vectors $\mathbf{u}_{n|b1}$, \mathbf{u}_{b2} , $\mathbf{u}_{n|b3}$ and \mathbf{u}_{b4} containing the unknown quantities. Partitioning the matrices $\hat{\mathbf{H}}_b$ and \mathbf{L}_b , Eq. (5.95) is recast

$$\begin{bmatrix} \hat{\mathbf{H}}_{b1} & \hat{\mathbf{H}}_{b2} & \hat{\mathbf{H}}_{b3} & \hat{\mathbf{H}}_{b4} \end{bmatrix} \begin{Bmatrix} \bar{\mathbf{u}}_{b1} \\ \mathbf{u}_{b2} \\ \bar{\mathbf{u}}_{b3} \\ \mathbf{u}_{b4} \end{Bmatrix} + \mathbf{G}_b \mathbf{b} = \begin{bmatrix} \mathbf{L}_{b1} & \mathbf{L}_{b2} & \mathbf{L}_{b3} & \mathbf{L}_{b4} \end{bmatrix} \begin{Bmatrix} \mathbf{u}_{n|b1} \\ \bar{\mathbf{u}}_{n|b2} \\ \mathbf{u}_{n|b3} \\ \bar{\mathbf{u}}_{n|b4} \end{Bmatrix}. \quad (5.96)$$

Carry out the multiplications and move unknown boundary values to the left-hand side of the equation. That is,

$$\begin{bmatrix} -\mathbf{L}_{b1} & \hat{\mathbf{H}}_{b2} & -\mathbf{L}_{b3} & \hat{\mathbf{H}}_{b4} \end{bmatrix} \begin{Bmatrix} \mathbf{u}_{n|b1} \\ \mathbf{u}_{b2} \\ \mathbf{u}_{n|b3} \\ \mathbf{u}_{b4} \end{Bmatrix} = \begin{bmatrix} -\hat{\mathbf{H}}_{b1} & \mathbf{L}_{b2} & -\hat{\mathbf{H}}_{b3} & \mathbf{L}_{b4} \end{bmatrix} \begin{Bmatrix} \bar{\mathbf{u}}_{b1} \\ \bar{\mathbf{u}}_{n|b2} \\ \bar{\mathbf{u}}_{b3} \\ \bar{\mathbf{u}}_{n|b4} \end{Bmatrix} - \mathbf{G}_b \mathbf{b}. \quad (5.97)$$

Due to the homogenous boundary condition, and the introducing matrix,

$$\mathbf{H}^b = \begin{bmatrix} \mathbf{L}_{b1} & -\hat{\mathbf{H}}_{b2} & \mathbf{L}_{b3} & -\hat{\mathbf{H}}_{b4} \end{bmatrix}, \quad (5.98)$$

and the vector

$$\mathbf{u}^b = \begin{Bmatrix} \mathbf{u}_{n|b1} \\ \mathbf{u}_{b2} \\ \mathbf{u}_{n|b3} \\ \mathbf{u}_{b4} \end{Bmatrix}, \quad (5.99)$$

all the unknown boundary values are represented by the vector \mathbf{b} ,

$$\mathbf{u}^b = (\mathbf{H}^b)^{-1} \mathbf{G}_b \mathbf{b}. \quad (5.100)$$

Next, recall the equation

$$\mathbf{u} = \mathbf{G}_d \mathbf{b}(t) - \mathbf{L}_d \mathbf{u}_{nb} + \mathbf{H}_d \mathbf{u}_b \quad (5.101)$$

of the response at the domain. Partition the matrices \mathbf{H}_d and \mathbf{L}_d in the same way,

$$\mathbf{H}_d = [\mathbf{H}_{d1} \quad \mathbf{H}_{d2} \quad \mathbf{H}_{d3} \quad \mathbf{H}_{d4}], \quad (5.102)$$

and

$$\mathbf{L}_d = [\mathbf{L}_{d1} \quad \mathbf{L}_{d2} \quad \mathbf{L}_{d3} \quad \mathbf{L}_{d4}]. \quad (5.103)$$

Denote the matrix with the corresponding columns of the known matrices,

$$\mathbf{H}^d = [-\mathbf{L}_{d1} \quad \mathbf{H}_{b2} \quad -\mathbf{L}_{b3} \quad -\mathbf{H}_{d4}]. \quad (5.104)$$

Substituting the boundary conditions and Eq. (5.32) into Eq. (3.44), the vector \mathbf{u} is represented by \mathbf{b} ,

$$\mathbf{u} = \mathbf{M}_1 \mathbf{b}, \quad (5.105)$$

where

$$\mathbf{M}_1 = \mathbf{G}_d + \mathbf{H}^d (\mathbf{H}^b)^{-1} \mathbf{G}_b. \quad (5.106)$$

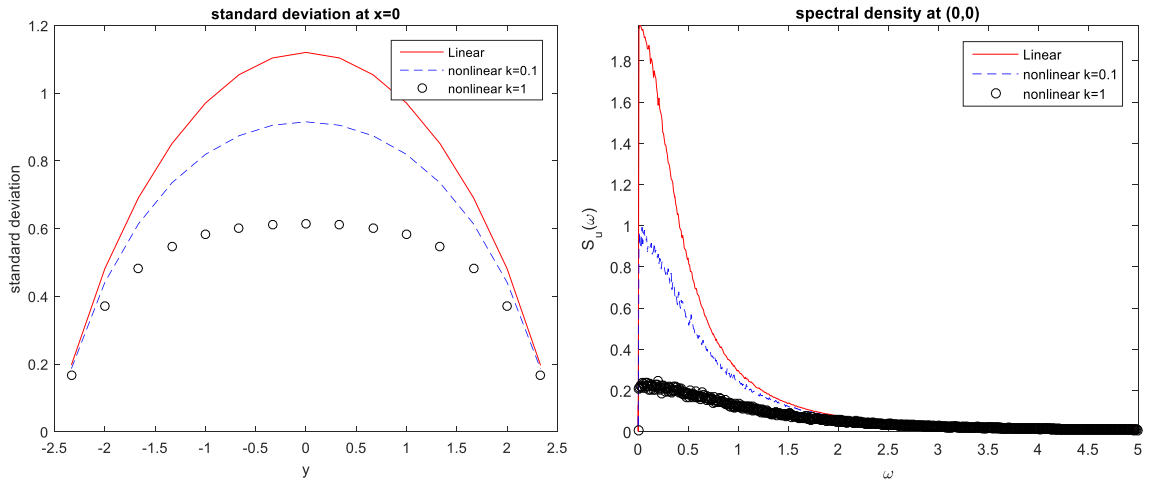


Fig. 5.16. Standard deviation of the response u along the line $x=0$ and the power spectral density of u at the point $(0,0)$ with white noise input and fractional order 1.9. The values of coefficient of the nonlinear term are: $k=0$ linear (continuous line); $k=0.1$ (dashed line); $k=1$ (circles).

Combining Eq. (5.105) with Eq. (5.108) yields,

$$(-\Delta)^{\alpha/2} \mathbf{u} = -\mathbf{M}_2 \mathbf{b}, \quad (5.107)$$

where

$$\mathbf{M}_2(i, j) = c(\alpha) \int_{\Omega_j} \frac{1}{|P_i - Q|^\alpha} d\Omega. \quad (5.108)$$

Further, substituting them into Eq. (5.76) yields,

$$\mathbf{u} - \mathbf{M}_2 \mathbf{M}_1^{-1} \mathbf{u} + k \mathbf{u}_3 = \mathbf{q}, \quad (5.109)$$

where \mathbf{u}_3 is the vector containing the values of u^3 at each node and \mathbf{q} is the vector of source terms. Eq. (5.109) is solved by the Runge-Kutta scheme.

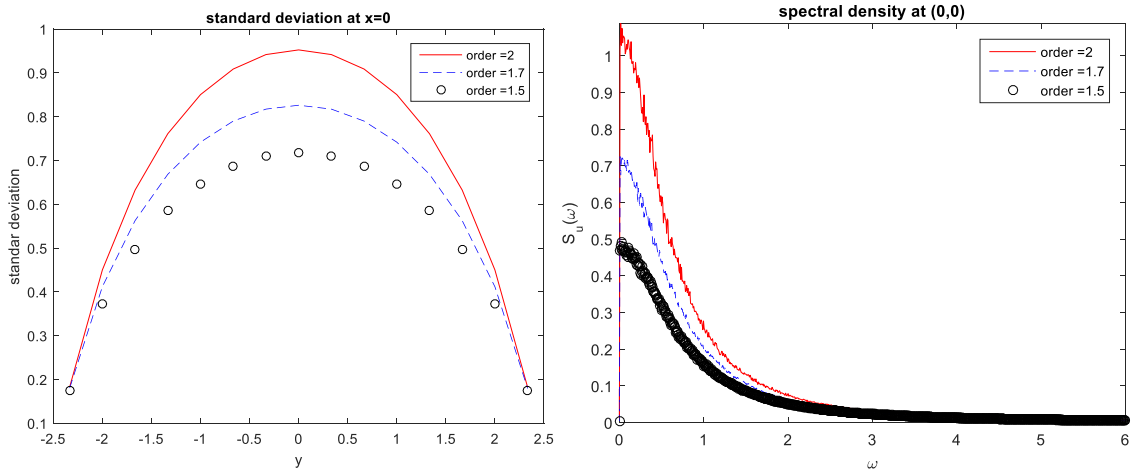


Fig. 5.17. Standard deviation of the response u along the line $x=0$ and the power spectral density of u at the point $(0,0)$ with white noise input and coefficient of the nonlinear term $k=0.1$. The values of fractional orders are: $\alpha=2$ classical Laplacian (continuous line); $\alpha=1.7$ (dashed line); $\alpha=1.5$ (circles).

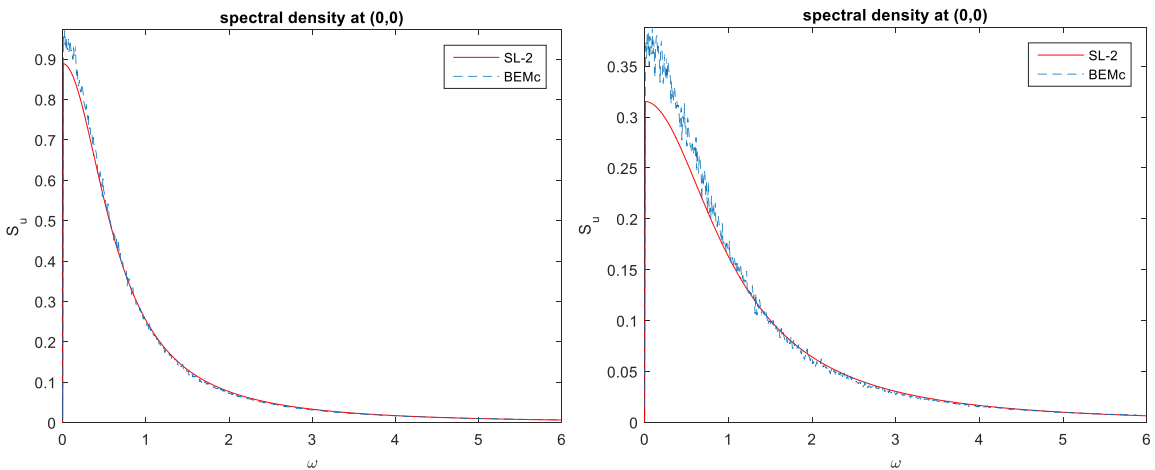


Fig. 5.18. Power spectrum of u at the point $(0,0)$ calculated by BEMc simulation and SL-2 (with 25 mode shapes) when $\alpha=1.9$. Nonlinear parameter $k=0.1$ (left) and $k=0.5$ (right).

Fig. 5.16 and Fig. 5.17 show standard deviation on the line $x=0$ and the power spectral density at the point $(0,0)$ calculated by the BEMc-based simulation results with different nonlinear parameter and fractional Laplacian order.

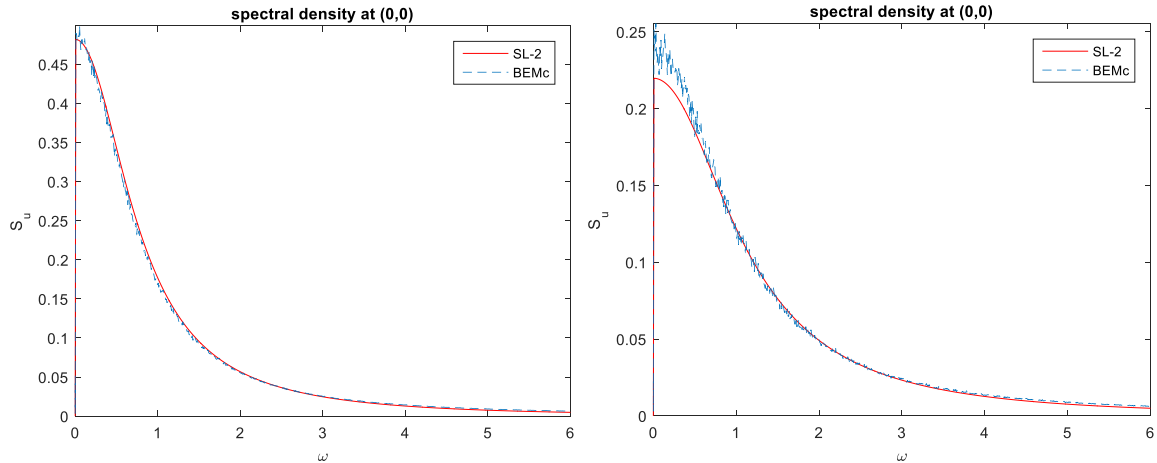


Fig. 5.19. Power spectrum calculated of u at the point $(0,0)$ by BEMc simulation and SL-2 (with 81 mode shapes) when $\alpha=1.5$. Nonlinear parameter $k = 0.1$ (left) and $k = 0.5$ (right).

Fig. 5.18 and Fig. 5.19 show the comparison of power spectral density calculated by statistical linearization method-2 and simulation based on BEMc. The left panel of each figure shows the calculated spectrum with nonlinear coefficient 0.1, while the right panel show shows the result with nonlinear coefficient 0.5.

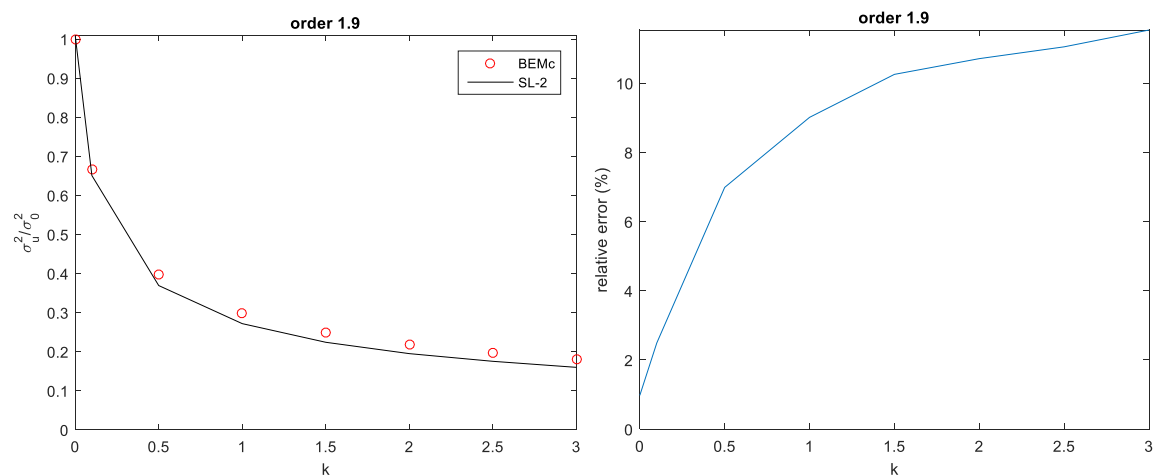


Fig. 5.20. Variance of u at the point $(0,0)$ by BEMc simulation and SL-2 (with 25 mode shapes) when $\alpha=1.9$ (left) and relative error (right).

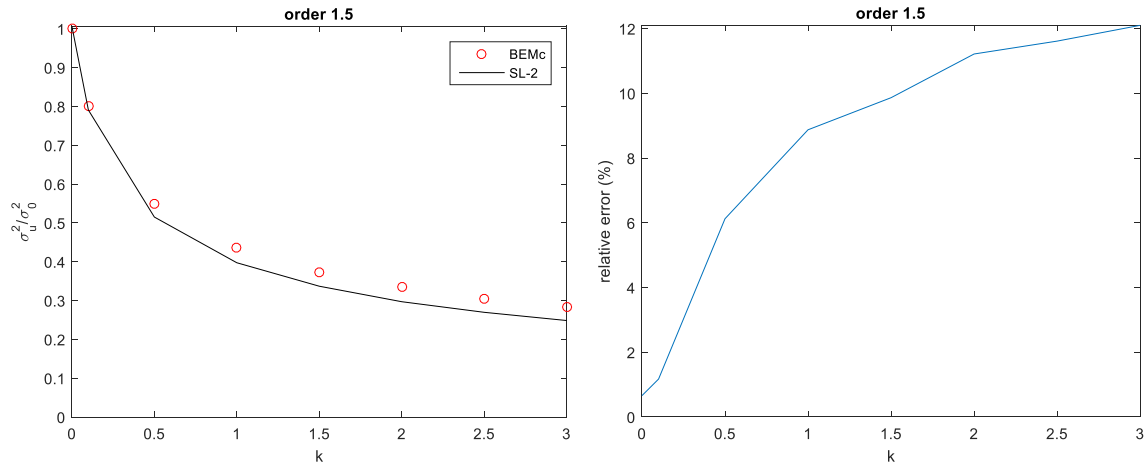


Fig. 5.21. Variance of u at the point $(0,0)$ by BEMc simulation and SL-2 (with 81 mode shapes) when $\alpha=1.5$ (left) and relative error (right).

Fig. 5.20 and Fig. 5.21 show the comparison of the variance computed by the BEMc simulation and statistical linearization-2. The relative error of the results is provided, where σ_0^2 is the variance of the linear response calculated by the simulation. As shown in the figures, the relative error is less than 12% for $\alpha = 1.9$ and about 13% for $\alpha = 1.5$, when the coefficient of nonlinear term $k=3$.

5.6 Synopsis

In this Chapter, first a method to obtain the expansion of the fractional Laplacian was proposed. The eigenfunctions were constructed via the Reisz potential of the linear modes of response in the classical diffusion equation with same boundary conditions. Evaluation of the proposed eigenfunctions and relating constants required discretization of the domain. The introduced eigenfunctions were defined in integration representation and hence is not orthogonal. Such property also pointed out the nonlocality of the fractional Laplacian.

Based on the novel eigenfunctions, frequency domain analysis of the fractional diffusion equation became feasible. Further, for the nonlinear diffusion equation endowed with a

fractional Laplacian, statistical linearization-based approaches were introduced for estimating the response of system. The first algorithm proposed in Section 5.3 is meant for a system where the order of the fractional Laplacian is close to 2. A system of nonlinear fractional ordinary differential equations describing the time-variation of the modes amplitudes was derived. Due to the assumption of orthogonality, a decoupled system was obtained.

In Section 5.4, another algorithm was introduced without orthogonality assumption, leading to a matrix differential equation. Numerical implementation of both methods requires truncation of the summation. In this context, the statistical linearization approach was implemented by minimizing a certain error in a mean square sense. The proposed methods were applied to numerical examples with different parameters to demonstrate the effectiveness.

Chapter 6

Concluding Remarks

The fractional Laplacian is the operator that is defined by a generalization of the classical Laplace operator. It can work as an interesting tool for mathematical modeling of the nonlocal behavior, such as anomalous diffusion, and nonlocal phase transitions (Bates and Chmaj, 1999). The work in this thesis focuses on the numerical analysis of diffusion equation with the fractional Laplacian. In brief, it contains three main parts: two Boundary Element Method based approaches for estimating the response a fractional diffusion equation; a modal expansion of the fractional Laplacian and frequency domain analysis of the fractional diffusion equation; two statistical linearization methods for the stochastic nonlinear dynamic system containing the fractional Laplacian.

Chapter 1 provides useful background and an outline of the thesis. The nonlocal property of the fractional derivative makes it a useful tool in engineering applications. However, most works of numerical analysis of the fractional differential equation focus on the time-derivative or one-dimensional space-derivative, while the analytical solution is not always available. Among different numerical methods, the Boundary Element Method and statistical linearization have been successfully implemented to the time-fractional partial differential equation. These two methods are further developed for the partial differential equation with the fractional Laplacian in the thesis.

Chapter 2 provides the mathematical background of the fractional Laplacian and the algorithms that can be generalized in the context. The anomalous diffusion is briefly introduced. Due to the nonlocal property of the operator, the fractional Laplacian is often defined via integration, which makes it difficult to deal with in the numerical analysis. To capture different representations of the fractional Laplacian, an implicit definition based on the Fourier transform is adopted. The Caputo-type representation is of more importance as it naturally includes the boundary conditions. Such properties make it quite useful in the application in a bounded domain. Then, the BEM and statistical linearization

method are briefly illustrated for the dynamic systems with time-fractional derivatives.

In Chapter 3, an approximate algorithm is proposed for fractional differential equation endowed with the fractional Laplacian. The algorithm BEM_{rm} is based on the Riesz-Marchaud definition. Different examples are presented to demonstrate the algorithm.

In Chapter 4, first, it is proved that Caputo-type fractional Laplacian converges to the standard Laplace operator, which is the desirable property that is expected as a generalized operator. Then, based on such representation, a BEM-based algorithm (BEM_c) is developed for the fractional diffusion equation. An analog equation is established at first, which is the classical Poisson equation with load to be determined by the BEM. The solution of the analog equation is represented as an integral equation about the fundamental solution of the Laplace equation. The fractional Laplacian is then evaluated by matrix transformation, where the matrix is determined by numerical integration. Through the proposed algorithm, a matrix differential equation is constructed, where the response in each element can be obtained.

Chapter 5 proposes a way to separate the variables of the fractional Laplacian in the diffusion equation. The expansion is developed on the Caputo-type representation and includes the information of the boundary conditions. The non-orthogonal eigenfunctions of the fractional Laplacian are developed from the linear modes of classical diffusion equation solution. Based on such expansion, statistical linearization is then applied to the nonlinear fractional diffusion equation. When the order of the operator is close to 2, i.e. the fractional Laplacian is close to the standard Laplace operator, the mode shape functions are also close to be orthogonal and hence a set of decoupled single-degree-of-freedom ordinary differential equations is developed. For the smaller order though, the non-orthogonality must be considered and via the statistical linearization method, a multi-degree-of-freedom ordinary differential equation is established. In both cases, the response statistics and power spectral density are calculated by an iterative procedure. In this thesis, the statistical linearization is in the

mean square sense. Numerical results are presented to demonstrate the efficiency of the methods. Comparison and parameter studies are provided for elucidating the influence of the order of the fractional Laplacian.

In this work, the methods are applied to fractional diffusion equation as illustration. But these algorithms could also be used to other differential equations with the fractional Laplacian for numerical analysis, such as a fractional wave equation.

There are several related works on the fractional calculus that need investigation. First, note that the implementation of the BEMs and statistical linearization requires the numerical integration of singular integral. It is possible to improve the performance of the proposed methods with better numerical algorithms. Different numerical method may be derived through other representation. Next, it is important to further understand the physical meaning of the boundary condition of the fractional diffusion equation, as it allows long-range interaction and long jump of the particles. In this context, it is worthwhile to investigate which representation is better for application in engineering problems.

There is another kind of fractional diffusion equation, which contains the time-fractional derivatives. The methods proposed in the thesis can be directly applied to the fractional diffusion equation with both time-fractional derivative and the fractional Laplacian. That is,

$$D_t^\alpha u + (-\Delta)^{s/2} u = f(u, x, t). \quad (6.1)$$

The Grunwald-Letnikov algorithm is implemented for such problems. Also, it is interesting to try the proposed BEM and statistical linearization on the Fractional Porous Medium Equation

$$\dot{u} + (-\Delta)^{\alpha/2} (u^m) = 0. \quad (6.2)$$

For the application of the fractional Laplacian, nonlocal diffusion in inhomogeneous media is also an interesting topic that is worth being further investigated.

There are also many different numerical analysis methods that could be generalized for the problems containing the fractional Laplacian. The deterministic linearization method has already been introduced to the time-fractional differential equation by Spanos and Evangelatos (2010). It is worth trying to see if it can be generalized for the fractional Laplacian system. Further, a different statistical linearization introduced by Fang and Elishakoff (1995) is possible to be applied to different systems including fractional Laplacian, where an equivalent system is constructed to minimize the error in the energy sense. Another theme can be the application of the Singular Boundary Method, which is considered by Chen and Pang (2016) for a different implication definition of the fractional Laplacian, as well as other techniques such as stochastic averaging method. Furthermore, as another tool to describe nonlocal behavior of a system (Weckner and Abeyaratne, 2005), it is worth investigating if there is some correlation between stochastic Peridynamics and the fractional calculus (Evangelatos & Spanos, 2011).

References

- Abe, S., & Thurner, S. (2005). Anomalous diffusion in view of Einstein's 1905 theory of Brownian motion. *Physica A: Statistical Mechanics and its Applications*, 356(2), 403-407.
- Agrawal, O. P. (2001). Stochastic analysis of dynamic systems containing fractional derivatives. *Journal of Sound and Vibration*, Volume 247, Issue 5, 927-938.
- Babouskos, N. G., & Katsikadelis, J. T. (2010). Nonlinear vibrations of viscoelastic plates of fractional derivative type: an AEM solution. *Open Mechanics Journal*, 4, 8-20.
- Bates, P. W., & Chmaj, A. (1999). An integrodifferential model for phase transitions: stationary solutions in higher space dimensions. *Journal of Statistical Physics*, 95(5), 1119-1139.
- Bayazitoglu, Y., & Ozisik, M. N. (1988). *Elements of heat transfer*. McGraw-Hill.
- Beck, J. V., Wright, N. T., Haji-Sheikh, A., Cole, K. D., & Amos, D. E. (2008). Conduction in rectangular plates with boundary temperatures specified. *International Journal of Heat and Mass Transfer*, 51(19-20), 4676-4690.
- Bucur, C. (2015). Some observations on the Green function for the ball in the fractional Laplace framework. *arXiv preprint arXiv:1502.06468*.
- Bucur, C., & Valdinoci, E. (2016). *Nonlocal diffusion and applications* (Vol. 20, pp. xii-155). Bologna: Springer.
- Caffarelli, L., & Silvestre, L. (2007). An extension problem related to the fractional Laplacian. *Communications in partial differential equations*, 32(8), 1245-1260.
- Chen, W. (2006). A speculative study of 2/3-order fractional Laplacian modeling of turbulence: Some thoughts and conjectures. *Chaos: An Interdisciplinary Journal of Nonlinear Science*, 16(2), 023126.

- Chen, W., & Holm, S. (2004). Fractional Laplacian time-space models for linear and nonlinear lossy media exhibiting arbitrary frequency power-law dependency. *The Journal of the Acoustical Society of America*, 115(4), 1424-1430.
- Chen, W., & Pang, G. (2016). A new definition of fractional Laplacian with application to modeling three-dimensional nonlocal heat conduction. *Journal of Computational Physics*, 309, 350-367.
- D'Abbicco, M., & Ebert, M. R. (2014). Diffusion phenomena for the wave equation with structural damping in the L_p - L_q framework. *Journal of Differential Equations*, 256(7), 2307-2336.
- D'Elia, M., & Gunzburger, M. (2013). The fractional Laplacian operator on bounded domains as a special case of the nonlocal diffusion operator. *Computers & Mathematics with Applications*, 66(7), 1245-1260.
- del Teso, F. (2014). Finite difference method for a fractional porous medium equation. *Calcolo*, 51(4), 615-638.
- Di Paola, M., Failla, G., & Pirrotta, A. (2012). Stationary and non-stationary stochastic response of linear fractional viscoelastic systems. *Probabilistic Engineering Mechanics*, 28, 85-90.
- Elishakoff, I., Fang, J., & Caimi, R. (1995). Random vibration of a nonlinearly deformed beam by a new stochastic linearization technique. *International journal of solids and structures*, 32(11), 1571-1584.
- Evangelatos, G. I., & Spanos, P. D. (2011). A collocation approach for spatial discretization of stochastic peridynamic modeling of fracture. *Journal of Mechanics of Materials and Structures*, 6(7), 1171-1195.
- Fang, J., Elishakoff, I., & Caimi, R. (1995). Nonlinear response of a beam under stationary random excitation by improved stochastic linearization method. *Applied mathematical modelling*, 19(2), 106-111.

- Gettoor, R. K. (1961). First passage times for symmetric stable processes in space. *Transactions of the American Mathematical Society*, 101(1), 75-90.
- Guan, Q. Y., & Ma, Z. M. (2005). Boundary problems for fractional Laplacians. *Stochastics and Dynamics*, 5(03), 385-424.
- Huang, Z. L., & Jin, X. L. (2009). Response and stability of a SDOF strongly nonlinear stochastic system with light damping modeled by a fractional derivative. *Journal of Sound and Vibration*, 319(3-5), 1121-1135.
- Huang, Y., & Oberman, A. (2014). Numerical methods for the fractional Laplacian: A finite difference-quadrature approach. *SIAM Journal on Numerical Analysis*, 52(6), 3056-3084.
- Huang, Y., & Oberman, A. (2016). Finite difference methods for fractional Laplacians. *arXiv preprint arXiv:1611.00164*.
- Jiao, Y., & Malara, G., & Spanos, P. D. (2018). Boundary Element Method Based Approach for Estimating the Response of a System Governed by a Stochastic Nonlinear Fractional Diffusion Equation. *COMPUTATIONAL STOCHASTIC MECHANICS* 8, Manuscript in preparation.
- Katsikadelis, J. T. (1990). A boundary element solution to the vibration problem of plates. *Journal of Sound and Vibration*, 141(2), 313-322.
- Katsikadelis, J. T. (1991). Special methods for plate analysis. In *Boundary element analysis of plates and shells* (pp. 221-311). Springer, Berlin, Heidelberg.
- Katsikadelis, J. T. (1994). The analog equation method- A powerful BEM-based solution technique for solving linear and nonlinear engineering problems. *Boundary element method XVI*, 167-182.
- Katsikadelis, J. T. (2002). The analog boundary integral equation method for nonlinear static and dynamic problems in continuum mechanics. *Journal of Theoretical and Applied Mechanics*, 40(4), 961-984.

Katsikadelis, J. T. (2002). *Boundary elements: theory and applications*. Elsevier, 13-84.

Katsikadelis, J. T. (2006). The meshless analog equation method. A new highly accurate truly mesh-free method for solving partial differential equations. *Boundary Elements and other mesh reduction methods XXVIII*, WIT Press, Southampton, 13-22.

Katsikadelis, J. T. (2008). A generalized Ritz method for partial differential equations in domains of arbitrary geometry using global shape functions. *Engineering analysis with boundary elements*, 32(5), 353-367.

Katsikadelis, J. T. (2009). Numerical solution of multi-term fractional differential equations. *ZAMM-Journal of Applied Mathematics and Mechanics/Zeitschrift für Angewandte Mathematik und Mechanik*, 89(7), 593-608.

Katsikadelis, J. T. (2011). The BEM for numerical solution of partial fractional differential equations. *Computers & Mathematics with Applications*, 62(3), 891-901.

Katsikadelis, J. T. (2014). A new direct time integration method for the equations of motion in structural dynamics. *ZAMM-Journal of Applied Mathematics and Mechanics/Zeitschrift für Angewandte Mathematik und Mechanik*, 94(9), 757-774.

Katsikadelis, J. T. (2014). *The boundary element method for plate analysis*. Elsevier.

Katsikadelis, J. T., & Babouskos, N. (2007). The post-buckling analysis of plates. A BEM based meshless variational solution. *Facta Universitatis, Series Mechanics, Automatic Control and Robotics*, 6, 113-118.

Katsikadelis, J., & Babouskos, N. (2009). Nonlinear flutter instability of thin damped plates: A solution by the analog equation method. *Journal of Mechanics of Materials and Structures*, 4(7), 1395-1414.

Katsikadelis, J. T., & Babouskos, N. G. (2010). Post-buckling analysis of viscoelastic plates with fractional derivative models. *Engineering analysis with boundary elements*, 34(12), 1038-1048.

- Katsikadelis, J. T., & Nerantzaki, M. S. (1994). Non-linear analysis of plates by the analog equation method. *Computational mechanics*, 14(2), 154-164.
- Katsikadelis, J. T., & Sapountzakis, E. J. (1991). A BEM solution to dynamic analysis of plates with variable thickness. *Computational Mechanics*, 7(5-6), 369-379.
- Katsikadelis, J. T., & Tsiatas, G. C. (2003). Large deflection analysis of beams with variable stiffness. *Acta Mechanica*, 164(1-2), 1-13.
- Katsikadelis, J. T., & Tsiatas, G. C. (2004). Non-linear dynamic analysis of beams with variable stiffness. *Journal of Sound and Vibration*, 270(4), 847-863.
- Nerantzaki, M. S., & Katsikadelis, J. T. (1996). An analog equation solution to dynamic analysis of plates with variable thickness. *Engineering Analysis with Boundary Elements*, 17(2), 145-152.
- Kilbas, A. A., Srivastava, H. M., & Trujillo, J. J. (2006). *Theory and Applications of Fractional Differential Equations*, Volume 204 (North-Holland Mathematics Studies).
- Luchko, Y. (2015). Wave–diffusion dualism of the neutral–fractional processes. *Journal of Computational Physics*, 293, 40-52.
- Malara, G., Jiao, Y., & Spanos P. D. (2018). Statistical Linearization Approach for Calculating the Response Statistics of a System Governed by a Nonlinear Fractional Diffusion Equation, *COMPUTATIONAL STOCHASTIC MECHANICS* 8, Manuscript in preparation.
- Malara, G., & Spanos, P. D. (2017). Nonlinear random vibrations of plates endowed with fractional derivative elements. *Probabilistic Engineering Mechanics*, Volume 54, 2-8.
- Miller, K. S., & Ross, B. (1993). *An introduction to the fractional calculus and fractional differential equations*. John Wiley & Sons, 44-125.
- Monje, C. A., Chen, Y., Vinagre, B. M., Xue, D., & Feliu-Battle, V. (2010). *Fractional-order systems and controls: fundamentals and applications*. Springer Science & Business Media.

Nerantzaki, M. S., & Katsikadelis, J. T. (1996). An analog equation solution to dynamic analysis of plates with variable thickness. *Engineering Analysis with Boundary Elements*, 17(2), 145-152.

Oh, T., & Tzvetkov, N. (2017). Quasi-invariant Gaussian measures for the two-dimensional defocusing cubic nonlinear wave equation. *arXiv preprint arXiv:1703.10718*.

Petráš, I. (2011). *Fractional-order nonlinear systems: modeling, analysis and simulation*, Springer Science & Business Media, 7-38.

Podlubny, I. (1998). *Fractional differential equations: an introduction to fractional derivatives, fractional differential equations, to methods of their solution and some of their applications* (Vol. 198), Elsevier, 41-112.

Pozrikidis, C. (2016). *The Fractional Laplacian*, CRC Press, 1-21.

Roberts, J. B., & Spanos, P. D. (2003). *Random vibration and statistical linearization*, Courier Corporation, 122-211,

Ros-Oton, X., & Serra, J. (2014). The Dirichlet problem for the fractional Laplacian: regularity up to the boundary. *Journal de Mathématiques Pures et Appliquées*, 101(3), 275-302.

Rossikhin, Y. A., & Shitikova, M. V. (1997). Application of fractional derivatives to the analysis of damped vibrations of viscoelastic single mass systems. *Acta Mechanica*, 120(1-4), 109-125.

Rossikhin, Y. A., & Shitikova, M. V. (1997). Application of fractional derivatives to the analysis of damped vibrations of viscoelastic single mass systems. *Acta Mechanica*, 120(1-4), 109-125.

Rossikhin, Y. A., & Shitikova, M. V. (1997). Applications of fractional calculus to dynamic problems of linear and nonlinear hereditary mechanics of solids. *Applied Mechanics Reviews*, 50(1), 15-67.

- Rossikhin, Y. A., & Shitikova, M. V. (2000). Analysis of nonlinear vibrations of a two-degree-of-freedom mechanical system with damping modelled by a fractional derivative. *Journal of engineering mathematics*, 37(4), 343-362.
- Rossikhin, Y. A., & Shitikova, M. V. (2001). A new method for solving dynamic problems of fractional derivative viscoelasticity. *International Journal of Engineering Science*, 39(2), 149-176.
- Rossikhin, Y. A., & Shitikova, M. V. (2001). Analysis of dynamic behaviour of viscoelastic rods whose rheological models contain fractional derivatives of two different orders. *ZAMM-Journal of Applied Mathematics and Mechanics/Zeitschrift für Angewandte Mathematik und Mechanik*, 81(6), 363-376.
- Rossikhin, Y. A., & Shitikova, M. V. (2006). Analysis of damped vibrations of linear viscoelastic plates with damping modeled with fractional derivatives. *Signal Processing*, 86(10), 2703-2711.
- Rossikhin, Y. A., & Shitikova, M. V. (2006). Analysis of free non-linear vibrations of a viscoelastic plate under the conditions of different internal resonances. *International Journal of Non-Linear Mechanics*, 41(2), 313-325.
- Rossikhin, Y. A., & Shitikova, M. V. (2010). Application of fractional calculus for dynamic problems of solid mechanics: novel trends and recent results. *Applied Mechanics Reviews*, 63(1), 010801.
- Rossikhin, Y., Shitikova, M., Chao, C. K., & Persada, D. B. (2008). Analysis of Rectangular Plate Vibrations in a Fractional Derivative Viscous Medium. ENOC 2008, Saint Petersburg, Russia, June, 30–July, 4 2008
- Rossikhin, Y. A., Shitikova, M. V., & Ngenzi, J. C. (2015). A new approach for studying nonlinear dynamic response of a thin plate with internal resonance in a fractional viscoelastic medium. *Shock and Vibration*, 2015.
- Samko, S. G., Kilbas, A. A., & Marichev, O. I. (1993). Fractional integrals and derivatives. Theory and Applications, Gordon and Breach, Yverdon, 1993, 44.

- Sapountzakis, E. J., & Katsikadelis, J. T. (1999). Dynamic analysis of elastic plates reinforced with beams of doubly-symmetrical cross section. *Computational Mechanics*, 23(5-6), 430-439.
- Sapountzakis, E. J., & Katsikadelis, J. T. (2000). Analysis of plates reinforced with beams. *Computational Mechanics*, 26(1), 66-74.
- Seide, P. (1976). Nonlinear stresses and deflections of beams subjected to random time dependent uniform pressure. *Journal of Engineering for Industry*, 98(3), 1014-1020.
- Shampine, L. F. (2008). Vectorized adaptive quadrature in MATLAB. *Journal of Computational and Applied Mathematics*, 211(2), 131-140.
- Shinozuka, M., & Deodatis, G. (1991). Simulation of stochastic processes by spectral representation. *Applied Mechanics Reviews*, 44(4), 191-204.
- Solomon, T. H., Weeks, E. R., & Swinney, H. L. (1994). Chaotic advection in a two-dimensional flow: Lévy flights and anomalous diffusion. *Physica D: Nonlinear Phenomena*, 76(1-3), 70-84.
- Spanos, P. D., & Evangelatos, G. I. (2010). Response of a non-linear system with restoring forces governed by fractional derivatives—Time domain simulation and statistical linearization solution. *Soil Dynamics and Earthquake Engineering*, 30(9), 811-821.
- Spanos, P. D., & Malara, G. (2014). Nonlinear random vibrations of beams with fractional derivative elements. *Journal of Engineering Mechanics*, 140(9), 04014069.
- Spanos, P. D., & Malara, G. (2017). Random Vibrations of Nonlinear Continua Endowed with Fractional Derivative Elements. *Procedia Engineering*, 199, 18-27.
- Stapf, S., Kimmich, R., & Seitter, R. O. (1995). Proton and deuteron field-cycling NMR relaxometry of liquids in porous glasses: evidence for Lévy-walk statistics. *Physical review letters*, 75(15), 2855.

- Thurner, S., Wick, N., Hanel, R., Sedivy, R., & Huber, L. (2003). Anomalous diffusion on dynamical networks: a model for interacting epithelial cell migration. *Physica A: Statistical Mechanics and its Applications*, 320, 475-484.
- Treeby, B. E., & Cox, B. T. (2010). Modeling power law absorption and dispersion for acoustic propagation using the fractional Laplacian. *The Journal of the Acoustical Society of America*, 127(5), 2741-2748.
- Varlamov, V. (1999). Nonlinear heat equation with a fractional Laplacian in a disk. In *Colloq. Math* (Vol. 81, No. 1, pp. 101-122).
- Vázquez, J. L. (2012). Nonlinear diffusion with fractional Laplacian operators. In *Nonlinear partial differential equations*(pp. 271-298). Springer, Berlin, Heidelberg.
- Vázquez, J. L. (2014). Recent progress in the theory of nonlinear diffusion with fractional Laplacian operators. *arXiv preprint arXiv:1401.3640*.
- Vázquez, J. L. (2017). The mathematical theories of diffusion: Nonlinear and fractional diffusion. In *Nonlocal and Nonlinear Diffusions and Interactions: New Methods and Directions* (pp. 205-278). Springer, Cham.
- Vlahos, L., Isliker, H., Kominis, Y., & Hizanidis, K. (2008). Normal and anomalous diffusion: A tutorial. *arXiv preprint arXiv:0805.0419*.
- Weckner, O., & Abeyaratne, R. (2005). The effect of long-range forces on the dynamics of a bar. *Journal of the Mechanics and Physics of Solids*, 53(3), 705-728.
- Weeks, E. R., Urbach, J. S., & Swinney, H. L. (1996). Anomalous diffusion in asymmetric random walks with a quasi-geostrophic flow example. *Physica D: Nonlinear Phenomena*, 97(1-3), 291-310.
- Yang, Q., Liu, F., & Turner, I. (2010). Numerical methods for fractional partial differential equations with Riesz space fractional derivatives. *Applied Mathematical Modelling*, 34(1), 200-218.

Yang, Q., Turner, I., Liu, F., & Ilić, M. (2011). Novel numerical methods for solving the time-space fractional diffusion equation in two dimensions. *SIAM Journal on Scientific Computing*, 33(3), 1159-1180.

Zoia, A., Rosso, A., & Kardar, M. (2007). Fractional Laplacian in bounded domains. *Physical Review E*, 76(2), 021116.